Part I

Nanofiber production

1

Electrospinning of nanofibers and the charge injection method

D. R. S A L E M, Charge Injection Technologies Inc., USA

1.1   Introduction

The use of electric charge to break up liquids into small particles has been well known and extensively studied for over a century, but commercial applications have been constrained by difficulties in surmounting flow rate limitations associated with the underlying physics of the process. This is true for both electrospraying, in which low-viscosity liquids can be atomized into droplets, and electrospinning, in which viscoelastic liquids can be transformed into filaments of submicrometer and nanometer dimensions.

In this chapter, we will start by reviewing the principal forces involved in electrostatic atomization, which also form the basis of the electrospinning process, and then discuss the development of the science and technology of electrospraying and electrospinning, with particular emphasis on efforts to increase the rate at which nanofibers can be electrospun. After reviewing advances in the conventional approach to charging liquids in electrospraying and electrospinning (usually referred to as the capillary or needle method) we will highlight an alternative charging technology, known as the charge injection method, which is being developed for the production of nanometer and submicrometer fibers at exceptionally high output rates.

1.2   Principles of electrostatic atomization

It has long been known that application of electric charge to a liquid droplet causes instability of the liquid, resulting in distortion of the droplet or meniscus and in the ejection of liquid filaments and/or satellite droplets.[1–4] The effect is explained as a competition between the Coulomb repulsion of like charges favoring droplet distortion/partitioning and surface tension opposing droplet division. For example, in the case of a droplet of a conductive fluid in an electric field (where the charge accumulates at the droplet surface and there is no electric field inside the droplet) the pressure balance is given by:

$$\Delta P = \frac{2\sigma}{R} - \frac{e^2}{32\pi^2\varepsilon_0 R^4} \qquad [1.1]$$

where e is the total droplet charge, R is the droplet radius, σ is the surface tension and ε_0 is the vacuum permittivity.

It is informative that the relationship between the pressure drop and droplet radius is not monotonic (Fig. 1.1) – the electrostatic pressure, $e^2/(32\pi^2\varepsilon_0 R^4)$, becomes dominant as droplet radius becomes smaller (charge density increases), so that the function passes through a maximum and then reaches a point at which the pressure in the atmosphere and the pressure in the droplet are the same ($p = 0$). This point is associated with the electrostatic Rayleigh criterion, and can be interpreted as the maximum charge density that a droplet of a given diameter can withstand. Rewritten as the charge per mass, the Rayleigh relation takes the more familiar form:[5]

$$\frac{e}{M} = \sqrt{\frac{288\varepsilon_0\sigma}{d^3\rho^2}} \qquad [1.2]$$

The non-monotonic relationship between pressure drop and droplet radius has important consequences for understanding and predicting droplet/vapor coexistence and the behavior of an evaporating charged droplet, for which the pressure balance can be expressed as:[6]

$$\ln P_v / P_0 = \frac{v}{kT}\Delta P = \frac{v}{kT}\left(\frac{2\sigma}{R} - \frac{e^2}{32\pi^2\varepsilon_0 R^4}\right) \qquad [1.3]$$
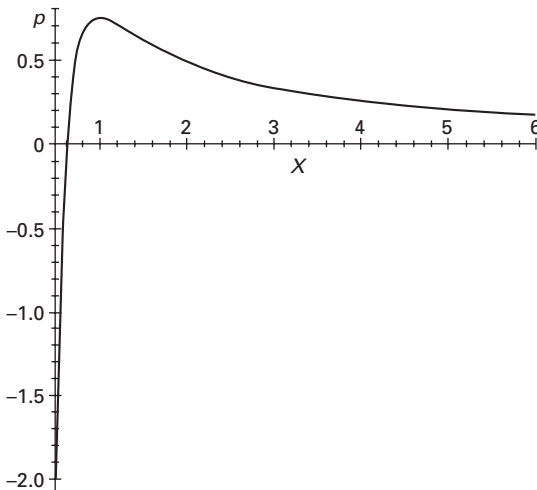
1.1 Dimensionless pressure drop $p = \Delta P\ell/2\sigma$ as a function of the dimensionless droplet radius $X = R/\ell$, where ℓ is the characteristic length scale.

where P_0 is the saturation pressure for a planar vapor/liquid uncharged surface. Kornev *et al.* have employed this relationship to anticipate the destiny of charged droplets surrounded by their own vapor under a range of pressure conditions.[6]

It is noteworthy, especially in relation to our later discussions on electrospinning, that cylindrical liquid columns are also subject to the Rayleigh-type instability, in which case the pressure balance is given by:[6]

$$\Delta P = \frac{\sigma}{R} - \frac{\kappa^2}{8\pi^2\varepsilon_0 R^2} \qquad [1.4]$$

where κ is the charge per unit length of the filament. Written in terms of charge density, the Rayleigh criterion for a charged liquid becomes:

$$\left.\frac{e}{M}\right|_{\text{column}} = \sqrt{\frac{64\sigma\varepsilon_0}{d^3\rho^2}} \qquad [1.5]$$

It is immediately apparent from Equations [1.2] and [1.5] that the charge required to reach the Rayleigh limit is about two times smaller for a column of liquid than for a droplet of the same radius.

The above analysis relates to charge-induced liquid break-up under static conditions, in order to provide an understanding of the primary forces involved, but the charge-induced break-up of flowing liquids is complicated by the superposition hydrodynamic perturbations and electrostatic instabilities that result in a variety of disruption behaviors, some of which will be discussed below.

1.3   Electrospraying and electrospinning by the capillary method

1.3.1   Operating modes

The earliest, and still the most widespread, practical use of electrostatic instabilities in liquids is electrospraying. It should be pointed out, however, that the term electrospraying is frequently applied to processes in which the primary liquid break-up is not generated by electrostatic forces, but by high pressure or some other mechanical method. In this case, the applied electric field mainly serves to charge the droplets so that they can be efficiently attracted to a grounded target and the technology is better described as electrostatically assisted spraying. Important commercial examples include electrostatic paint guns and agricultural sprayers, where large volumes of charged particles must be generated.

Electrospraying in which the primary break-up process (as well as any subsequent droplet division) occurs as a direct result of electrostatic forces is often referred to as electrohydrodynamic (EHD) atomization, and tends to

find application where flow rates can be low or minuscule. This is because EHD atomization using conventional charging technologies (often referred to as the capillary method) cannot operate at high rates of liquid delivery.

In a common set-up, a conductive liquid is delivered to the tip of a metal capillary, which is at high negative or positive potential (Fig. 1.2). As a result of the electric field generated, charge accumulates at the surface of the pendant droplet formed at the tip of the capillary and creates an instability that deforms the hemispherical droplet into a cone shape, often referred to as a Taylor cone.[3, 4, 7] At a sufficiently high field strength, a jet of liquid is continuously ejected from the apex of the cone and breaks up into charged particles. In this cone-jet mode of operation,[8] a stable, continuous stream of charged particles can be generated.

The break-up of the jet may be via an axisymmetric varicose instability, a bending/whipping instability or, more rarely, a ramified mode involving distortion of the jet's circular cross-section and emission of lateral sub-jets (Fig. 1.3).[10, 11] The varicose instability occurs at relatively low surface charge and is similar in manner to the break-up of a neutral jet. This mode can produce charged sprays with highly monodisperse droplet diameters and mean diameters ranging from a few nanometers to hundreds of micrometers, depending on field strength and fluid properties such as conductivity and viscosity.

As surface charge on the jet increases (by raising the flow rate[11–14] or the applied voltage[11, 13, 15] to increase current), the axisymmetric break-up mode
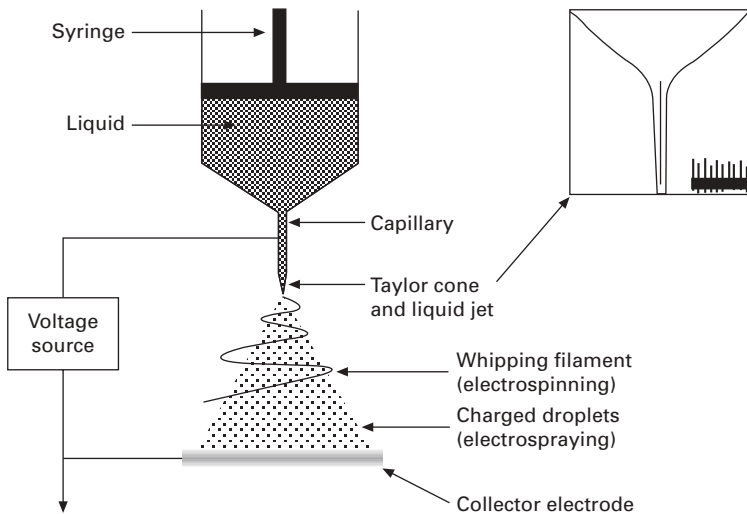
1.2 Typical set-up for electrospraying/electrospinning by the capillary method. The inset is an example of a pendant droplet, distorted by the electric field, and the emitted jet (adapted from Ref. 9).

Axisymmetric   Bending/whipping   Ramified
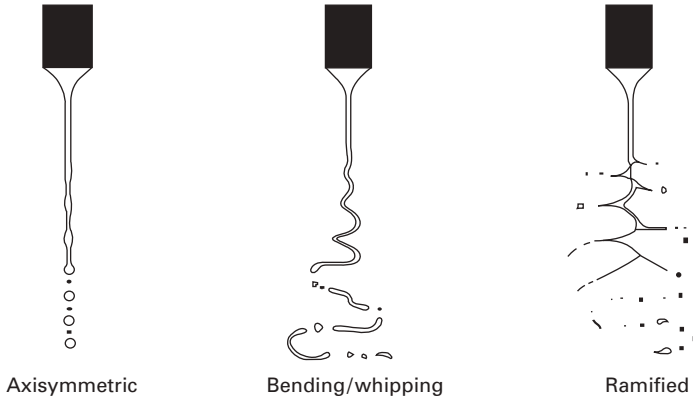
1.3 Principal jet break-up modes (adapted from Ref. 11).

transitions to the bending/whipping instability.[10, 11, 16] The whipping motion rapidly thins the jet and breaks it into a spray with polydisperse droplet diameters having mean values usually of the order of tens of micrometers.

If the jet is highly charged, the electric stresses can overcome surface tension, causing the cross-section of the jet to deform or bulge in one or more locations, from which fine sub-jets are released.[10, 11] This ramified mode is of course related to the electrostatic Rayleigh break-up mode anticipated by Equation [1.4], although this equation cannot be directly used to indicate the charge threshold for Coulombic rupture in a column of liquid that is flowing. For example, it has been shown that the stretching of a charged liquid column, as in an accelerating jet, not only introduces hydrodynamic perturbations, but also modifies (compared with a static liquid column) the relationship between Laplacian pressure and electrostatic pressure in a way that tends to stabilize the column against Coulombic disruption.[6]

Ramified jet break-up is seldom observed in the capillary method of electrospraying because corona discharge prevents reaching the required field strength. However, it may be noted that dramatic Coulombic explosion of a liquid helium jet was observed by Tsao *et al.* using capillary electrospraying.[17] No Taylor cone was formed, and the shattering of the helium jet into droplets of 1–10 μm diameter was attributed to charge densities that – owing to high current and exceptionally low surface tension – were computed to be 50 times the Rayleigh limit (for a stationary liquid cylinder). In this case, the ratio of electric stress to surface tension was evidently sufficient to overwhelm any stabilizing effects of the accelerating jet.

If the charged droplets from any electrospraying process evaporate sufficiently rapidly, they may undergo further disruption and division after the initial break-up, since the shrinking droplets (both parent and daughter droplets) will repeatedly attain the threshold charge for electrostatic Rayleigh

division.[18–21] This phenomenon led to the ground-breaking application of cone-jet electrospraying in mass spectroscopy, where the droplets become so small from repeated division that the electric field due to the high surface charge density is strong enough to desorb ions from the droplets into the ambient gas.[22] 'Quasi-molecules' suitable for mass analysis are produced when solute species are attracted to desorbing cations and anions. Single and few-chain polymer particles have been produced by this multiple-fission method.[23]

Electrospinning of fibers from polymer solutions is usually carried out by the capillary method of Fig. 1.2. In a typical experiment, a pendant droplet of the polymer solution at the capillary tip is subject to the electric field created by the potential difference between the capillary and a grounded collector.[9, 24, 25, 26] Although polymer solutions are subject to the same competition between axisymmetric and whipping instabilities described for electrospraying,[27, 28] the viscoelastic properties of these solutions delay or completely suppress the break-up of the fluid into droplets. Consequently, the jet rapidly thins as it is accelerated from the cone apex and, at high enough field strengths, is further attenuated as it undergoes the whipping instability.[9, 27–30] Evaporation of the solvent in the course of this draw-down process results in the accumulation of solid filaments at the collector with mean diameters typically in the range 100–500 nm, and sometimes well below 100 nm.[31, 32] An example of nanofibers produced by capillary electrospinning is shown in Fig. 1.4.

5 µm
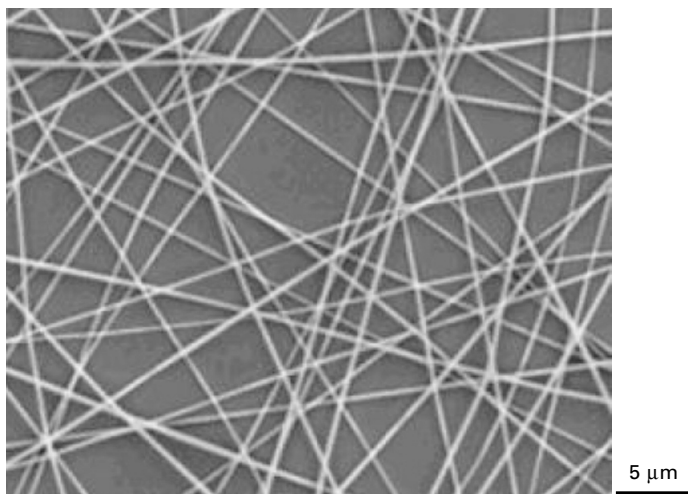
1.4 SEM image of poly(vinyl pyrrolidone) nanofibers electrospun by the 'capillary' method. (Adapted from D. Li and Y. Xia, *Adv. Mater.* (2004) **16**, p. 1151.)

Nevertheless, droplet creation – both isolated droplets and 'beads on a string'[9, 31–34] – can occur in electrospinning when the solution is insufficiently elastic. Inadequate solution elasticity usually arises from lack of molecular entanglements in solutions that are too dilute, and the polymer concentration generally needs to be well above the critical concentration for chain overlap.[34] The essential importance of elasticity in electrospinning has been confirmed recently in a systematic study by Yu *et al.* using model fluids with different degrees of elasticity.[35] They demonstrated that a critical value of elastic stress indicates the complete suppression of the instability responsible for jet break-up into droplets, and marks a transition from bead-on-a-string morphology to the formation of uniform fibers.

On the basis that the whipping of the jet arises when surface tension is insufficient to stabilize the jet against perturbations that grow with increasing surface charge, Fridrikh *et al.*[36] have shown that the terminal diameter h_t of a polymer solution undergoing the whipping instability is controlled by the flow rate Q, electrical current I and surface tension γ. Thus, at a given polymer concentration:

$$h_t = \left(\gamma \bar{\varepsilon} \frac{Q^2}{I^2} \frac{2}{\pi^2 (2 \ln \chi - 3)} \right)^{1/3} \qquad [1.6]$$

where $\bar{\varepsilon}$ is the dielectric constant of the outside medium and χ is the dimensionless wavelength of the instability responsible for the normal displacements. This relationship (which assumes negligible solvent evaporation during draw-down and neglects elastic effects) confirms that a valuable strategy to minimize fiber diameter is to increase the charge-carrying capacity of the fluid. This has been demonstrated in a number of experimental studies where conductive additives were introduced into the solution.[26, 32, 37]

An interesting modification of the capillary method, explored recently, involves the application of AC voltage instead of DC,[38] or, more optimally, AC voltage with biased DC voltage.[39] As a result of short charge segments of alternating polarity along the jet, the net charge was reduced and the whipping instability was thereby diminished or suppressed. Yet under optimized AC frequency and DC bias conditions, draw-down from the straight jet was sufficient to produce aligned fibers with diameters ranging from 100 to 200 nm.

1.3.2   Output limitations and recent developments

The greatest drawback of both electrospraying and electrospinning by the standard capillary method is the very low rates at which they can usefully generate sprays or nanofibers. Typically, output of fluid from a single capillary is in the range 1–5 milliliters per hour.

The rate of fluid flow is largely determined by the strength of the electric field, since the field is responsible for accelerating the jet from the cone apex. However, the field strength that can be applied is limited by the electrical breakdown strength of the atmosphere (usually air) in which the droplets or fibers are forming, in addition to which the space charge field from the charged droplets or filament can increasingly attenuate the applied electric field as flow rate (and current) increases. It is also well documented that with the standard capillary method, the diameters of the droplets or fibers increase with flow rate, so that – even before reaching the limiting flow rate imposed by electrical breakdown – the dimensions of these entities may be too large to be of practical interest. Furthermore, it is noteworthy that despite volume flow rates of milliliters per hour, the jet velocity must be in the range 100–300 m/s in existing electrospinning practice for fibers to attain dimensions of a few hundred nanometers. It is therefore improbable that a substantial increase of these, already high, velocities is likely to arise from manipulation of electric fields alone.

For these reasons, most efforts to increase output from electrospraying and electrospinnng have centered on multiplexing the liquid output source, either by stacking an array of capillaries as closely together as possible, or by attempting to operate in the so-called multi-jet mode. Both these approaches are complex, and are difficult to implement robustly, although some significant improvements in output have been reported recently.

The multi-jet mode, in which several cone-jets emanate from a single capillary tube, appears within a narrow range of voltages and flow rates, and the individual jets are prone to interruption and positional instability. Duby et al.[40] have recently demonstrated, however, that by introducing a number of grooves in the tube circumference to intensify the electric field at these locations, the stability of the multi-jet mode in electrospraying was much improved. Fifty cone-jets per cm^2 could be achieved, capable of delivering sprays with mean droplet diameters in the range 7–20 μm at rates between about 0.2 and 1.5 ml/min per cm^2 of spray-head area. This delivery rate remains far too low for most commercial applications, and in any case the multi-jet approach has not, to our knowledge, been successfully applied to electrospinning.

Assembling an array of capillaries or orifices to increase output in electrospraying and electrospinning has been explored by several groups, but the fundamental difficulty with this tactic is that each jet is subject to electric-field shielding and space-charge interference from adjacent jets.[41–45] Consequently, at orifice densities that would significantly improve output, only the outermost jets in an array will function effectively, and addressing this problem requires careful configuration of the electric field at each jet.

In the case of electrospraying, a systematic attempt to configure the electric fields was made by Deng et al.[41] who microfabricated an array of orifices

etched in silicon with a density of 250 orifices/cm^2. Reduction of cross-talk between jets and minimization of space-charge feedback were achieved by positioning an extractor electrode (consisting of a plate with holes concentric with the output orifices) at a distance from the orifices that was comparable to the inter-orifice spacing of 0.5 mm. It would appear that, under optimal conditions, monodisperse sprays with flow rates of the order of 5 ml/min per cm^2 of spray-head area can be delivered by this type of device.

For electrospinning, similar attempts have been made to configure the electrical fields using secondary external electrodes[42, 43] but so far the achievable packing density of spinneret orifices for successful nanofiber spinning appears to be considerably less than in the case of electrospraying. Reasonable jet stability in electrospinning seems to require inter-orifice spacing in the range of several millimeters to centimeters with packing densities of the order of two jets/cm^2. Consequently, in these multiplexed systems, output per unit area of the spinneret head remains very modest.

Electrospinning apparatus appearing to provide a relatively high nanofiber output is, however, described in a recent US patent.[46] In this disclosure, block-type nozzles emit charged jets of a polymer solution from an array of pins. In one example, 200 blocks were deployed, comprising a total of 40 000 pins. However, no information is given on inter-pin spacing or strategies used for minimizing electrical interference between jets: rather, the patent focuses on the application of a device that intermittently delivers solution to each nozzle block (held at high voltage), thereby charging discrete quantities of the fluid consecutively. This is claimed to reduce the deterioration of electric forces that occur when the high voltage is applied to the whole spinning solution. In the case where 40 000 pins were used (delivering ~0.003 g/min of solid polyamide fiber per pin), a 0.6 m wide web was produced at 60 m/min and had a base weight of 3 g/m^2.

1.3.3   Viscosity limitations and recent developments

It would be preferable to spin nanofibers from molten polymer than from polymer solution because the solvents used are generally flammable and/or toxic. For nanofiber production on an industrial scale, the use of solvents presents a significant environmental hazard, and the need for expensive safety precautions and solvent recovery equipment provides an additional obstacle to commercial scale-up of the technology.

Whereas fibers can certainly be electrospun from the melt, they generally have diameters in the micrometer range. Resistance to nanofiber formation is largely due to the high viscosity of the polymer melt, being one to two orders of magnitude higher than typical solution viscosities, and this problem is no doubt compounded by the rapid increase in viscosity taking place as the thinning (and whipping) filament cools to ambient temperature. Furthermore,

melt electrospinning does not benefit from the contribution of solvent evaporation to the thinning process.

Electrospinning into a heated chamber is likely to reduce the tendency for premature solidification of the molten filament during the electrically driven draw-down process, and this approach has been investigated recently by Zhou et al.[47] Under optimized operating conditions, they electrospun molten polylactic acid (PLA) from a single capillary into fibers with a mean diameter of about 800 nm. The flow rate was 0.01 ml/min, and the spinning mode was characterized by a typical whipping instability.

Another method to assist draw-down of high-viscosity polymer fluids in electrospinning involves subjecting the electrified polymer jet to a hot air stream, thereby decreasing the viscosity of the fluid and adding a mechanical pulling force to the jet. This has been developed into a multiple jet 'electroblowing' (or 'blowing-assisted electrospinning') system and is considered by its inventors to be suitable for molten polymers.[43] The only published data to date, however, are from electroblowing of hyaluronic acid (HA) solutions, which exhibit unusually high viscosity at relatively low concentrations and could not be spun by unassisted electrospinning.[48, 49] Via the electroblowing method, consistent fabrication of HA fiber membranes was achieved with mean fiber diameter of about 70 nm. It may be noted, however, that despite the pulling force of the heated air stream on the jet, the output of this process is not appreciably higher than an unassisted multiple-jet electrospinning system, even when applied to lower-viscosity polymer solutions.

1.4   Electrospraying and electrospinning by the charge injection method

1.4.1   Principle of operation

Electrohydrodynamic atomization of liquids by charge injection is an alternative approach to the capillary method, and offers distinct advantages in terms of output and efficiency. One configuration of the charge injection method, shown in Fig. 1.5, comprises two electrodes immersed in a (non-conducting) fluid. The sharpened point of the 'emitter electrode', held at high electric potential, is centered over a grounded orifice ('blunt electrode'). Owing to the small distance between electrodes (typically one to three orifice diameters), an intense electric field is set up in the fluid, which is much larger than that provided by the capillary method. The fluid is continuously forced through the orifice under high pressure and becomes highly charged as it passes between the electrodes. Most of this charge remains in the liquid because of the low mobility of electrons in an insulating fluid and due to the very short residence time of the fluid prior to exiting the orifice, the applied flow rate
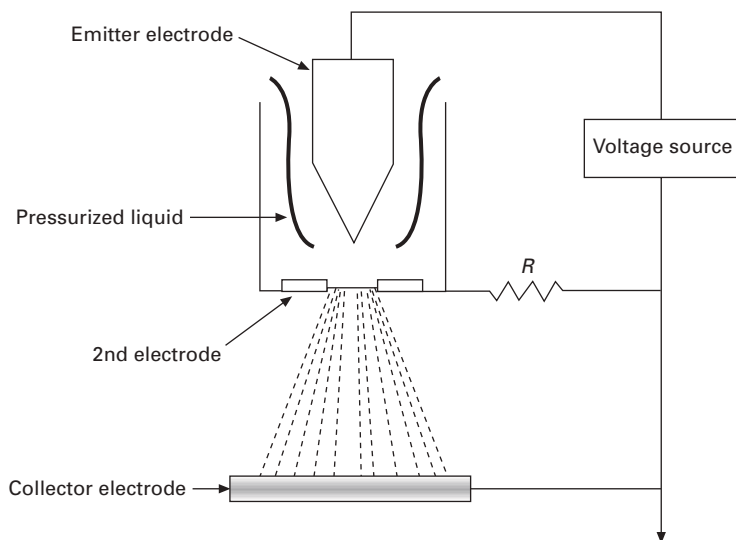
1.5 An example of the 'triode' configuration of the charge injection method.

being typically between 0.2 and 5 ml/s (three orders of magnitude greater than in the capillary method). After emerging from the orifice, the charged droplets or filaments can be attracted towards a third (collector) electrode in the form of a grounded (or oppositely charged) object, or they may be allowed to disperse freely in the environment.

Unlike the capillary method, the charge injection system does not involve the formation of a Taylor cone, and the velocity of the fluid stream is determined by the (mechanical) pressure applied, not by the strength of the external electric field. In this way, charge injection electrospraying/electrospinning overcomes throughput limitations by decoupling the fluid flow from the field strength.

Whereas the capillary method is applicable to conductive liquids, it is clear that charge injection technology can only be used with insulating or weakly conducting fluids, and much of the development of this technology has been related to the atomization of hydrocarbon fuels for combustion applications. For electrospinning fibers, however, there is no shortage of suitable polymer–solvent combinations with dielectric properties, and the non-conducting nature of polymer melts should make them particularly amenable to electrospinning by charge injection.

1.4.2 Operating regimes and limits

Spray behavior from charge injection atomizers has been studied and described in some detail by Kelly,[50–52] a pioneer of this technology, and it will be

useful to review the series of events that occur to a stream of (low molecular weight) fluid issuing from the orifice of such a device as the applied voltage is increased. Starting as a uniform column, the stream starts to disrupt into droplets at some distance from the orifice once the voltage attains a threshold value (dependent on fluid properties, flow rate, device configuration, etc.). As the voltage is raised higher (further increasing the spray current and charge density of the fluid) column disruption occurs closer and closer to the orifice, atomization progressively intensifies, the droplets become smaller and the lateral dispersion of the spray increases. A voltage level is finally reached, however, at which the spray current falls precipitously due to electrical breakdown phenomena, causing the atomization to halt abruptly and the spray to collapse back to a flowing column of liquid (Fig. 1.6). Since the liquid breaks up most energetically at the maximum charge density, just prior to the breakdown voltage, a feedback controller for optimization of performance has been designed which detects trichel discharge events that occur as the breakdown limit is approached and then automatically adjusts the voltage back to stay just below this limit, providing stable operation for unlimited run times.[50f]

Shrimpton and Yule[54] have identified subcritical and supercritical flow regimes delineated by different types of electrical breakdown. At subcritical flow rates, the spray is not finely atomized and it is limited by electrical breakdown of the fluid within the atomizer. At supercritical flow rates, fine atomization occurs and spraying is limited by electrical breakdown of the air outside the orifice, which results from the high surface charge density of the exiting liquid column. It has been found, however, that the maximum achievable charge density increases with increasing stream velocity and decreasing orifice diameter.[51, 54]

The break-up behavior of a charge-injected columnar stream is depicted in Fig. 1.7. Although the orifice diameter is relatively large and the liquid is
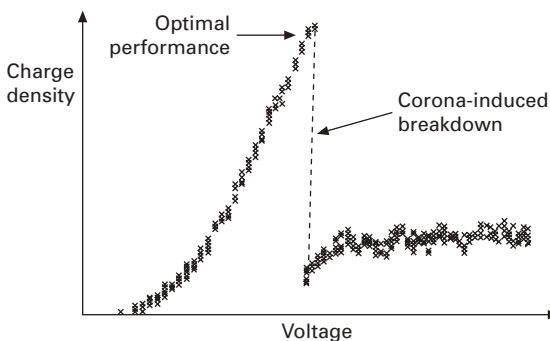
1.6 Charging behavior of a fluid in a triode-type charge injection device (adapted from Ref. 53).
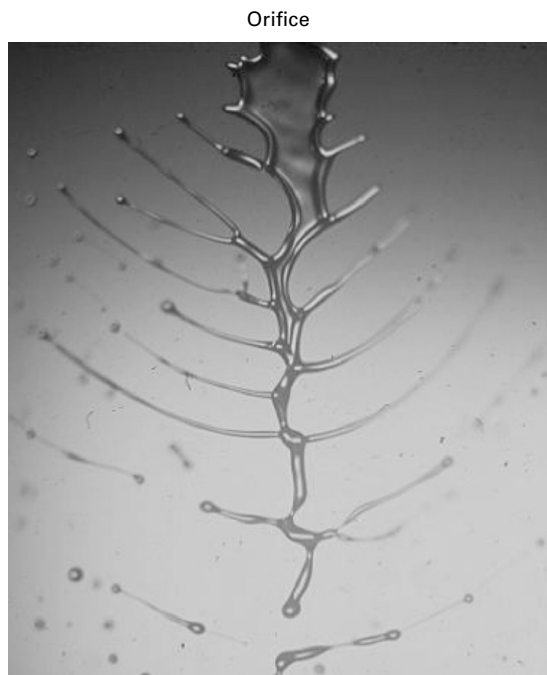
Orifice

1.7 Break-up of a liquid column of mineral oil just after exiting the orifice of a triode-type charge injection device (adapted from Ref. 52). Flow direction is from top to bottom of the image.

weakly charged in this example (0.15 C/m^3), the column disruption is quite dramatic and revealing. Just after issuing (downwards) from the orifice, the column distorts laterally due to charge repulsion. The charge, and the fluid that carries it, tend to migrate to the edges and concentrate there, forming a thick rim around the extended core region. The high charge density in the rim creates additional instabilities, and lateral jets are emitted from localities at which Coulombic forces have overcome surface tension. This behavior is clearly reminiscent of the ramified jet mode, observed in cone-jet electrospraying at very high electric fields, and is indicative of Rayleigh-type Coulombic rupture.

As charge density increases, this break-up mode becomes more vigorous and, in the absence of electrical breakdown phenomena, would be expected to progress towards explosive disruption at the fluid exit point. The observed form of Coulombic rupture appears to be favored by the charge injection method in both electrospraying and electrospinning, and the whipping mode is rarely observed. In the quest to improve the productivity of electrospinning, it is clear that stream-splitting instabilities in which multiple filaments are generated from a single liquid column are much more desirable than instabilities that generate a single, thinning filament from an intact column. Optimization

of column splitting or bursting in charge injection electrospinning is therefore of significant interest.

Nanofiber webs spun by the charge injection system were first produced by A. J. Kelly in 2000. Research and development work has shown that the morphology of charge injection fiber webs is dependent on the polymer/ solvent system and on process variables (which for proprietary reasons cannot be detailed in this chapter). For example, polyurethane fibers produced at 1 ml/s under one set of conditions have significantly more network junctions than is typically found in webs produced by the capillary method, but show little direct evidence of being generated by a column-bursting mechanism (Fig. 1.8). On the other hand, fibers spun from the same polyurethane at the same flow rate under different operating conditions, display a distinct hierarchical structure in which interconnected networks of larger diameter fibers are further interconnected by networks of smaller diameter fibers (Fig. 1.9). The latter morphology is consistent with other evidence that the predominant mechanism of fiber formation in charge injection electrospinning involves expansion and splitting of two-dimensional films, propagated from a stretched and disrupted liquid column.

These bimodal, interconnected membrane structures should be of significant commercial value, since the majority of filaments are nanofibers (providing, for example, ultra-efficient filtration properties) and the larger fibers are interconnected in such a way as to provide structural integrity and strength to the web. To our knowledge, however, the charge injection method has so
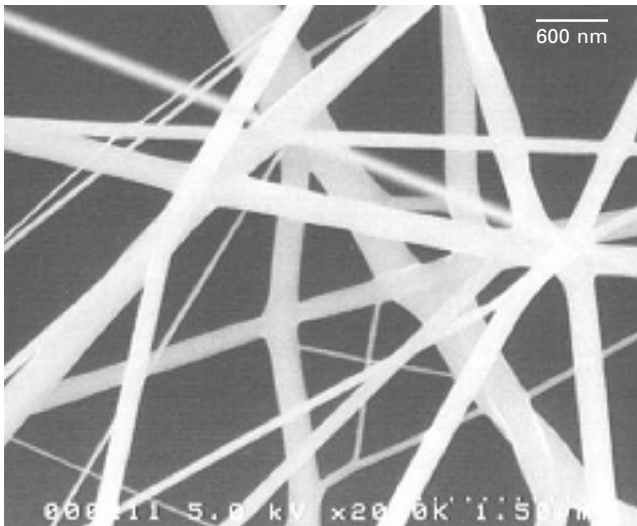
1.8 SEM image of polyurethane nanofibers electrospun by the charge injection method.
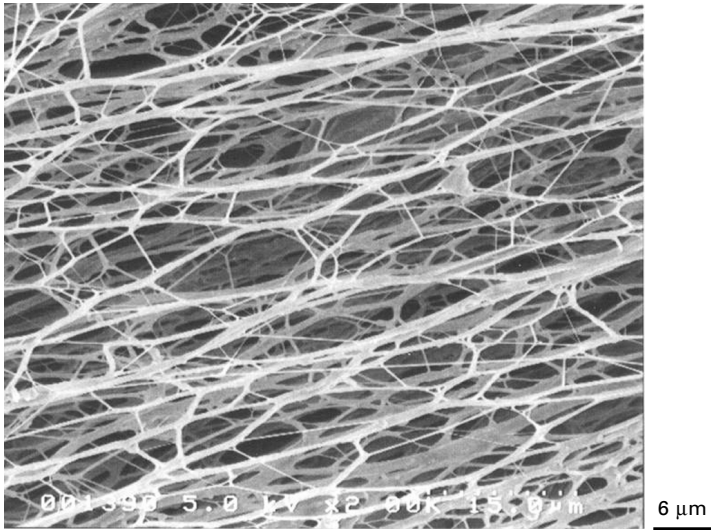
(a)
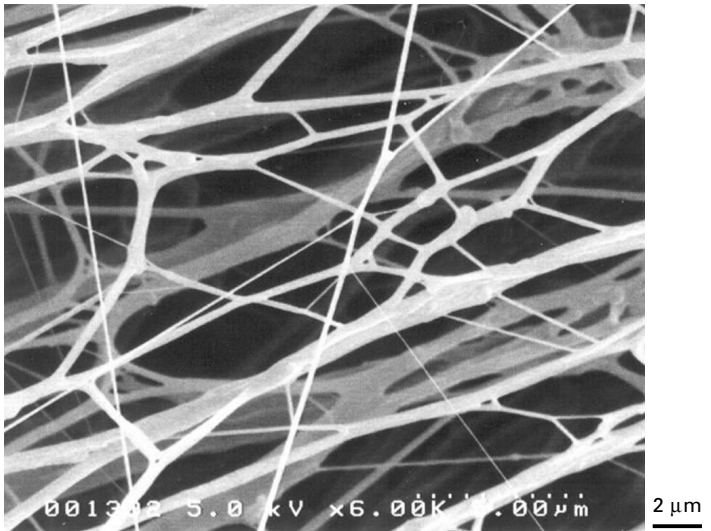
(b)

1.9 SEM images of polyurethane nanofibers electrospun by the charge injection method, illustrating highly interconnected networks of fibers with smaller and larger diameters.

far been unable to produce webs in which the majority of the polymer has been converted into nanofibers. The membranes either contain nanofibers with unconverted polymer or they are fully fibrillar but comprise a mixture of nanofibers and microfibers.

Under yet another set of operating conditions, electrospinning from a solution of polypropylene and decalin at elevated temperature (below the solvent's boiling point), we observed scattered instances of hollow droplets that appear to have partially transformed into nanofibers as a result of explosive rupture (Fig. 1.10). As discussed by Kornev et al.,[55] we attribute this to a charge-induced cavitation process that can be predicted from theory.


2 μm

(a)

600 nm
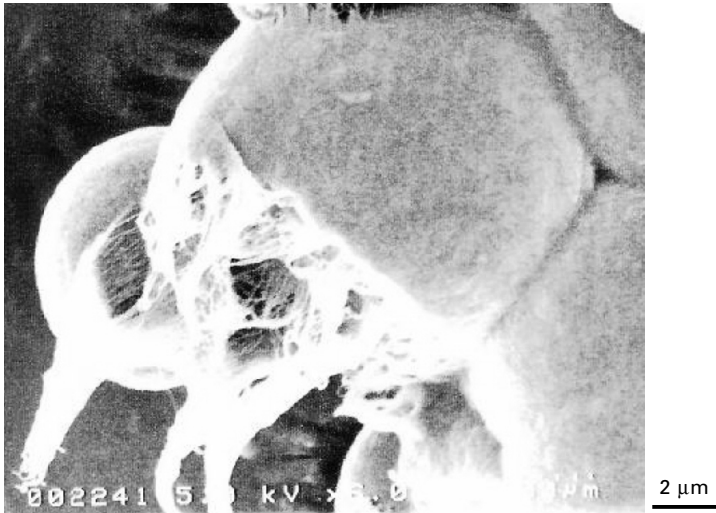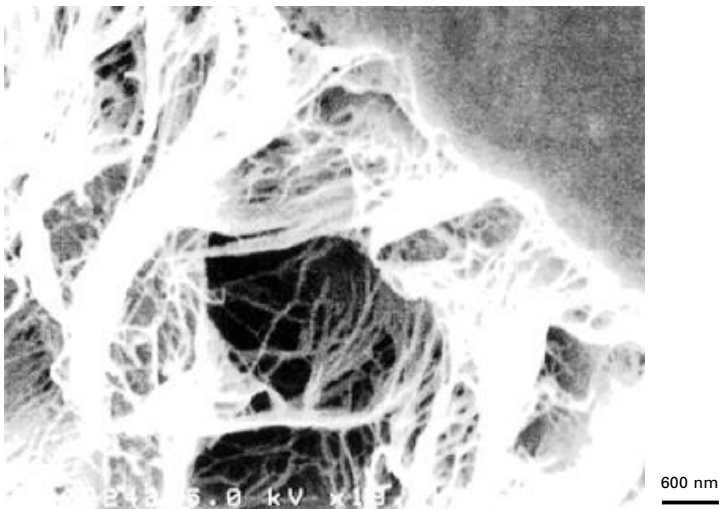
(b)

1.10 SEM images of nanofibers produced from 'exploded' droplets in charge injection electrospinning of a polypropylene/decalin solution.[55] (The lower image is a section of the upper image at higher magnification.)

Efforts to increase nanofiber yield in solution and to achieve nanofiber production from molten polymer using charge injection are focusing on increasing the charge density beyond the limits (of about $6\,C/m^3$) currently imposed by electrical breakdown phenomena, and improving the uniformity of charge distribution across the orifice diameter (since it is known that charge density is generally lower at the center of the exiting fluid column than in the outer regions).[51] Some strategies are outlined below.

1.4.3   Strategies for further development

A patented strategy for increasing charge density above the corona-induced breakdown point is to pulse the voltage of the charge injection device from a base value below the breakdown limit to a value above the breakdown limit, for a time shorter than that required for breakdown.[50g] It has been shown that under typical spraying condition, pulses of a few milliseconds duration should allow voltage to exceed the threshold level without a corona discharge effect occurring.

Another approach is to use a sealed electron beam gun (Fig. 1.11).[50d] The fluid is passed over an electron-transparent window of the sealed gun, which injects energetic electrons into the fluid as it sweeps by. This method could provide highly efficient charging of the fluid and may be the key to obtaining nanofibers from the melt at high throughput. Implementation is difficult in practice, however, because small, robust e-beam guns must be custom made, and the electron-permeable window must be strong enough to withstand the fluid pressure and thin enough to be highly transparent to electrons.
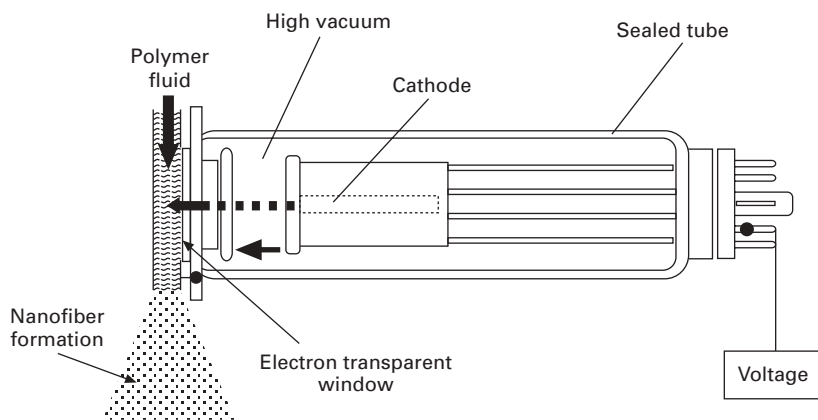
1.11 Schematic representation of charge injection into a flowing polymer fluid by means of a miniature electron beam device.

1.5   **References**

1. Rayleigh, F.R.S., *Phil. Mag.* (1882) **44**, p. 184
2. Zeleny, J., *Phys. Rev.* (1917) **10**, p. 1
3. Taylor, G.I., *Proc. R. Soc. London* (1966) **A291**, p. 145
4. Taylor, G.I., *Proc. R. Soc. London* (1969) **A313**, p. 453
5. Schweizer, J.W. and Hanson, D.N., *J. Colloid Interface Sci.* (1971) **35**, p. 417
6. Kornev, K. Kurtz, S. and Salem, D.R., To be published
7. Pantano, C., Ganan-Calvo, A.M. and Barrero, A., *J. Aerosol Sci.* (1994) **25**, p. 1065
8. Cloupeau, M. and Prunet-Foch, B., *J. Electrostatics* (1989) **22**, p. 135
9. Fong, H. and Reneker, D.H. in *Structure Formation in Polymeric Fibers*, D.R. Salem (Ed) (2001) p. 225
10. Cloupeau, M. and Prunet-Foch, B., *J. Aerosol Sci.* (1994) **25**, p. 1021
11. Hartman, R.P.A., Brunner, D.J., Camelot, D.M.A., Marijnissen, J.C.M. and Scarlett, B., *J. Aerosol Sci.* (2000) **31**, p. 65
12. Fernandez de la Mora, J. and Loscertales, I.G., *J. Fluid Mech.* (1994) **260**, p. 155
13. Ganan-Calvo, A.M., Davila, J. and Barrero, A., *J. Aerosol Sci.* (1997) **28**, p. 249
14. Ganan-Calvo, A.M., *Phys. Rev. Lett.* (1997) **79**, p. 217
15. Gomez, A. and Tang, K., *Proc. 5th Int. Conf. on Liquid Atomization and Spray Systems* (1991) p. 805
16. Magarvey, R.H. and Outhouse, L.E., *J. Fluid Mech.* (1962) **13**, p. 151
17. Tsao, C.C., Lobo, J.D., Okumura, M. and Lo, S.Y., *J. Phys. D: Appl. Phys.* (1998) **31**, p. 2195.
18. Doyle, A., Moffett, D.R. and Vonnegut, B., *J. Colloid Sci.* (1964) **19**, p. 136
19. Roth, D.G. and Kelly, A.J., *IEEE Trans. Ind. Appl.* (1983) **IA-19**, p. 771
20. Duft, D., Achtzehn, T., Muller, R., Huber, B.A. and Leisner, T., *Nature* (2003) **421**, p. 128
21. Lopez-Herrera, J.M. and Ganan-Calvo, A.M., *J. Fluid. Mech*. (2004) **501**, p 303
22. Fenn, J.B., Mann, M., Meng, C.K., Wong, S.F. and Whitehouse, C.M., *Science* (1989) **246**, p. 64
23. Festag, R., Alexandratos, S.D., Cook, K.D., Joy, D.C., Annis, B. and Wunderlich, B., *Macromolecules* (1997) **30**, p. 6238
24. Formhals, A., US Patent 2,349,950 (1944)
25. Baumgarten, P.K., *J. Colloid and Interface Sci.* (1971) **36**, p. 71
26. Bornat, A., US Patent 4,323,525 (1982)
27. Hohman, M.M., Shin, M., Rutledge, G. and Brenner, M.P., *Phys. Fluids* (2001) **13**, p. 2201
28. Hohman, M.M., Shin, M., Rutledge, G. and Brenner, M.P., *Phys. Fluids* (2001) **13**, p. 2221
29. Reneker, D.H., Yarin, A.L., Fong, H. and Koombhongse, S., *J. Appl. Phys.* (2000) **87**, p. 4531
30. Yarin, A.L., Koombhongse, S. and Reneker, D.H., *J. Appl. Phys.* (2001) **89**, p. 3018
31. Fong, H. and Reneker, D.H., *Polymer* (1999) **40**, p. 4585
32. Zong, X., Kim, K., Fang, D., Ran, S., Hsiao, B.S. and Chu, B. *Polymer* (2002) **43**, p. 4403
33. Lee, K.H., Kim, H.Y., Bang, H.J., Jung Y.H. and Lee, S.G., *Polymer* (2003) **44**, p. 4029
34. McKee, M.G., Wilkes, G.L., Colby, R.H. and Long, T.E., *Macromolecules* (2004) **37**, p. 1760

35. Yu, J.H., Fridrikh, S.V. and Rutledge, G.C., *Polymer* (2006) **47**, p. 4789
36. Fridrikh, S.V., Yu, J.H., Brenner, M.P. and Rutledge, G.C., *Phys. Rev. Lett.* (2003) **90**, p. 144502-1.
37. Hou, H., Jun, Z., Reuning, A., Schaper, A., Wendorff, J.H. and Greiner, A., *Macromolecules* (2002) **35**, p. 2429
38. Kessik, R., Fenn, J.B. and Tepper, G., *Polymer* (2004) **45**, p. 2981
39. Sarkar, S. and Tepper, G., The Fiber Society Fall Annual Meeting and Technical Conference, October 2006, 5A
40. Duby, M.H., Deng, W., Kim, K., Gomez, T. and Gomez, A., *J. Aerosol Sci.* (2006) **37**, p. 306
41. Deng, W., Klemic, J., Li, X., Reed, M. and Gomez, A., *J. Aerosol Sci.* (2006) **37**, p. 696
42. Chu, B., Hsiao, B.S. and Fang, D., US Patent 6,713,011 (2004)
43. Burger, C., Hsiao, B.S. and Chu, B., *Annu. Rev. Mater. Res.* (2006) **36**, p. 333
44. Theron, S.A., Yarin, A.L., Zussman, E. and Kroll, E., *Polymer* (2005) **46**, p. 2889
45. Tomaszewski, W. and Szadkowski, M., *Fibers Textiles E. Eur.* (2005) **13**, p. 22
46. Kim, H.Y., US Patent 6,991,702 (2006)
47. Zhou, H., Green, T.B. and Joo, Y.L., *Polymer* (2006) **47**, p. 7497
48. Um, I.C., Fang, D., Hsiao, B.S., Okamoto, A. and Chu, B., *Biomacromolecules* (2004), **5**, p. 1428
49. Wang, X.F., Um, I.C., Fang, D., Okamoto, A. and Chu, B., *Polymer* (2005) **46**, p. 4853
50. Kelly, A.J., US Patents (a) 4,255,777 (1981), (b) 4,380,786 (1983), (c) 4,630,169 (1986), (d) 5,093,602 (1992), (e) 6,206,307 (2001), (f) 6,227,465 (2001), (g) 6,656,394 (2003), (h) 6,964,385 (2005)
51. Kelly, A.J., *Aerosol Sci. Tech.* (1990) **12**, p. 526
52. Kelly, A.J., *J. Aerosol Sci.* (1994) **25**, p. 1159
53. Lehr, W. and Hiller, W., *J. Electrostatics* (1993) 30, p. 433
54. Shrimpton, J.S. and Yule, A.J., *Exp. Fluids* (1999) **26**, p. 490
55. Kornev, K., Kurtz, S. and Salem, D.R. To be published

2

Producing nanofiber structures by electrospinning for tissue engineering

F. K. K O, The University of British Columbia, Canada and
M. R. G A N D H I, Drexel University, USA

2.1 Introduction

Biocompatible and biodegradable polymeric biomaterials are used to develop biological matrices or scaffolds not only for tissue engineering but also for various biomedical applications including wound dressings, membrane filters and drug delivery. These materials include synthetic polymers such as poly-(lactide-co-glycolide), poly-(lactic acid), poly-(glycolic acid) and poly-(caprolactone) and natural biopolymers such as silk, mussel adhesive protein, keratin, elastin and collagen. The natural materials are of considerable interest due to their structural properties and superior biocompatibility. Electrospinning is a unique method capable of producing nanoscale fibers. We have utilized this technique in our laboratory to fabricate nanofibrous scaffolds from both synthetic as well as natural polymers. The strength of a biomaterial is very important for the design of scaffolds meant for biomedical applications. They should provide the initial framework for the cells to withhold the natural loading conditions. The architecture of an engineered scaffold is also important in the design of a synthetic tissue replacement. Thus scaffolds should mimic the mechanical and geometrical properties of the replacing tissue. We have generated various structures including nonwoven mesh, 3D braided fibers, microspheres and foams as scaffolds for tissue engineering.

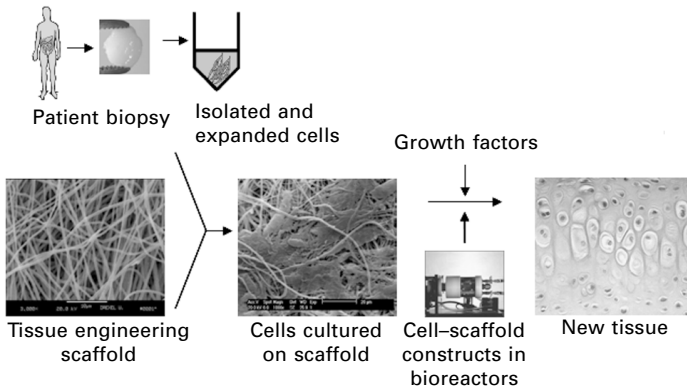### 2.1.1 Tissue engineering concept

Tissue engineering was identified by the United States National Science Foundation some ten years ago as an emerging area of national importance and defined as:[1]

'Tissue Engineering is the application of principles and methods of engineering and the life sciences towards the fundamental understanding of structure/function relationships in normal and pathological mammalian tissues and the development of biological substitutes to restore, maintain or improve functions.'

22

Fueled by the exciting progress made in biotechnology in recent years, tissue engineering is quickly becoming a method of choice for the development of implants in surgery. It is expected that it will become a viable option in the healthcare industry and it is on the verge of breaking into a rapid growth mode in the next decade. For example, in orthopedic reconstruction, surgeons often replace damaged tissue resulting from trauma, pathological degeneration or congenital deformity with autogenous grafts.[1] Reconstructive surgery is based upon the principle of replacing these types of defective tissues with viable, functioning alternatives.

The grafting of bone in skeletal reconstruction has become a common task of the orthopedic surgeon, with over 863 200 grafting procedures performed each year in the United States. For cartilage replacement, there are over 1 000 000 procedures of various types performed each year, and for ligament repairs, there are approximately 90 000 procedures performed per year.[1] Currently, autograft[2,3] (tissue taken from the patient) and allograft[4–6] (tissue taken from a cadaver) are the most common replacement sources for the treatment of musculoskeletal problems. In repair of anterior cruciate ligament injuries, a segment of the patellar tendon has frequently been used.[3] For cartilage and bone repair, transplantation of autogenous grafts has been the current treatment of choice. Unfortunately, these gold standards possess certain disadvantages. For any type of autogenous tissue, the key limitations are donor site morbidity where the remaining tissue at the harvest site is damaged by removal of the graft, and the limited amount of tissue available for harvesting. The use of allograft attempts to alleviate these problems. However, this type of graft is often rejected by the host body because of an immune response to the tissue. Allografts are also capable of transmitting disease. Although a thorough screening process eliminates most of the disease-carrying tissue, this method is not 100% effective.[4] As a result of the limitations with conventional reconstructive graft materials, surgeons have looked to the field of tissue engineering for synthetic alternatives.[1,6–12]

As articulated succinctly by Professors Vacanti and Mikos,[13] the key challenges in tissue engineering are the synthesis of new cell adhesion-specific materials and the development of fabrication methods to produce reproducible 3D synthetic or natural biodegradable polymer scaffolds with tailored properties. These properties include porosity, pore size distribution and connectivity, mechanical properties for load-bearing applications and rate of degradation. Scientists around the globe have tried to address these issues by fabricating a 3D surface having the properties equivalent to the replacing tissue. These artificial 3D matrices, called scaffolds, provide the structural integrity similar to the natural extracellular matrix in the body. The scaffold is then seeded with the cells taken from the patient's normal tissue or from the donor. The cells used for seeding tissue engineered scaffolds can be stem cells or mature adult cells. The biochemical and/or mechanical

*2.1* Concept of tissue engineering.

signals are then provided for the differentiation of the cells into tissues. These signals are mostly in the form of growth factors. Ideally, the tissue will form and the scaffolds will degrade, leaving behind the regenerated tissue. Thus, the classic 'triad' of tissue engineering is based on the three basic tissue components: a *scaffold* on which *cells* are incorporated and *signals* provided to build and differentiate the tissue. Figure 2.1 describes the concept of tissue engineering.

2.1.2   Scaffolds for tissue engineering

It is well known that biological tissues consist of well-organized hierarchical fibrous structures[14] ranging from nanometer to micrometer scale as described in Fig. 2.2. The successful regeneration of biological tissue and organs calls for the development of fibrous structures with fiber architectures conducive to cell deposition and cell proliferation. Of particular interest in tissue engineering is the creation of reproducible and biocompatible 3D scaffold for cell ingrowth, resulting in bio-matrix composites for repair and replacement of various tissues.

A large family of fiber architectures is available for surgical implants (Fig. 2.3). The design and selection of these fiber architectures for tissue engineering can be carried out on the fiber and structural levels resulting in a wide range of dimensional scale, fiber tortuosity and fabric porosity as characterized by the fiber volume fraction-orientation map.[15]

Since the 1950s, many of the textile structures illustrated in Fig. 2.3 have been used for surgical implants with considerable success. Some of the structures and their respective applications are summarized in Table 2.1. These fibrous structures are mostly from non-absorbable polymers consisting of fibers larger than 10 μm in diameter. Unfortunately, these fibers were developed primarily for clothing rather than for medical applications. It is
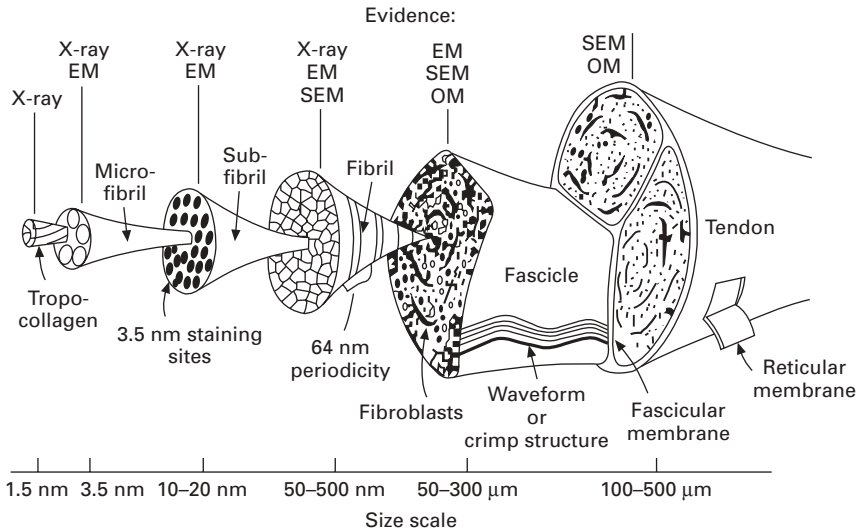
2.2 Hierarchical fiber architecture of tendons (EM, electron microscope; SEM, scanning electron microscope; OM, optical microscope; see Ref. 14 for more details).
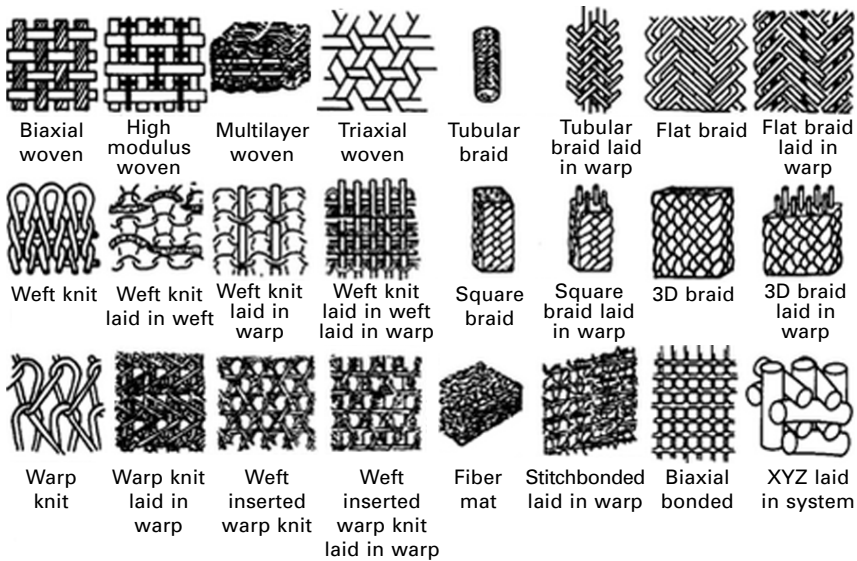
2.3 Fiber architecture for surgical implants (see Ref. 15 for more details).

necessary to build scaffolds that mimic the mechanical properties of the native tissue as they provide the basic 3D mechanical framework for the cells to attach to and proliferate before they can differentiate into a tissue. Not only the mechanical properties but also the hierarchical geometry of the

Table 2.1 Textile structures for surgical implants (see Ref. 16 for more details)

Application	Material	Structure	
		Yarn	Fabric
Arteries	Polyester Dacron 56 Teflon	Textured	Weft/warp knit Straight tube bifurcation Plain woven Straight tube, nonwoven
Tendon	Polyester Dacron 56 Kevlar	Low twist filament	Plain woven narrow tape coated with silicon rubber
Hernia repair	Polypropylene	Monofilament	Tricot jersey knit
Esophagus	Regenerated collagen	Multifilament	Plain weave
Heart valve	Polyester Dacron 56	Multifilament	Plain weave Knit
Patches	Polyester Dacron 56	Textured	Knitted velour
Sutures	Polyester Nylon Collagen Silk	Monofilament Multifilament	Braid Woven tapes
Ligament	Polyester Teflon Polyethylene	Multifilament	Braid
Bone and joints	Carbon in thermoset or thermoplastic matrix	Multifilament	Woven Braid

tissue plays a major role in engineering the design for scaffolds. In the natural tissues the cells are embedded in the extracellular matrix mainly made up of collagen and elastin. The scaffolds for the tissue engineering application should mimic the mechanical properties and hierarchical organization of the natural extracellular matrix. The scaffolds replacing a tissue should be fibrous as well as nanoscale to mimic the natural extracellular matrix.

As stated earlier not only the mechanical properties but also the geometry of the extracellular matrix plays a role in scaffold fabrication. In order to take the 3D and nanofibrous nature of biological tissue into consideration, we have developed an integrated hierarchical design methodology for the manufacturing of scaffolds for tissue engineering. A schematic of the hierarchical structural design of a braided structure fabricated in our laboratory for anterior cruciate ligament is shown in Fig. 2.4.
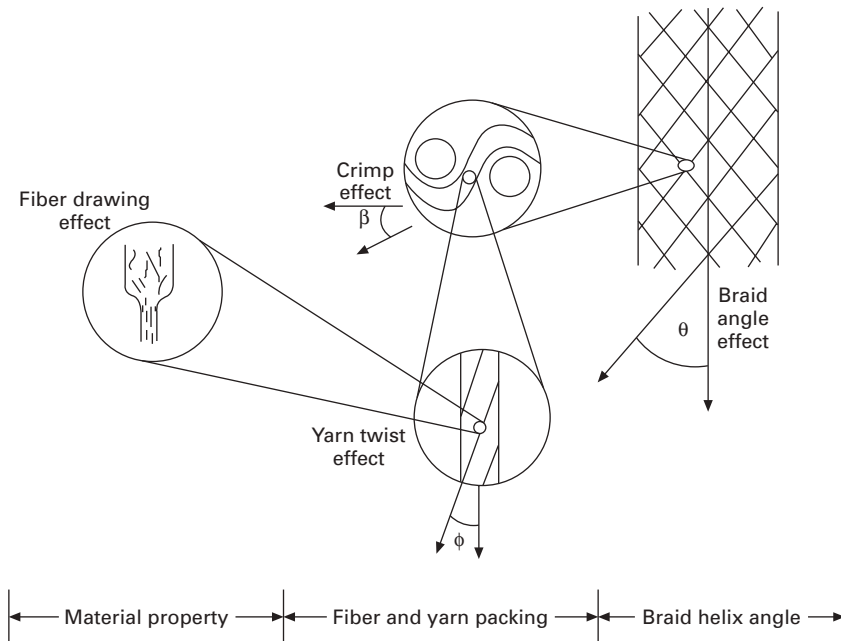
2.4 Structural hierarchy of fibrous assemblies.

2.1.3   Scaffold fabrication and electrospinning procedure

Several methods have been developed to fabricate highly porous biodegradable scaffolds, including fiber bonding, braiding, solvent casting, particle leaching, phase separation, emulsion freeze drying, gas foaming and 3D printing techniques. Using these methods in our laboratory, we have successfully made scaffolds with various geometries including sponges, microspheres, 3D braid and nanofibers. However the simplicity of the electrospinning process to generate nanofibers makes it an ideal process for scaffold fabrication. The further discussion in this chapter will be focused strongly on nanofibrous scaffold fabrication and characterization. In the next sections more specific examples on the use of nanofibrous scaffolds are mentioned followed by a brief description of various experiments conducted in our laboratory. The electrospinning technique is a process of generating ultrafine fibers in the nanometer to micrometer scale.[17–19] In the electrospinning process an electric field is generated between an oppositely charged polymer fluid and a collection screen, the electrode. A polymer solution is added to a glass syringe with a capillary tip. An electrode is placed in the solution with another connection made to a metal screen. As the power is increased, the charged polymer solution is attracted to the screen. Once the voltage reaches a critical value, the charge overcomes the surface tension of the polymer cone formed on the
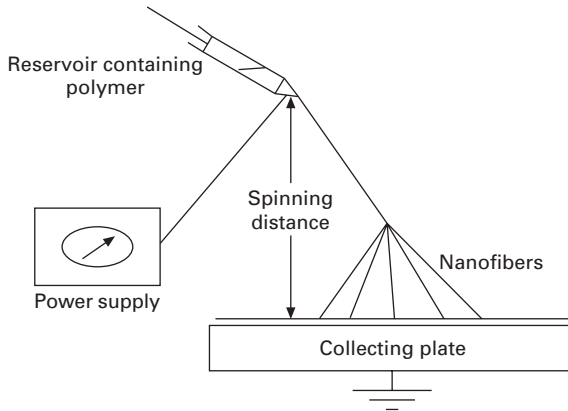
2.5 Schematic of the electrospinning process.

capillary tip of the syringe and a jet of ultrafine fibers is produced. As the charged fibers are splayed, the solvent quickly evaporates and the fibers are accumulated randomly on the surface of the collection screen. This results in a nonwoven mesh of nano- to micrometer scale fibers. A schematic drawing of the electrospinning process is shown in Fig. 2.5.

2.2   Fabrication of nanofibrous scaffolds

2.2.1   Polymeric nanofibers

Tissue engineering scaffolds should have the following characteristics:

- porosity for cell migration;
- balance between surface hydrophilicity and hydrophobicity for cell attachment;
- mechanical properties comparable to natural tissue to withstand natural loading conditions;
- degradation capability so that it gets completely reabsorbed after implantation;
- nontoxic byproducts;
- 3D matrix.

Scientists around the globe have used various biocompatible and biodegradable synthetic polymeric biomaterials including polylactic (PLA) and glycolic acids (PGA), and their copolymers (PLAGA), polycaprolactone, polydioxanone, polyanhydrides, polyorthoester, polytrimethylene carbonate and poly-phosphazene for scaffold fabrication. Various nondegradable materials such as polyester, polypropylene, polytetrafluoroethylene, polyethylene and polycarbonates are used as well. The main advantages of synthetic polymers

are they are available in bulk and their properties are tailorable. However they lack cell recognition signals and sometimes their degraded products may be toxic. PLA, PGA and PLAGA are the most abundantly used polymers for scaffold fabrication. These are US Food and Drug Administration (FDA) approved polymers and their mechanical and degradable properties can be tailored by varying the ratio of PLA to PGA. We have electrospun a number of polymers including PLA, PGA and PLAGA in our laboratory. We have optimized the spinning process by varying the parameters such as choice of solvent, charge density, spinning distance, viscosity, concentration and molecular weight of polymer. Continuous, uniform and nanoscale fibers were produced by the electrospinning process. These electrospun nanofibrous scaffolds have a large surface area to volume ratio, high porosity and a variety of pore size distribution, giving all the important features necessary for ideal tissue engineering scaffolds.

2.2.2   Protein nanofibers

Natural materials such as collagen, elastin, keratin, silk, fibrin clot, chitosan and mussel proteins are ideal candidates for scaffold fabrication. Of particular interest are protein material from silkworm silk and spider silk because of their superior biocompatibility and unique mechanical properties of combined strength and toughness. The big advantages of natural materials over synthetic ones are favorable cell interaction and nontoxic degradation products. The disadvantages include limited supply and restricted design flexibility. Various proteins that we have electrospun are collagen, elastin and silk. Recently our laboratory has done extensive study on silkworm silk and spider silk to fabricate nanofibrous scaffolds.[20–23] Silkworm silk fibers from *Bombyx mori* cocoons were utilized. The silk protein from silkworm silk contains two fibroin proteins held together by a glue-like protein called sericin. Sericin causes T-cell mediated hypersensitivity if introduced in the body. Sericin is removed from the cocoon fibers by a process called degumming. The degummed *Bombyx mori* silk fibers are biocompatible. Silkworm silk, unlike spider silk, is readily available from cocoons but one has to go through a procedure to make it spinnable by the electrospinning process. We have established a protocol to make a spinnable dope from *Bombyx mori* cocoon fibers. Briefly the procedure includes dissolving degummed *Bombyx mori* silk fibers in 50% aqueous $CaCl_2$ and dialyzing it against deionized water. The dialyzed fibroin solution should then be frozen for 24 h at –20 °C and lyophilized to obtain regenerated sponge. This regenerated silk fibroin sponge can be dissolved in the appropriate solvent to carry out electrospinning. As described earlier, silkworm silk is available from cocoons and can be obtained by sericulture. Spider silk has better properties than silkworm silk but it is not possible to grow spiders in a farm because of their cannibalistic nature.

Dragline silk from major ampullate glands of the spider *Nephila clavipes* is a fibrous protein having crystalline regions of anti-parallel β-sheet interspersed with elastic amorphous segments. These two segments are represented by two different proteins, MaSp1 (Major Ampullate Spidroin 1) and MaSp2 (Major Ampullate Spidroin 2), coded by different genes. Nexia Biotechnologies Inc. in 1999 introduced an innovative technology of using a transgenic approach for large-scale production of spider silk. They produced recombinant spider silk, Biosteel[R] in the BELE[R] (Breed Early Lactate Early) goat system. The milk produced by transgenic goats contained MaSp1 and MaSp2 proteins which can be isolated and purified to homogeneity. We have electrospun MaSp1 and MaSp2 in our laboratory to generate nanofibrous scaffolds.

2.2.3 Nanocomposite nanofibers

Sometimes it is necessary to have more than one material in nanofibers to mimic the structural and mechanical properties of the natural extracellular matrix. This can be done by a process called co-electrospinning, whereby blends of two different materials are electrospun to fabricate the scaffolds. Depending on the application one can make blends of different polymers or proteins or a combination of both. In our laboratory we have carried out extensive work on nanocomposite nanofibers fabricated from carbon nanotubes (CNTs). CNTs are a layer of graphite, one atom thick, rolled into a cylinder. CNT has a Young's modulus in the order of 1 TPa.[24–26] The toughness of CNT ranges from 6 to 30%. Incorporation of CNTs in polymeric and/or protein scaffolds not only improves the mechanical properties but gives unique electrical conductivity as well. We have fabricated co-electrospun scaffolds from various proteins, polymers and CNT.

2.3   Characterization of nanofibrous scaffolds

2.3.1 Porosity and pore size distribution

In the remaining sections we will discuss the findings of different experiments carried out in our laboratory to demonstrate various concepts. In one such experiment we fabricated three scaffolds from PLAGA. These were: (1) 150–300 μm PLAGA sintered spheres; (2) 3D braided structure consisting of 20 bundles of 20 μm filaments of PLAGA; and (3) electrospun nanofibrous scaffolds from PLAGA. The porosity of these scaffolds was characterized by mercury porosimetry measurement to characterize their pore size distributions. The detailed description of fabrication techniques of these scaffolds can be obtained from various papers.[18,27–29] The concept we want to demonstrate here is the differences in porosity and pore size distribution of these scaffolds having different architectures. The pore size and distribution were characterized using a Micrometrics Autopore III porosimeter. As shown in Fig. 2.6, a

Log differential intrusion vs diameter
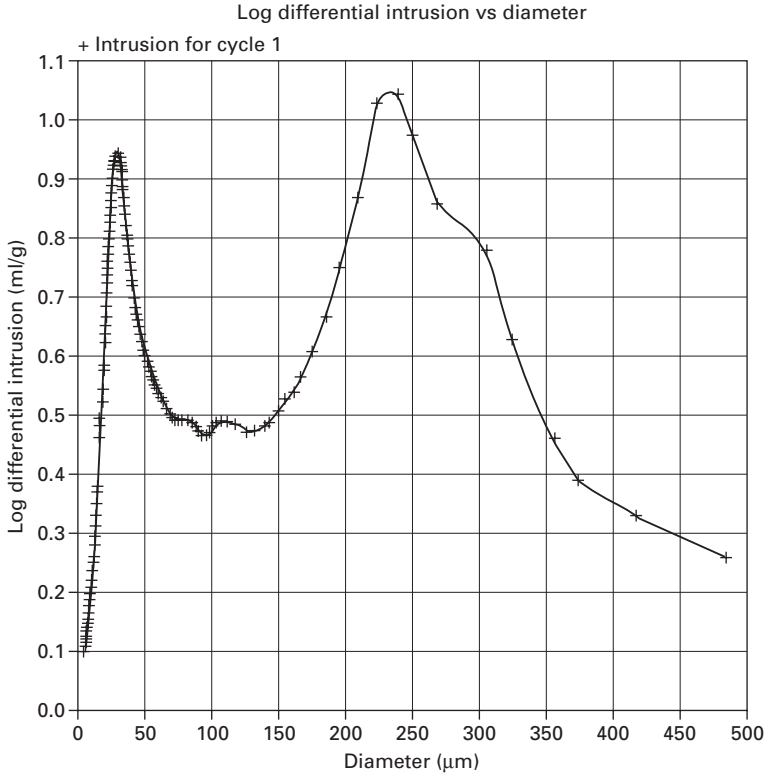
2.6 Pore size distribution of braided structure.

bimodal distribution of pores was observed for the 3D braided structures showing the existence of large interstitial pores of the order of 250 μm and interfiber pores having a diameter of the order of 30 μm. On the other extreme, as shown in Fig. 2.7, the nanofiber structures show a predominant concentration of pores with an average pore size of 14 μm. The pore surface of the nanofibrous structures was $0.823\,m^2/g$, an order of magnitude greater than that in the 3D braided structure at $0.0045\,m^2/g$. The sintered spheres show a single mode pore diameter distribution over the range of 200–600 μm as shown in Fig. 2.8, depending on the sphere diameter.

2.3.2 Morphology and fiber diameter distribution

In this section we will discuss our experiment with electrospun spider silk proteins. The MaSp1 and MaSp2 proteins obtained from Nexia Biotechnologies were dissolved in various ratios (1:0, 1:1, 1:3, 3:1, 0:1) in an appropriate solvent to prepare the spinning dope for electrospinning. The spinning dope was placed in a 3 ml syringe (18-G and spinning angle 45°). The tip-to-

Log differential intrusion vs diameter

+ Intrusion for cycle 1
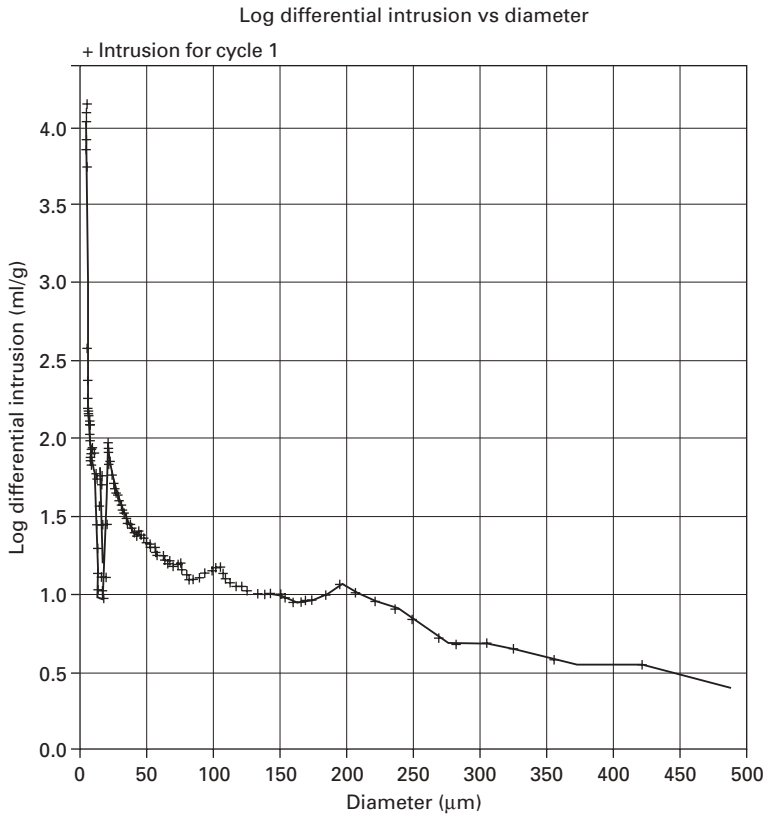
2.7 Pore size distribution of nanofibrous structure.

collection plate (covered with aluminum foil) distance was varied from 5 to 10 cm. The electric field applied between the collecting plate (cathode) and the needle tip (anode) ranged from 1 to 6 kV/cm. The morphology of the gold sputtered electrospun fibers was examined and their diameters were determined by field emission environmental scanning electron microscope (Phillips XL-30 ESEM). The average fiber diameter and its distribution were determined based on 100 random measurements. Figure 2.9 shows the morphology and fiber diameter distribution of silk fibers at 10 cm spinning distance and electric field of 3 kV/cm. A 12% concentration of MaSp1 at these conditions produced continuous uniform fibers with diameter 100.7 ± 36.43 nm. MaSp2 was spinnable at these conditions but produced beads at 12% with fiber diameter of 28.7 ± 17.48. The 3:1 ratio of MaSp1 to MaSp2 was spinnable at 12% but for 1:1 and 1:3, the viscosity was too high and the concentration had to be reduced to 10% and 6% respectively to obtain continuous and uniform fibers. A 3:1 ratio at 12% concentration, 10 cm spinning distance and charge density of 3 kV/cm produced fibers with diameter

Log differential intrusion vs diameter
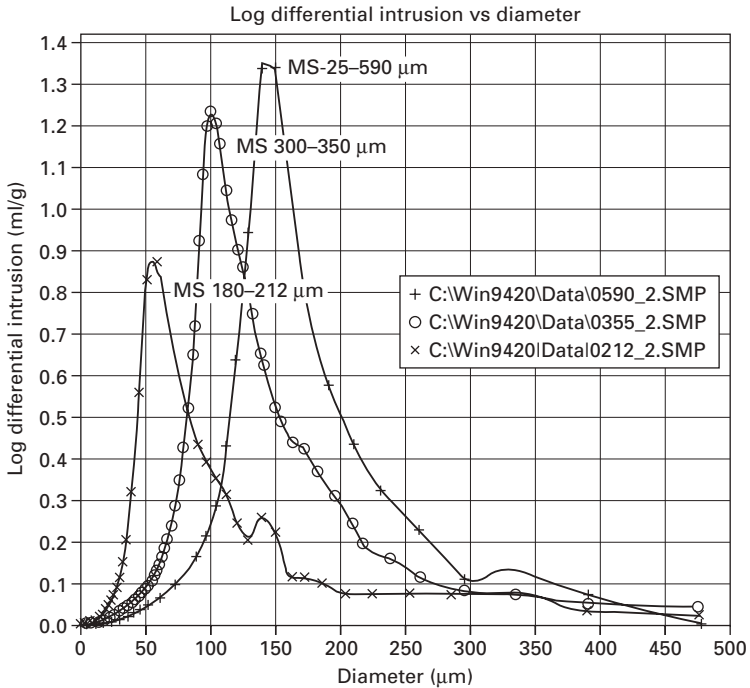
2.8 Pore size distribution of sintered spheres.

of 81.1 ± 29.73 nm. A 1:1 ratio at 10% concentration, 10 cm spinning distance and electric field of 3 kV/cm generated 63.3 ± 25.17 nm size fibers and 1:3 ratio at 6% concentration, 10 cm spinning distance and electric field of 3 kV/cm delivered fibers with diameter of 57.4 ± 25.75 nm. This experiment demonstrates the importance of optimization techniques that need to be carried out during electrospinning in order to generate continuous, uniform nanoscale fibrous scaffolds. The fiber diameter can be controlled by varying the processing parameters such as solution concentration, viscosity, applied charge and charge density, type of solvent employed, distance from tip of capillary to the collection plate, flow rate, diameter and angle of spin of the spinneret.
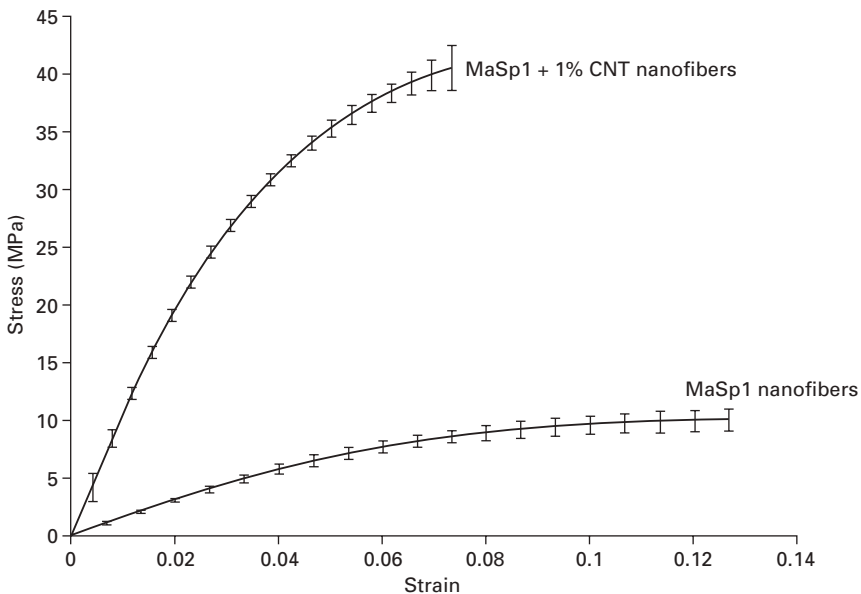
2.3.3   Tensile properties

We will again discuss our experiment with spider silk. For this experiment we co-electrospun spider silk protein and 1% CNT. Aligned nanofibers were generated using MaSp1 and 1% CNT. We calculated tensile properties of aligned MaSp1 nanofibers with and without CNT. The mechanical properties of fibers were determined by KES-G1 Kawabata micro tensile tester at the
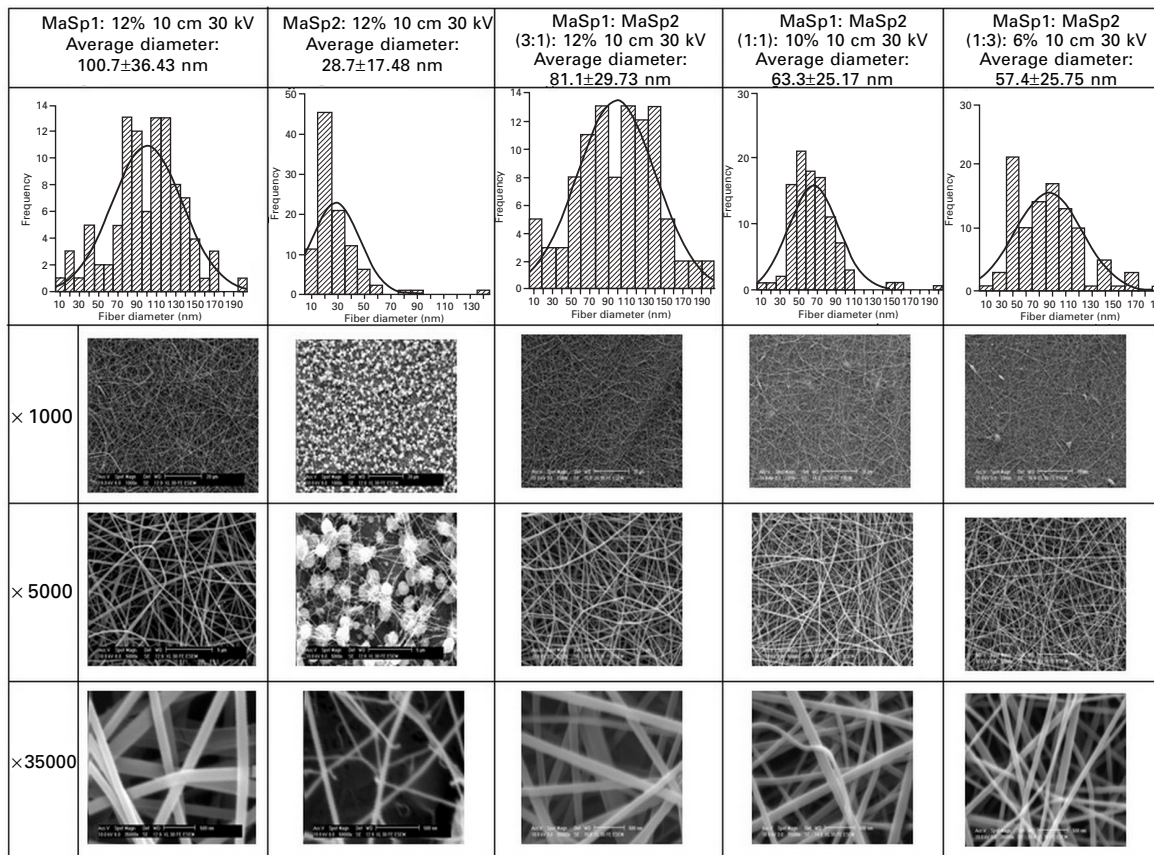
2.9 Fiber morphology and diameter distribution of electrospun spider silk.

elongation rate of 0.2 mm/s. The aligned fibers were rolled into a yarn. The 4 cm long sample was glued from both sides on a paper frame having 1 cm length. This gives us the gauge length of about 3 cm. These samples were then mounted on a Kawabata micro tensile machine and the tensile properties were measured from the average of five samples. The modulus of MaSp1 nanofibers was 123.29 MPa. The ultimate tensile stress was found to be 9.59 MPa and the elongation at break was 14.33%. The incorporation of 1% CNT improves the mechanical properties significantly. The modulus of MaSp1 with 1% CNT was 1004.36 MPa. The ultimate tensile stress increased to 40.74 MPa; however elongation at break was reduced to 7.39%. Figure 2.10 shows the stress–strain curve generated from the average of five samples. This experiment demonstrates the concept of co-electrospinning protein with CNT and thereby improving the mechanical properties. In spite of the significant improvement of mechanical properties of the pristine MaSp1 silk by the addition of 1% CNT, we feel that we still have not made use of the expected potential of CNT. Considering the modulus of MaSp1 as 100 MPa and CNT as 1 TPa, if we apply the rule of mixture for the properties of composite material then the modulus of MaSp1 with 1% CNT should be ~10 000 MPa. Our experimental results indicated that the modulus of the composite silk was 1000 MPa. This means that the silk could be made even stronger. We can improve the efficiency of property translation from the CNT to the silk matrix by improving the interfacial bonding between the CNT and the matrix.

*2.10* Tensile properties of aligned MaSp1 with and without CNT.

Further improvement can be made by improving the alignment of CNTs within the MaSp1 matrix and the alignment of the nanofibrils. A better dispersion of the CNT will facilitate the alignment of the CNT, and the functionalization of the CNT will promote a higher level of bonding between the CNT and the silk matrix.

2.3.4   Other specific characterization techniques

Characterization techniques to be employed for nanofibrous scaffolds is one of the most important and rapidly growing fields of tissue engineering. Morphology and fiber diameter distribution can be characterized by environmental scanning electron microscope. Porosity can be determined by mercury porosimeter. We need to know the mechanical properties of our scaffolds. Thus our scaffolds should pass through a battery of characterization before we can test them with cell culture. Apart from the characterization methods described here there are many other investigations that we need to carry out depending on the scaffolds. For example if we co-electrospin our material with CNT we need to know whether these CNTs are inside the fiber or on the surface. Raman spectroscopy provides a good way of determining this. Transmission electron microscopy can also be used to locate CNTs in the nanocomposite. The structure and composition of a material can be characterized by Fourier transform infrared spectrometry and X-ray diffraction study. Figure 2.11 shows the Raman spectroscopy of electrospun MaSp1 with and without CNT. The electrospun MaSp1 having 1% CNT showed characteristic Raman peaks of CNT between 195 and 270 cm^{-1}, indicating radio breathing mode, and 1570 and 1593 cm^{-1}, indicating tangential mode for CNT. This confirms successful incorporation of CNT in nanocomposite fibers.

2.4   Cell–scaffold interaction

To study the effect of CNT and fiber size on cell proliferation, silkworm silk natural micrometer sized fibers, silkworm silk nanofibers with and without CNT and spider silk nanofibers with and without CNT were used. Human chondrosarcoma cells (ATCC HTB94) were maintained in culture using DMEM (Dulbecco's modified Eagle's medium; Mediatech) supplemented with 10% fetal bovine serum (FBS), 1% penicillin-streptomycin and 1% L-glutamine. For cell seeding on scaffolds, cells from the tissue culture flasks were trypsinized for 5 minutes at 37 °C, neutralized with DMEM, centrifuged for 5 minutes at 1200 rpm and resuspended in DMEM. A sum of 1 000 000 cells was seeded per scaffold over 48 hours on a shaker at 37 °C. The culture medium was supplemented with ascorbic acid (40 μg/ml) on the first day. The cell–scaffold constructs were maintained in the culture environment and
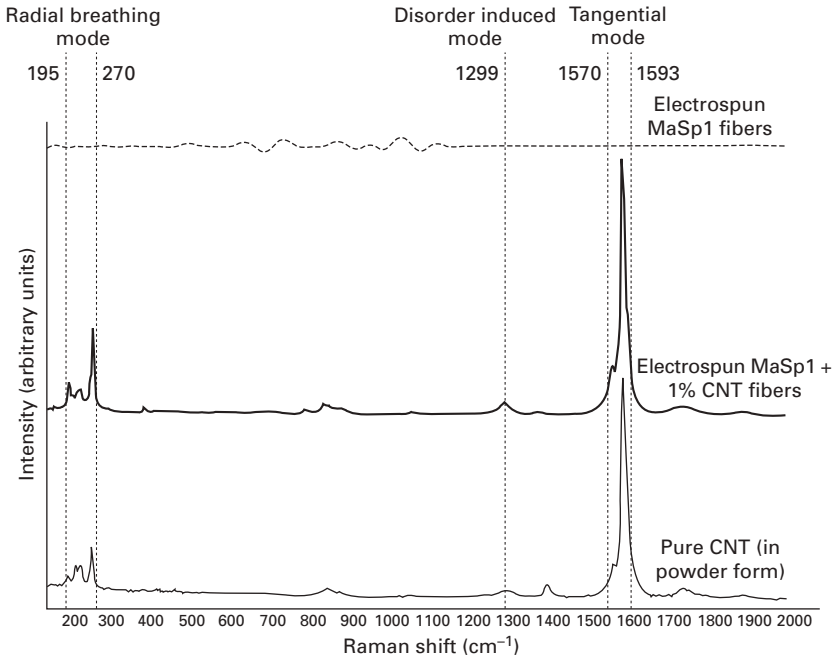
2.11 Raman spectra of electrospun MaSp1 fibers with and without CNT confirming successful incorporation of CNT in the composite fiber.

were studied for morphology and proliferation on days 3, 7 and 14. They were removed from the culture media on 3, 7 and 14 days. They were washed twice with 1× phosphate buffered saline (PBS) and then subjected to a gradient of ethanol (20%, 50%, 70%, 90%, 100%), each for 10 min. They were refrigerated overnight at 4 °C. The scaffolds were immediately coated with palladium. The morphology of cells on scaffolds was examined by Phillips XL-30 ESEM. A cell proliferation assay was carried out at 3, 7 and 14 days. Scaffolds being assayed were fed incubated for 2.5 h with serum-free media supplemented with 3-(4,5-dimethylthiazol-2-yl)-2,5-diphenyltetrazolium bromide solution (MTT). The concentration used was 2.5 mg MTT/ml of 1× PBS. The scaffolds were then vortexed with 500 μl acidic isopropanol (0.04 M HCl in absolute isopropanol). The intensity of 200 μl of this solution was measured at 595 nm.
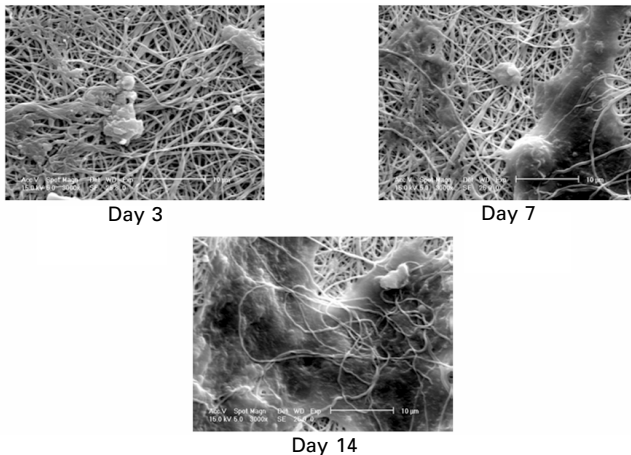
2.4.1 Co-electrospinning effect

Figure 2.12 shows the morphology of cells after 3, 7 and 14 days on spider silk nanofibers. Figure 2.13 shows the morphology on spider silk nanofibers with 1% CNT. On day 3 the cells were attached to the nanofibrous scaffolds
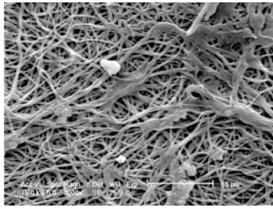
Day 3

Day 7

Day 14
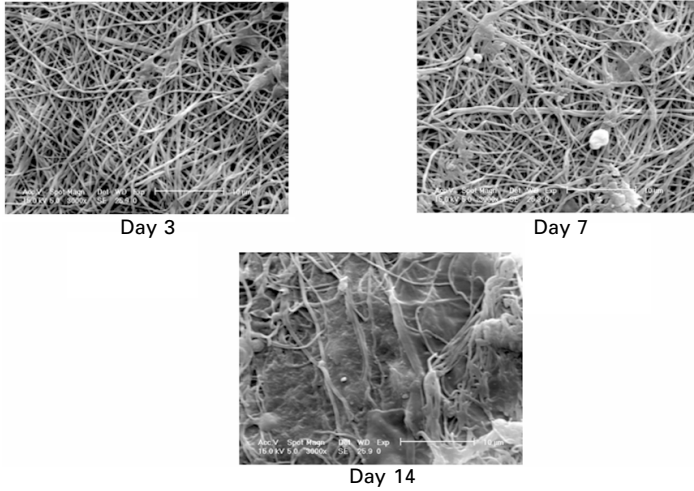
2.12 Morphology of cells after 3, 7 and 14 days on spider silk nanofibers.
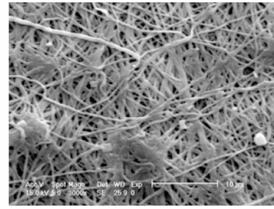

Day 3

Day 7

Day 14

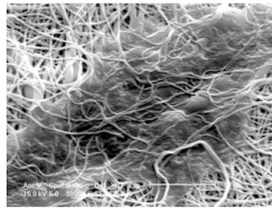*2.13* Morphology of cells after 3, 7 and 14 days on spider silk nanofibers with 1% CNT.

which acted as a support, providing a 3D framework for cells. The cells migrated and proliferated over time and that was evident by the production of extracellular matrix. By day 7 there were more cells and they formed bridges over the nanofiber scaffolds. The entire scaffold was covered with the cells by day 14. Overall, there were fewer cells on the scaffolds having CNT but the morphology remained the same. Figure 2.14 shows the morphology of cells after 3, 7 and 14 days on silkworm nanofibers. Figure 2.15 shows the morphology on silkworm nanofibers with 1% CNT.
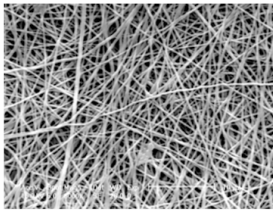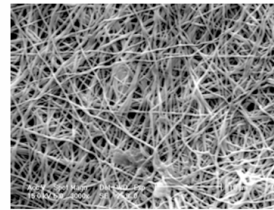
Day 3

Day 7

Day 14
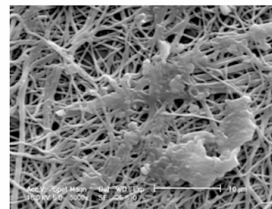
2.14 Morphology of cells after 3, 7 and 14 days on silkworm nanofibers.

Day 3

Day 7

Day 14

2.15 Morphology of cells after 3, 7 and 14 days on silkworm nanofibers with 1% CNT.

2.4.2   Size effect

The cells were able to proliferate over the micrometer-sized natural cocoon fibers but the morphology was significantly different (Fig. 2.16). The cells were not able to attach and spread well on microfibers. They were seen rotated around the fiber whereas on nanofibers they were attached over the number of fibers and were able to spread and make contacts with underlying
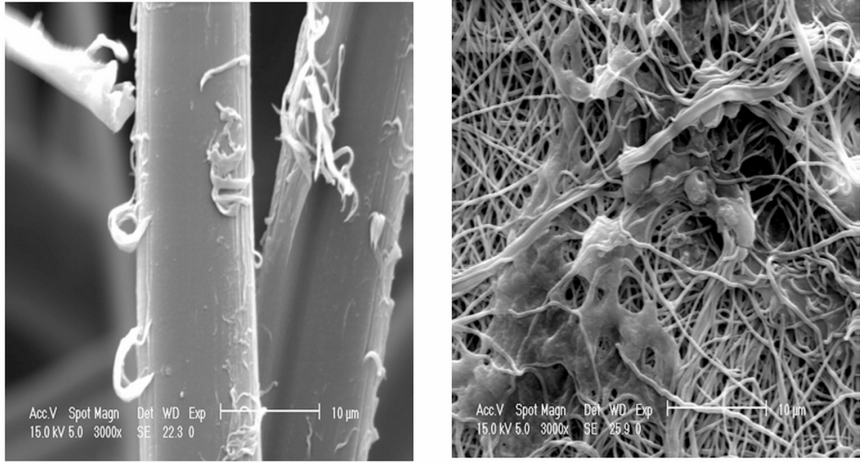
Natural silk fibers (micrometer size)   Nanofibers

2.16 Morphology of cells on natural silkworm silk fibers and nanofibers after 7 days in culture.
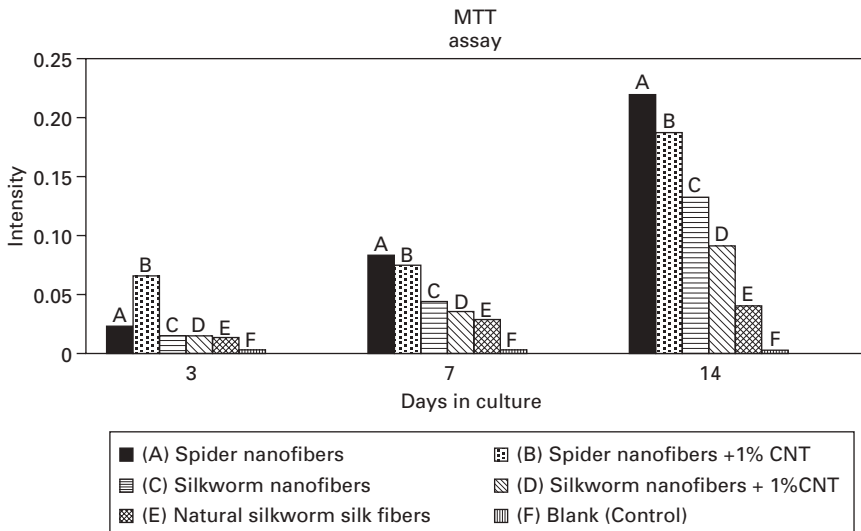

2.17 Cell proliferation (MTT) assay.

nanofibers. Figure 2.17 shows the result of MTT assay. It can be seen that the nanofibers had the maximum number of cells after 14 days in culture compared with the micrometer-sized fibers. Also, incorporation of CNT did not change the cell proliferation significantly. This study shows the importance of nanofibers over microfibers. The tissue engineering scaffolds act as an artificial extracellular matrix until the cells start producing their own. During

this time cells should attach, migrate and proliferate over the scaffolds. The nanofiber scaffolds from silk have a greater advantage over the micrometer-sized natural fibers. The study also proved that nanofibers with 1% CNT supported cell attachment and proliferation.

2.4.3   Architecture effect

The three types of scaffolds described in Section 2.3.1 were used to study the cell–scaffold interaction on different architectures of scaffolds. Osteoblasts isolated from neonatal rat calvarias and grown to confluence in Ham's F-12 medium (GIBCO), supplemented with 12% Sigma's fetal bovine were seeded on all three scaffolds: (1) 150–300 μm PLAGA sintered spheres, (2) 3D braided structure consisting of 20 bundles of 20 μm filaments of PLAGA and (3) electrospun nanofibrous scaffolds from PLAGA. Briefly, cells were seeded on the UV sterilized PLAGA matrices at a density of 100 000 cells/ cm^2. The osteoblasts were cultured on the scaffolds for durations ranging from 1 to 21 days. They were prepared according to established procedures by fixing in gluteraldehyde and dehydrated through a series of ethanol dilutions. The seeded cells were labeled with [^{3}H]-thymidine and the thymidine uptake were measured at 1, 3, 7, 10 and 11 day intervals. The cell proliferation, as shown in Fig. 2.18, is expressed in terms of the amount of [^{3}H]-thymidine uptake as a function of time. It can be seen that there is a consistent increase in cell population with time. The nanofibrous structure demonstrated the most cell growth whereas the tightly woven 3D braided structure showed the least proliferation. On the other hand, the cell growth on fused microsphere structure is between that of the 3D braid and the nanofibrous structures showing a surprising drop after the 10th day.
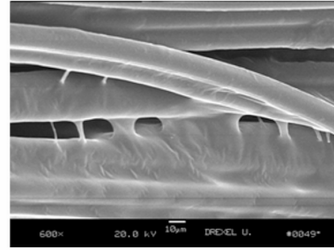
Scanning electron microscopy pictures are shown in Fig. 2.19. It can be seen that, in responding to the large spheres wherein the cells are more than 10× smaller than the spheres (Fig. 2.19a), the cells tend to spread over the
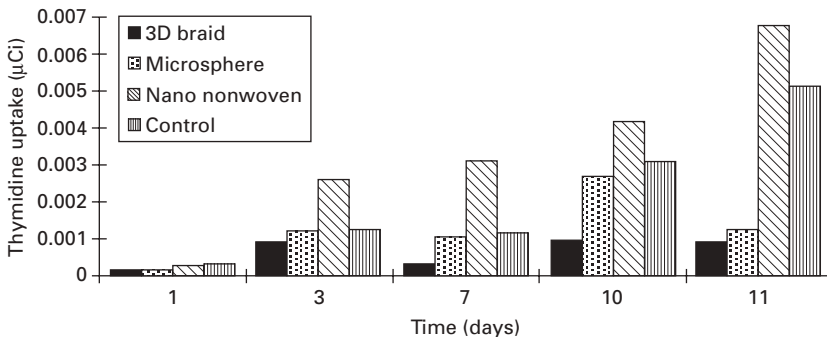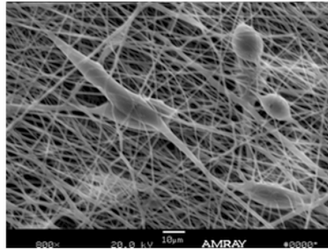

2.18 Cell proliferation of fibrous scaffolds.
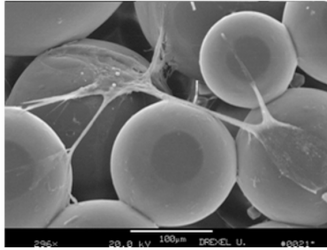
(a) Microspheres

(b) 3D braid

(c) Nanofibers

2.19 Cell–fiber architecture interaction.

surface of the sphere before connecting to the adjacent spheres and eventually forming an interconnected cellular network. In the case of 20 μm filaments in unidirectional bundles and 3D braid (Fig. 2.19b) wherein the cells are about the same order of magnitude in dimension, the cell–matrix reaction appears to be similar. The cells tend to slide off the matrix at the moment of seeding. Those cells that remain on the surface of the substrates tend to grow around the filaments and bridge onto the adjacent filaments along the length. The most intensive cell deposition was seen in the nanofibrous structure (Fig. 2.19c). Extensive cell spreading was observed along the length of the fibrils and through the thickness.

2.5   Summary and conclusion

Tissue engineering is a rapidly growing field wherein cells either from the patient or a donor are seeded on an artificial scaffold made up of protein or polymer. It is a good alternative to traditional options. Nanoscale fibrous materials are the ideal candidates for tissue engineering scaffolds because of their high surface area to volume ratio, greater porosity and pore size distribution. Electrospinning is a simple method to generate nanofibrous scaffolds. The scaffolds from natural protein material have better biocompatibility as the degraded products are nontoxic. Silk protein has a clear advantage over other natural resources because of a unique combination

of strength and toughness. One can incorporate carbon nanotubes in the scaffolds and increase mechanical properties and electrical conductivity without much harm to cell proliferation.

2.6   Acknowledgments

2.7   References

1. R. Skalak, C.F. Fox and Y.C. Fung. Preface, in *Tissue Engineering*, edited by R. Skalak and C.F. Fox. Proceedings of NSF workshop on Tissue Engineering, Granlibakken, Lake Tahoe, California, Feb. 26–29, 1988.
2. R. Langer and J.P. Vacanti. *Science* **260**, 920 (1993).
3. O.H. Friedman, J.M. Sherman, *et al*. *Clin. Ortho*. **196**, 9 (1985).
4. G.E. Jackson, R. Windler and T.M. Simon. *Amer. J. Sports Med*. **18**, 1 (1990).
5. A.R. Gadzag, J.M. Lane, D. Glaser and R.A. Forster. *J. Amer. Acad. Ortho. Surg*. **3**, 1 (1995).
6. M. Shino, S. Inoue, *et al*. *J. Bone Joint Surg*. **70B**, 556 (1988).
7. D.W. Jackson, J.T. Heinrich, M. Timothy and M.S. Simon. *Arthroscopy* **10**, 442 (1994).
8. M.A. Attawia, J.E. Devin and C.T. Laurencin. *J. Biomed. Mater. Res*. **29**, 843 (1995).
9. C.N. Cornell. *Tech. Orthop*. **7**, 55 (1992).
10. D.W. Jackson, Ed. *The Anterior Cruciate Ligament: Current and Future Concepts*. Raven Press: New York; 1993.
11. C.B. Frank, S.L.-Y. Woo, T. Andriacchi, *et al*. *Injury and Repair of the Musculoskeletal Soft Tissues*, edited by S.L.Y. Woo and J.A. Buckwalter. American Academy of Orthopaedic Surgeons: Park Ridge; 1988, p. 45.
12. R.P. Lanza, R. Langer and W.L. Chick, Eds. *Principles of Tissue Engineering*. R.G. Landes Company and Academic Press, Inc.: San Diego, CA; 1997.
13. C.A. Vacanti and A.G. Mikos. Letter from the Editors, *Tissue Engineering*, Vol. **1**, (1) (1995).
14. J. Kastelic, A. Galeski and E. Baer. *J. Connective Tissue Res*. **6**, 11–23 (1978).
15. F.K. Ko. *Ceramic Bull*. February (1989).
16. F.K. Ko. *Textile Asia* April (1997).
17. A. Formhals. US Patent 1,975,504 (1934).
18. F.K. Ko, C.T. Laurencin, M.D. Borden and D. Reneker. 'The dynamics of cell–fiber architecture interaction,' Proceedings, Annual Meeting, Biomaterials Research Society, San Diego, April, 1998.
19. J. Doshi and D. Reneker. *J Electrostatics* **35**, 151 (1995).
20. J. Ayutsede *et al. Biomacromolecules* **7**, 208 (2006).
21. J. Ayutsede *et al. Polymer* **46**, 1625 (2005).

22. S. Sukigara, M. Gandhi, J. Ayutsede, M. Micklus and F. Ko. *Polymer* **44**, 5721 (2003).
23. S. Sukigara, M. Gandhi, J. Ayutsede, M. Micklus and F. Ko. *Polymer* **45**, 3701 (2004).
24. J.P. Lu *et al*. *Phys. Rev. Lett.* **79**, 1297 (1997).
25. A. Krishnan *et al*. *Phys. Rev. B.* **58**, 14013 (1998).
26. E.W. Wong *et al*. *Science* **277**, 1971 (1997).
27. F.K. Ko. Three dimensional fabrics for composites, in *Textile Structural Composites*, Edited by T.W. Chou and F.K. Ko. Elsevier: Amsterdam; 1989.
28. M. Borden, S.F. El-Amin, M. Attawia and C.T. Laurencin. *Biomaterials* **24**, 597 (2003).
29. W.J. Li, C.T. Laurencin, E.J. Caterson, R.S. Tuan and F.K. Ko. *J. Biomed. Mater. Res.* **60**, 613 (2002).

3
Continuous yarns from electrospun nanofibers

E. SMIT, U. BÜTTNER and R. D. SANDERSON,
Stellenbosch University, South Africa

3.1 Introduction

Electrospinning is a simple but extremely versatile method for obtaining continuous nano- and microfibers of natural and synthetic polymers, as well as of inorganic oxide materials. The process itself has been discussed in the first two chapters. Additional information for the interested reader can be found in reviews on the topic.[1,2]

   The focus of this chapter is on the manufacture of continuous yarns from electrospun fibers. Section 3.2 provides a brief overview of the potential applications of electrospun fiber yarns and some important textile terms related to this field. The importance of, and the underlying principles related to, controlling fiber orientation during electrospinning will then be discussed in Section 3.3. Section 3.4 describes how some of the principles of controlling fiber orientation during electrospinning have been applied for obtaining short or noncontinuous yarns. The different approaches taken to obtain continuous yarns from electrospun fibers are discussed in Section 3.5. Section 3.6 includes a discussion of some likely future trends in the field and a short review of some sources of further information is given in Section 3.7.

3.2 Using electrospun nanofibers: background and terminology

The three inherent properties of nanofibrous materials that make them very attractive for numerous applications are their high specific surface area (surface area/unit mass), high aspect ratio (length/diameter) and their biomimicking potential. These properties lead to the potential application of electrospun fibers in such diverse fields as high-performance filters, absorbent textiles, fiber-reinforced composites, biomedical textiles for wound dressings, tissue scaffolding and drug-release materials, nano- and microelectronic devices, electromagnetic shielding, photovoltaic devices and high-performance electrodes, as well as a range of nanofiber-based sensors.

45

In many of these applications the alignment, or controlled orientation, of the electrospun fibers is of great importance and large-scale commercialization of products will become viable only when sufficient control over fiber orientation can be obtained at high production rates. In the past few years research groups around the world have been focusing their attention on obtaining electrospun fibers in the form of yarns of continuous single nanofibers or uniaxial fiber bundles. Succeeding in this will allow the processing of nanofibers by traditional textile processing methods such as weaving, knitting and embroidery. This, in turn, not only will allow the significant commercialization of several of the applications cited above, but will also open the door to many other exciting new applications.

Incorporating nanofibers into traditional textiles creates several opportunities. In the first instance, the replacement of only a small percentage of the fibers or yarns in a traditional textile fabric with yarns of similar diameter, but now made up of several thousands of nanofibers, can significantly increase the toughness and specific surface area of the fabric without increasing its overall mass. Alternatively, the complete fabric can even be made from nanofiber yarns. This has important implications in protective clothing applications, where lightweight, breathable fabrics with protection against extreme temperatures, ballistics, and chemical or biological agents are often required. On an aesthetic level, nanofiber textiles also exhibit extremely soft handling characteristics and have been proposed for use in the production of artificial leather and artificial cashmere.

In biomedical applications the similarity between certain electrospun polymeric nanofibers and the naturally occurring nanofibrous structures of connective tissues such as collagen and elastin gives rise to the opportunity of creating artificial biomimicking wound dressings and tissue engineering scaffolds. Several studies on nonwoven nanofiber webs of biocompatible polymers such as poly(ε-caprolactone),[3] poly(lactide-co-glycolide),[4] poly(L-lactic acid),[5] collagen[6] and regenerated silkworm silk[7] have already shown potential in this area. Simple three-dimensional constructs for vascular prostheses have also been manufactured by electrospinning onto preformed templates.[8] Although these initial studies show that enhanced cell adhesion, cell proliferation and scaffold vascularization can be obtained on porous, nonwoven nanofiber webs, the simplicity of the constructs and the fragile nature of nonwoven webs still limit their applicability to small areas.

Creating complex three-dimensional scaffold structures with fibers aligned in a controlled fashion along the directions of the forces that are usually present in dynamic tissue environments, as for instance in muscles and tendons, will lead to significant improvements in the performance of tissue engineering scaffolds. With continuous nanofiber yarns it will become possible to create such aligned fiber structures on a large scale, simply by weaving. In addition, the age-old techniques of knitting and embroidery can then be applied to

create very complicated, three-dimensional scaffolds, with precisely controlled porosity, and yarns placed exactly along the lines of dynamic force.

Several other fields will also benefit from the availability of continuous yarns from electrospun fibers. Owing to the high fiber-aspect ratios and increased fiber–matrix adhesion caused by the high specific surface areas, aligned nanofiber yarns can lead to stronger and tougher, lightweight, fiber-reinforced composite materials. The incorporation of nanofiber-based sensors into textiles can lead to new opportunities in the fields of smart and electronic textiles. Aligned nanofiber yarns of piezo-electric polymers and other micro-actuator materials may lead to better performance in advanced robotics applications.

Since the revival of electrospinning in the early 1990s, several research groups have worked on controlling the orientation of electrospun fibers. This is an important step on the road towards obtaining aligned nanofiber yarns and will be discussed in more detail in Section 3.3. A number of approaches to obtaining yarns from electrospun fibers have already been proposed in the open literature and will be discussed in greater detail in Sections 3.4 and 3.5. First, however, a brief discussion on terminology is required.

Those who have worked in the field of electrospinning over the past decade have come from various disciplinary backgrounds, including physics, chemistry and polymer science, chemical and mechanical engineering, and also from the traditional textiles field. The result of this has been that literature on the topic of electrospinning, and especially yarns from electrospun fibers, is plagued with terminology from different disciplines, which often leads to misunderstanding and even self-contradictory statements. So, for instance, in a paper on the electrospinning of individual fibers of a novel polymer some authors might use the term *yarn* when they are actually referring to an individual *fiber*, or authors might refer to spinning a *filament* when they are actually spinning a *yarn*.

In an attempt to avoid this kind of confusion, the authors propose the use of generally accepted terminology from the textiles industry. Some of the terms used in the following sections are defined below.

- **Fiber** – a single piece of a solid material, which is flexible and fine, and has a high aspect ratio (length/diameter ratio).
- **Filament** – a single fiber of indefinite length.
- **Tow** – an untwisted assembly of a large number of filaments; tows are cut up to produce staple fibers.
- **Sliver** – an assembly of fibers in continuous form without twist. The assembly of staple fibers, after carding but before twisting, is also known as a sliver.
- **Yarn** – a generic term for a continuous strand of textile fibers or filaments in a form suitable for knitting, weaving or otherwise intertwining to form a fabric.

- **Staple fiber** – short-length fibers, as distinct from continuous filaments, which are twisted together (spun) to form a coherent yarn. Most natural fibers are staple fibers, the main exception being silk which is a filament yarn. Most artificial staple fibers are produced in this form by slicing up a tow of continuous filaments.
- **Staple fiber yarn** – a yarn consisting of twisted together (spun) staple fibers.
- **Filament yarn** – a yarn normally consisting of a bundle of continuous filaments. The term also includes monofilaments.
- **Core-spun yarn** – a yarn consisting of an inner core yarn surrounded by staple fibers. A core-spun yarn combines the strength and/or elongation of the core thread and the characteristics of the staple fibers that form the surface.
- **Denier** – a measure of linear density: the weight in grams of 9000 meters of yarn.
- **Tex –** another measure of linear density: the weight in grams of 1000 meters of yarn.

3.3   Controlling fiber orientation

As stated in the previous section, achieving control over the orientation of electrospun fibers is an important step towards many of their potential applications. However, if one considers the fact that fiber formation occurs at very high rates (several hundreds of meters of fiber per second) and that the fiber formation process coincides with a very complicated three-dimensional whipping of the polymer jet (caused by electrostatic bending instability), it becomes clear that controlling the orientation of fibers formed by electrospinning is no simple task.

Various mechanical and electrostatic approaches have been taken in efforts to control fiber alignment. The two most successful methods are the following:

- *Spinning onto a rapidly rotating surface* – several research groups have been routinely utilizing this technique to obtain reasonably aligned fibers.[9–12] The rapid rotation of a drum or disk and coinciding high linear velocity of the collector surface allows fast take-up of the electrospun fibers as they are formed. The 'point-to-plane' configuration of the electric field does, however, lead to fiber orientations that deviate from the preferred orientation. A special instance of the rotating drum set-up involves spinning onto a rapidly rotating sharp-edged wheel, which utilizes an additional electrostatic effect, since the sharp edge of the wheel creates a stronger converging electrostatic field, or a 'point-to-point' configuration, which has a focusing effect on the collected fibers (see Fig. 3.1). This in turn leads to better alignment of the fibers.[13]
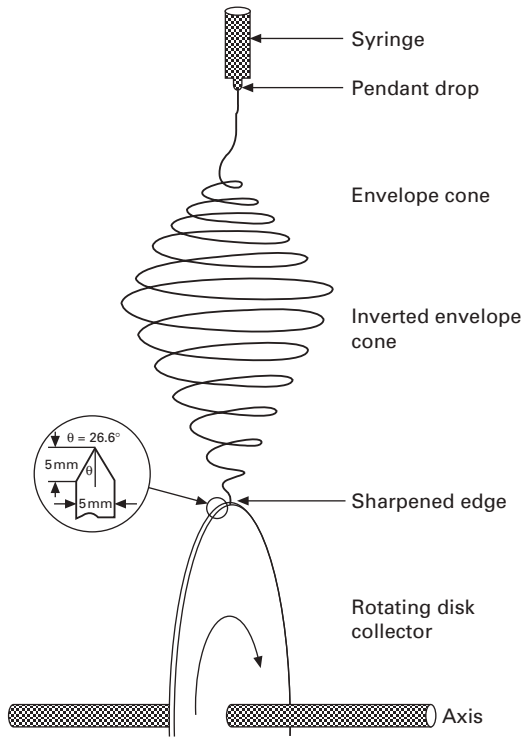
3.1 Converging electrostatic field on sharp-edged wheel electrode. Reprinted from reference 1. Copyright (2003), with permission from Elsevier.

- *The gap alignment effect* – uniaxially aligned arrays of electrospun fibers can be obtained through the gap alignment effect, which occurs when charged electrospun fibers are deposited onto a collector that consists of two electrically conductive substrates, separated by an insulating gap. This electrostatic effect (see Fig. 3.2) has been observed by various groups.[1,14,15] Recently this was investigated in more detail by Li *et al.*[16–18] Briefly, the lowest energy configuration for an array of highly charged fibers between two conductive substrates, separated by an insulating gap, is obtained when fibers align parallel to each other.

3.4   Producing noncontinuous or short yarns

Both spinning onto a rapidly rotating collector and the gap alignment effect have been used to obtain short yarns for experimental purposes.
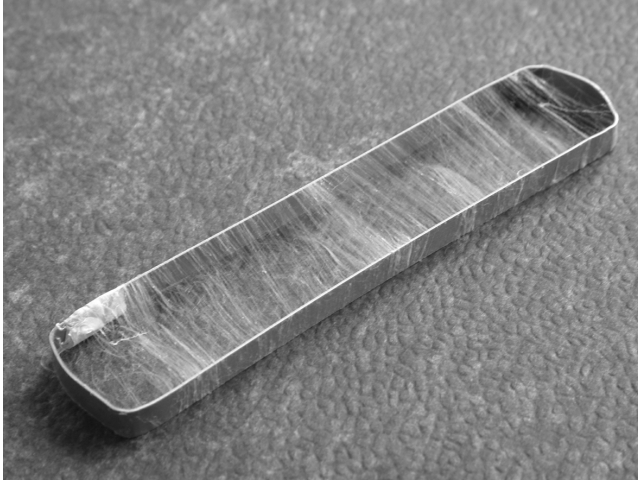
3.2 Aligned fibers obtained through the gap alignment effect. Reprinted from reference 14 and kindly supplied by R. Dersch. Copyright (2003), with permission from John Wiley & Sons Inc.

Rings of aligned nanofibers
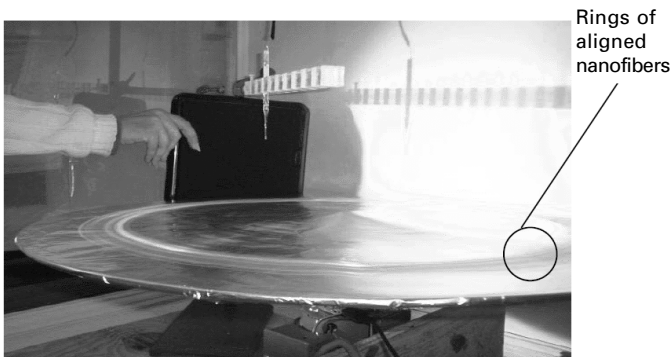
3.3 Aligned fiber tows on rotating disk collector. Reprinted with permission from reference 19 with kind permission from the author.

3.4.1   Rotating collector method

In work performed at Drexel University[19] poly(ethylene oxide) (PEO) fibers were spun onto a rapidly rotating disk (Fig. 3.3), where the shearing force of the rotating disk led to aligned fibrous assemblies with good orientation. These oriented fibers could then be collected and manually twisted into a yarn (Fig. 3.4).

Fennessey and Farris[20] collected tows of aligned polyacrylonitrile (PAN) fibers using a rotating drum set-up. The tows, measuring *ca*. 32 cm × 2 cm, were then linked together and twisted using a Roberta-type electric twister.

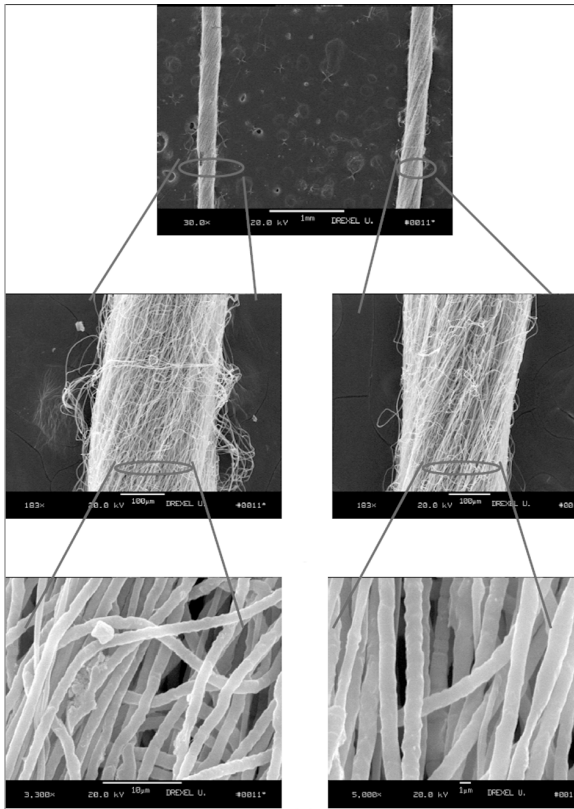*3.4* Twisted yarns obtained from tows spun on a rotating disk collector. Reprinted with permission from reference 19 with kind permission from the author.

Twisted yarns of PAN nanofibers with twist angles of between 1.1° and 16.8° were prepared, with a denier between 326 and 618 and an average denier of 446. The stress–strain behaviour of the yarns was examined and the modulus, ultimate strength and elongation at the ultimate strength were measured as a function of twist angle.

3.4.2   Gap alignment method

Deitzel *et al.*[21,22] made short yarns by quickly passing a wooden frame through the electrospinning jet several times (for up to an hour), in a process also known as 'combing', resulting in a tow of reasonably aligned fibers, which were then 'gently twisted' to form a yarn. Fong *et al.*[23] also used the combing technique, by rapidly oscillating a grounded frame within the jet.

Dalton *et al.*[24] used a modified version of the gap method of alignment by electrospinning poly(ε-caprolactone) onto two parallel grounded rings that
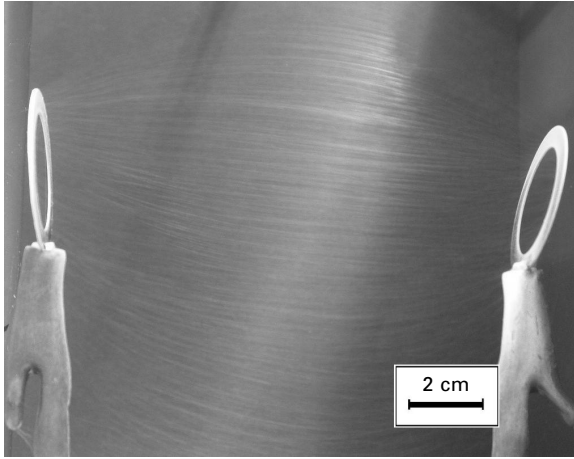
3.5 Fibers aligned between two parallel ring collectors. Reprinted from reference 24 and kindly supplied by P. D. Dalton. Copyright (2005), with permission from Elsevier.
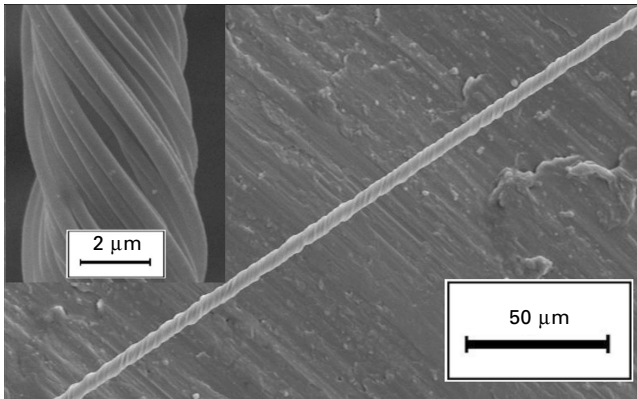
3.6 Twisted poly(ε-caprolactone) yarn. Reprinted from reference 24 and kindly supplied by P. D. Dalton. Copyright (2005), with permission from Elsevier.

were placed 80 mm horizontally apart (Fig. 3.5), resulting in 1.26 μm diameter fibers, neatly aligned between the two rings. When one of the collection rings was rotated at high speed, a wound multifilament yarn with a diameter of less than 5 μm and a length of 50 mm was obtained (Fig. 3.6).

3.5   Producing continuous yarns

A common misconception in recent electrospinning literature is that the first literature on electrospinning dates back to 1934 when Formhals patented a

method for manufacturing yarns from electrospun fibers.[25] Some of the first publications on electrospinning date back as far as 1902, when first Cooley[26] and then Morton[27] patented processes for dispersing fluids. In both patents, the authors describe processes for producing very fine artificial fibers by delivering a solution of a fiber-forming material, such as pyroxylin, a nitrated form of cellulose, dissolved in alcohol or ether, into a strong electric field. The reason for this oversight is unclear, but it could possibly be blamed on differences in terminology since the term 'electrospinning' has only become popular with the revival of the process in the mid-1990s.

Another more puzzling oversight, which has recently led several authors to bemoan the lack of processes for making continuous yarns from electrospun fibers, is that Formhals actually registered a series of seven patents over a period of ten years between 1934 and 1944[25,28–33] and that all these patents describe processes and/or improvements to processes for the manufacture of continuous yarns from electrospun fibers. Since the youngest of these patents is more than 60 years old, one could speculate that these processes did not really work, which would explain the absence of commercially available electrospun fiber yarns. An alternative explanation could be that, since Formhals lived in Mainz, Germany, and since the last patent application was filed in 1940, the disruption of World War II and the ensuing years simply led to the processes being forgotten. Closer inspection of the patents, aided by more recent knowledge of the electrospinning process, also leads us to believe that at least some of the described processes are viable and that they deserve further consideration. The patents of Formhals show a gradual evolution of his yarn production process over time and in many instances he applied the same fundamental practical aspects of electrospinning that have re-occurred in the recent literature. These included obtaining aligned fibers by spinning onto conductive strips or rods that were separated in space from each other by an insulating material (gap alignment effect), increasing production rates by using multiple spinnerets, regulating the electric field between the source and the collector by adding additional electrostatic elements, using corona discharge to discharge the electrospun fibers, and post-treating the electrospun fibers by submerging them in a liquid bath.

The fact that a recent patent[34] (discussed in Section 3.5.2) closely resembles the first process patented by Formhals in 1934 also supports the viability of his patents and so our group is currently re-evaluating the processes disclosed in the patents; results will be forthcoming in future publications. For the sake of comprehensiveness, the Formhals processes are included in the following discussion. At present, there are 13 different methods for making continuous yarns from electrospun fibers discussed in the open literature. Formhals patented four of these methods between 1934 and 1944, while the other nine appeared only after 2001.

3.5.1   Rotating dual-collector yarn

Formhals's original patent[25] relates to the manufacture of slivers of cellulose acetate fibers by electrospinning from a cogwheel source onto various collector set-ups. In these collector set-ups fibers are first spun onto a rotating collector and then removed in a continuous fashion, onto a second take-up roller. The first of these collector set-ups consisted of a solid conductive wheel or ring with string attached to the edge. In this set-up the wheel was rotated for a short period while fibers were spun onto its edge. The process was then stopped, the string was loosened and then drawn over rollers and/or through twist-imparting rings to a second take-up roller, and the spinning process restarted. The newly spun sliver or semi-twisted yarn was then drawn off continuously onto the second take-up roller. Another collector set-up consisted of a looped metal belt with fixtures to push or blow the fiber sliver off the belt before the fiber sliver was collected on a second take-up roller. The concept of using multiple spinnerets for increasing production rates was also introduced in this patent.

Formhals later identified several problems related to his first design and hence in subsequent patents he made various additions and/or alterations to the original design, which were intended to eliminate these problems. These problems and their solutions included the following:

- *Problem*: Fibers flying to-and-fro between the source and the collector. *Solution*: In his second patent,[28] Formhals claimed that one cause of the fibers flying to-and-fro between the jet and collector was that the collector was at too high a voltage of opposite polarity and that resulting corona discharge from the collector reversed the charge of the fibers while they were passing between the jet and the collector. This in turn caused them to change direction and fly back to the source. He proposed to eliminate this problem by adding a voltage regulator on the collector-side of the circuit in order to down-regulate the voltage of the collector.
- *Problem*: Fibers not drying sufficiently between source and collector. *Solution*: Formhals later designed various additions to his spinning system for regulating the shape and intensity of the electrical field in the vicinity of the spinning source.[30] This was done in order to direct the formed fibers along a longer, predetermined and constant path towards the collecting electrode and was achieved by placing, in close proximity to the fiber-stream, conductive strips, wires, plates and screens, which were connected to the same potential as the fiber source. These additions allowed a more thorough drying of fibers before they were deposited on the collector.

An additional problem, which is not specifically discussed in Formhals's patents, but which can be foreseen when examining his first collector design,[25] is that fiber alignment would be less than ideal when spinning onto a solid

wheel or belt. It appears, however, that Formhals did encounter this problem and that he overcame it by utilizing the gap alignment effect in the design of subsequent collectors. The design consisted of a picket-fence-like belt, with individual, pointed electrodes, separated from each other by an air gap.

3.5.2   Multi-collector yarn

In this patented process from the Korea Research Institute of Chemical Technology,[34] continuous slivers or twisted yarns of different polymers, but especially of polyamide–polyimide copolymers, are claimed to be obtained by electrospinning first onto one stationary or rotating plate or conductive mesh collector, where the charges on the fibers are neutralized, and then continuously collecting the fibers from the first onto a second rotating collector. A diagram depicting the process is given in Fig. 3.7. The underlying principle of this process closely resembles the rotating dual-collector yarn process patented by Formhals in 1934.[25]

3.5.3   Core-spun yarn

In his 1940 patent,[31] Formhals described a method for making composite yarns by electrospinning onto existing cotton, wool or other pre-formed yarn. It was also proposed that a sliver of fibers, such as wool, could be coated with the electrospun fibers before twisting the product into an intimately blended yarn.
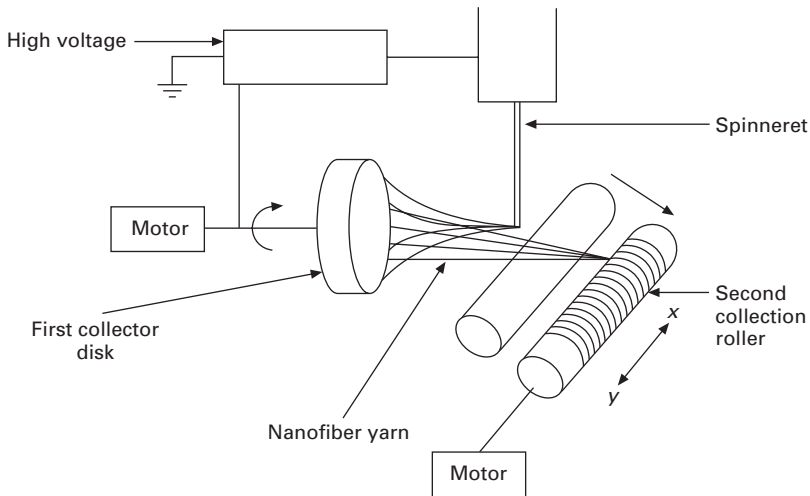
3.7 Multi-collector yarn process diagram. Reprinted from reference 34. Copyright (2005), with permission from Korea Research Institute of Chemical Technology.

3.5.4   Staple fiber yarn

Formhals developed a method for controlling the length of the electrospun fibers,[29] with the main objective being to manufacture fibers with a controlled and comparatively short length. This goal was achieved by modulating the electric field using a spark gap. In this modulation, it was preferable to periodically switch the field strength to at least 35% and preferably 20% of its original voltage in order to interrupt the electrospinning process for a short period and thereby create a sliver of short fibers, which could then be spun into a staple fiber yarn.

3.5.5   Continuous filament yarn

Instead of spinning directly onto the counter-electrode, Formhals altered the process[33] so that the polarity of the charge on the fibers was changed *before* reaching the counter-electrode. This was achieved by using high voltage of opposite polarity on a sharp-edged or thin wire counter-electrode. The high voltage led to corona discharge, which initially reduced and eventually inverted the charge on the fiber while it was travelling from the source to the collector. This caused the fibers to turn away from the collector electrode and they could then be intercepted at a point below the counter-electrode and rolled up as a continuous filament yarn on a take-up roller. In a final improvement on the system, the entire spinning apparatus was encased in a box with earthed conductive siding.[32] This avoided build-up of charges in the panels, which could lead to disturbance of the electric field inside the spinning chamber and disruption of the spinning process. In addition, variable voltage power on the source and collector electrodes allowed the tuning and moving of the position of the neutral zone in which the yarn formation process takes place, which in turn allowed better control over the continuity of the spinning process.

3.5.6   Self-assembled yarn

The self-assembled yarn process was developed by Ko *et al.* at Drexel University.[19, 35, 36] When a solution of pure PAN, or a PAN-containing polymer blend, was electrospun onto a solid conductive collector under appropriate conditions, the fibers did not deposit on the collector in the form of a flat nonwoven web as is usually observed. Instead, initial fibers deposited on a relatively small area of the collector and then subsequent fibers started accumulating on top of them and then on top of each other, forming a self-assembled yarn structure that rapidly grew upwards from the collector towards the spinneret. The formation of a self-assembled yarn is illustrated in Fig. 3.8. The self-assembling yarn, suspended in the space between the spinneret

3.8 Self-assembled yarn formation. Reprinted with permission from reference 19 with kind permission from the author.

and the collector, continued to grow in this fashion until it reached a critical point somewhere in the vicinity of the spinneret. At this critical point, a branched tree-like fiber structure formed and newly formed fibers deposited on the branches of the tree. The yarn could then be collected by slowly taking up the fibers collected on one of the tree branch structures, or by slowly moving the target electrode away from the spinneret. Post-processing of the yarn, including twisting, could be done in a second step.

Ali[36] proposed that the charge on the electrospun PAN fibers, which is induced through the high voltage in the spinneret, is dissipated through the evaporation of the solvent during the electrospinning process, so that the fibers are essentially neutral when they reach the collector electrode. This could explain why the initial fibers deposit on such a small area on the collector. If the fibers on the collector are charged, they repel incoming fibers leading to an expanding random web. Neutral fibers would not have the same repelling effect on incoming fibers and so the fibers would collect on a smaller area. Neutral fibers, deposited on top of each other, and therefore closer to the spinneret than the target electrode surface, also form an attractive

target for incoming fibers. This would explain why subsequent fibers selectively deposit on the tip of the self-assembling yarn.

3.5.7   Conical collector yarn

A method for the production of poly(ε-caprolactone) hollow fibers by the electrospinning process was reported by Kim *et al.*[37] The conventional electrospinning device was modified to include a conical collector and an air-suction orifice to generate hollow and void-containing, uniaxially aligned electrospun fibers. Use of the conical collector allowed for the collection of aligned yarns with diameters of approximately 157 µm.

3.5.8   Spin-bath collector yarn

In this recently published method, developed by our group at Stellenbosch University,[38] continuous uniaxial fiber bundle yarns are obtained by electrospinning onto the surface of a liquid reservoir counter-electrode. The web of electrospun fibers, which forms on the surface of the spin-bath, is drawn at low linear velocity (*ca.* 0.05 m/s) over the liquid surface and onto a take-up roller. A diagrammatic representation of the electrospinning set-up is given in Fig. 3.9. All the yarns obtained using this method exhibit very high degrees of fiber alignment (see Fig. 3.10) and bent fiber loops are observed in all the yarns.

The process of yarn formation is illustrated in Fig. 3.11. It can be described in three phases. In the first phase, a flat web of randomly looped fibers forms
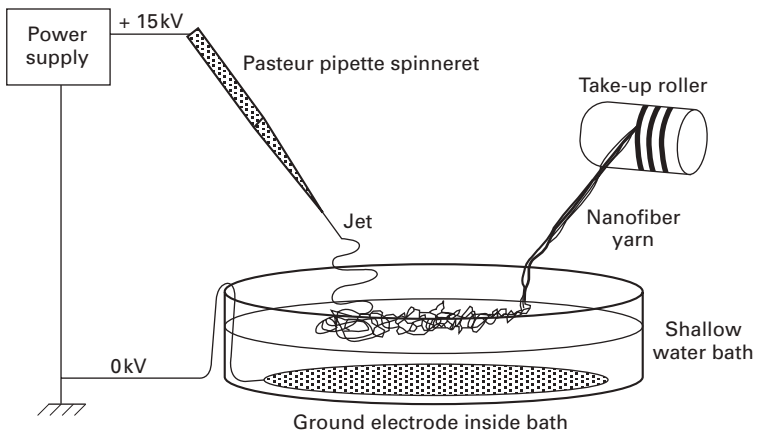
3.9 Yarn-spinning set-up with grounded spin-bath collector electrode. Reprinted from reference 38. Copyright (2005), with permission from Elsevier.
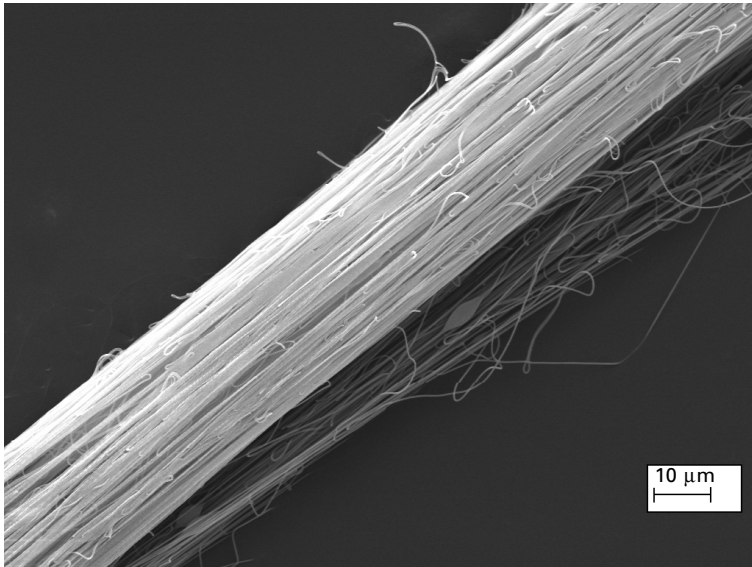
3.10 Electrospun fiber yarn of poly(vinyl acetate) showing high degree of fiber alignment.
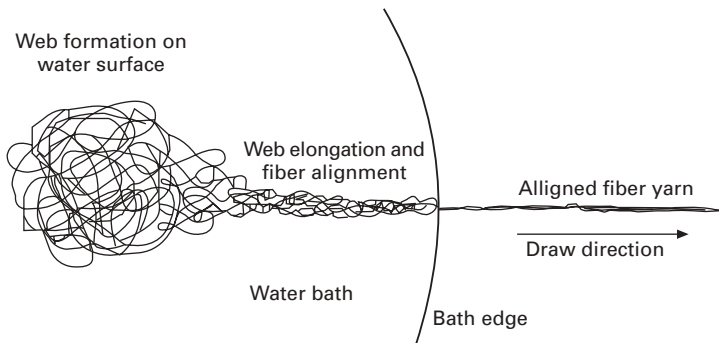

3.11 Top view of the yarn formation process. Reprinted from reference 38. Copyright (2005), with permission from Elsevier.

on the surface of the liquid. In the second phase, when the fibers are drawn over or through the liquid, the web is elongated and alignment of the fibers takes place in the drawing direction. The third phase consists of drawing the web off the liquid and into air. The surface tension of the remaining liquid on the web pulls the fibers together into a three-dimensional, round yarn structure.

The average yarn obtained in a single-spinneret electrospinning set-up contains approximately 3720 fibers per cross-section and approximately 180 m of yarn can be spun per hour. The yarns obtained are very fine, with calculated linear densities in the order of 10.1 denier. Figure 3.12 shows a comparison
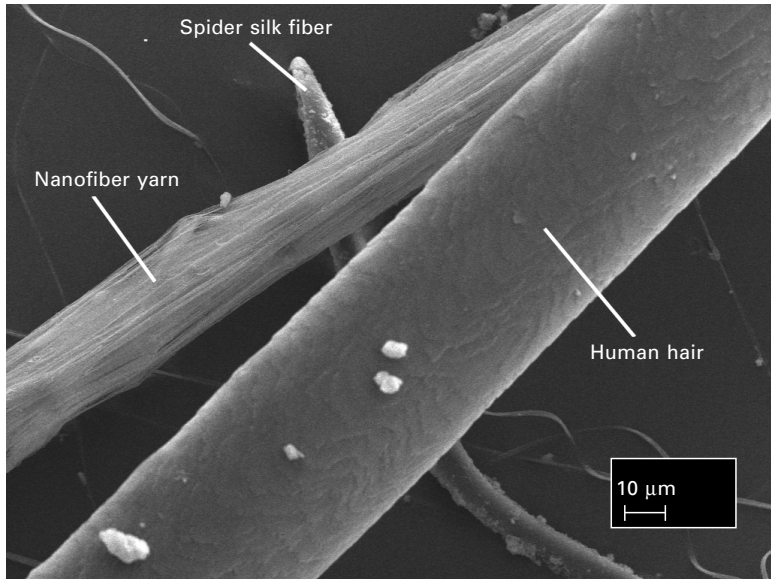
3.12 Relative sizes of nanofiber yarn, spider silk fiber and human hair.

between the nanofiber yarn, a spider silk fiber and a human hair. Although higher linear densities can be obtained by reducing the yarn take-up rate, this is accompanied by a decrease in fiber alignment within the yarn. Currently investigations are focused on various options to overcome these challenges by, for instance, combining aligned yarns from multiple spinnerets into single yarns.

3.5.9   Twisted nonwoven web yarn

This method, patented by Raisio Chemicals Korea Inc.,[39] involves electrospinning nanofibers through multiple nozzles to obtain a nonwoven nanofiber web, either directly in a ribbon form or in a larger form, which is then cut into ribbons, and subsequently passing the nanofiber web ribbons through an air twister to obtain a twisted nanofiber yarn. A diagram depicting the process is given in Fig. 3.13. Table 3.1 shows process variables and yarn characteristics for three polymer yarns that have been spun through this process.

3.5.10   Grooved belt collector yarn

In a recent patent by Kim and Park,[40] a ribbon-shaped nanofiber web is prepared by electrospinning onto a collector consisting of an endless belt-
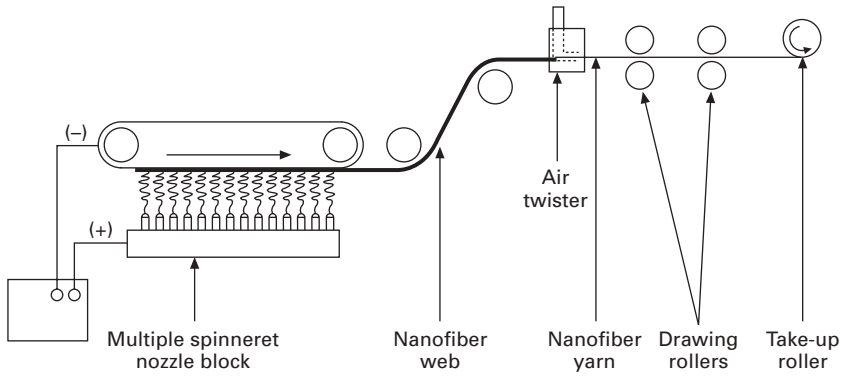
3.13 Spinning process used to prepare a twisted nonwoven web yarn. Reprinted from reference 39. Copyright (2005), with permission from inventor.

Table 3.1 Process variables and yarn characteristics of twisted nonwoven web yarns

Polymer	Poly(ε-caprolactone) M_w = 80 000	70% Polyurethane (M_w = 80 000), 30% PVC (n = 800)	Nylon-6
Solvent	75:25 (v/v) methylene chloride/DMF	5:5 (v/v) DMF/THF	Formic acid
Concentration (wt%)	13	12.5	15
Unit width of web (cm)	2.5	60 cm wide web cut to 2 cm ribbons	1.8
Number of nozzles in block	800	400	1000
Throughput rate per nozzle (mg/min)	1.6	2.0	1.2
Yarn twist rate (turns/m)	60	45	80
Drawing elongation (times)	2	1.2	2
Yarn production rate (m/min)	64.2	30	50
Fineness (denier)	75	120	75
Strength (g/denier)	1.3	1.4	3.0
Elongation (%)	32	50	36

DMF, *N*, *N*-dimethyl formamide; THF, tetrahydrofuran.

type nonconductive plate with grooves formed at regular intervals along a lengthwise direction and a conductive plate inserted into the grooves of the nonconductive plate. The nanofiber webs are electrospun onto the conductive

Table 3.2 Characteristics of grooved belt collector yarns

Polymer	Nylon	70% Polyurethane (M_w = 80 000), 30% PVC (n = 800)
Linear density (denier)	75	75
Strength (g/denier)	4.5	3.4
Elongation (%)	42	45
Nanofiber diameter (nm)	186	480

plates in the grooves and later separated from the collector, focused, drawn and wound into a yarn. Table 3.2 shows yarn characteristics of two yarns made through this process.
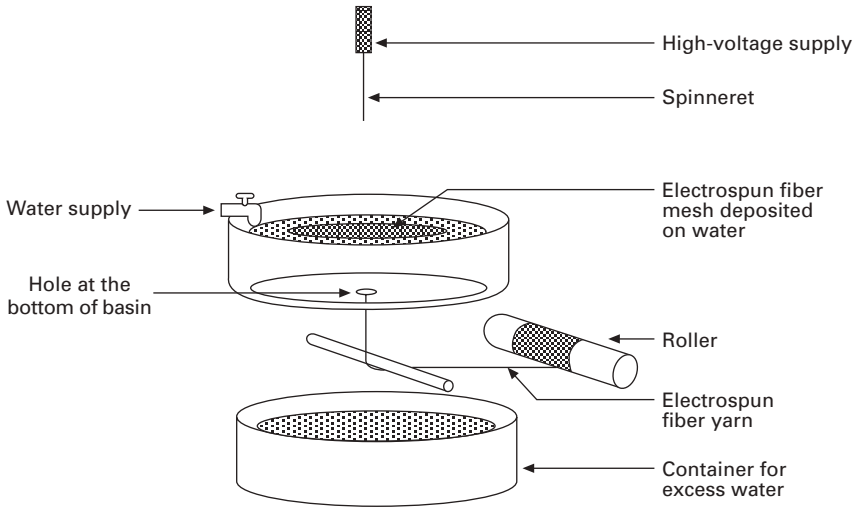
3.5.11 Vortex bath collector yarn

In this patent pending process developed at the National University of Singapore,[41] a basin with a hole at the bottom is used to allow water to flow out in such a manner that a vortex is created on the water surface. Electrospinning is carried out over the top of the basin so that electrospun fibers are continuously deposited on the surface of the water. Owing to the presence of the vortex, the deposited fibers are drawn into a bundle as they flow through the water vortex. Generally, a higher feed rate or multiple spinnerets are required to deliver sufficient fibers on the surface of the water so that the resultant fiber yarn has sufficient strength to withstand the drawing and winding process. Figure 3.14 shows the set-up used for the yarn drawing process.

Yarn drawing speeds as high as 80 m/min have been achieved and yarns made of poly(vinylidene fluoride) (PVDF) and polycaprolactone have been fabricated using this process. Figure 3.15 shows a PVDF yarn formed through this process. The diameter of the yarn is dependent on the amount of fibers deposited on the surface of the water, the diameter of the fibers that make up the yarn as well as the speed of water flowing through the hole.

3.5.12 Gap-separated rotating rod yarn

This method developed by Doiphode and Reneker at the University of Akron[42] utilizes the gap alignment effect in a very similar way to the work published by Dalton *et al.*[24] discussed in Section 3.4. The process is described with reference to Fig. 3.16. Fibers are electrospun between a 2 mm metal rod on the right and a hollow 25 mm metal rod with a hollow hemisphere attached to its end on the left. Both the geometries are grounded and placed at a distance of a few centimeters. Fibers are collected across the gap between

3.14 Vortex bath collector yarn process. Reprinted with permission and kindly supplied by W. E. Teo and S. Ramakrishna.
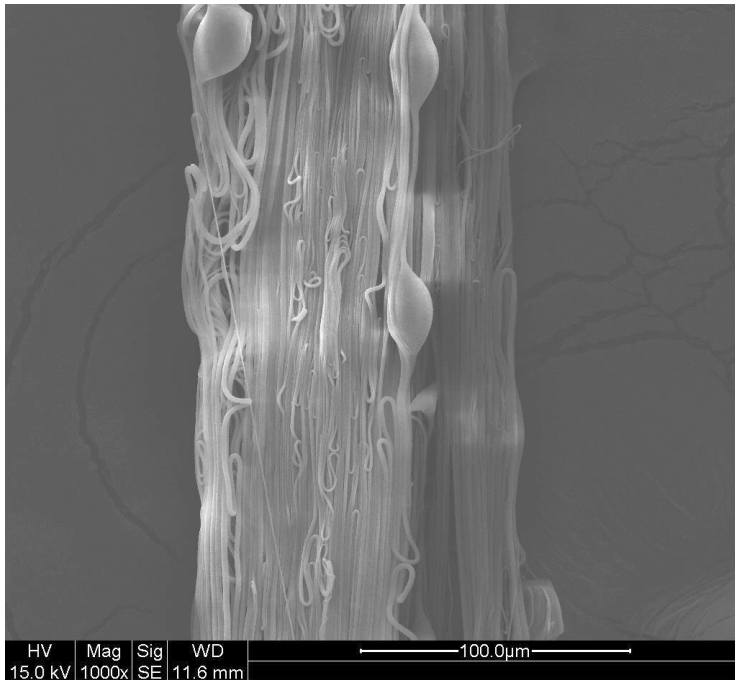
3.15 PVDF yarn obtained through the vortex bath collector process. Reprinted with permission and kindly supplied by W. E. Teo and S. Ramakrishna.
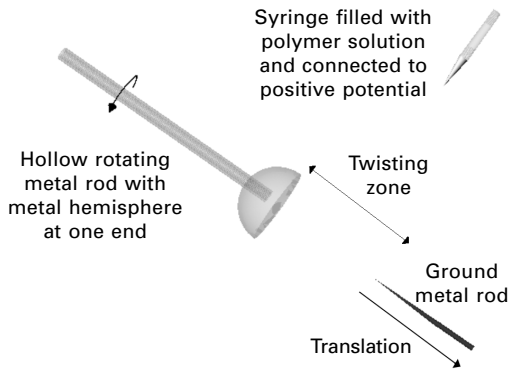
3.16 Schematic diagram for gap-separated rotating rod yarn set-up. Figure kindly supplied by Sphurti V. Doiphode and Darrell H. Reneker.

these two collector surfaces and are given a twist by rotating the hemispherical collector. Yarn collected in this manner on the tip of the metal rod can be translated away from the rotating collector, thereby drawing the yarn and producing yarn continuously. Yarns with lengths up to 30 cm were produced by this method and the creators of the process believe that optimizing the winding mechanism can lead to production of continuous yarns. An electron microscope image of a Nomex® yarn spun through this process is given in Fig. 3.17.
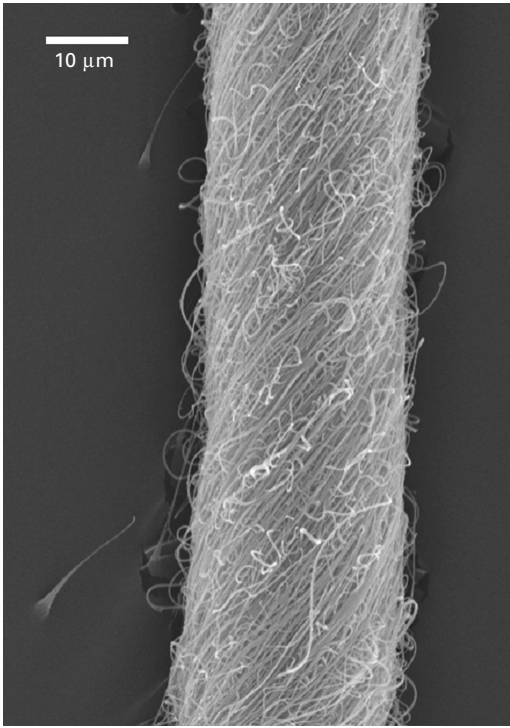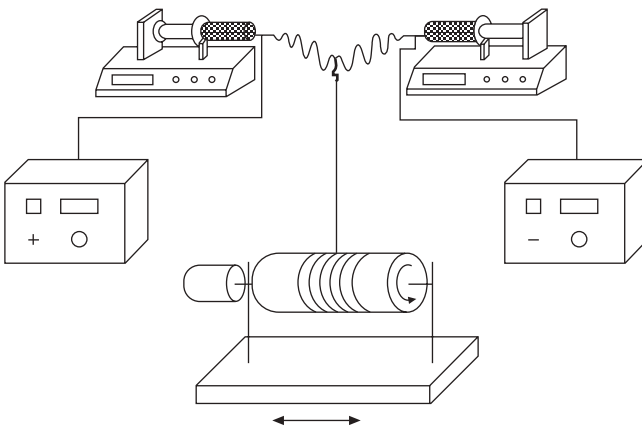
3.5.13 Conjugate electrospinning yarn

Methods for making continuous nanofiber yarns based on the principle of conjugate electrospinning were recently published and patented by Xinsong Li *et al.* at Southeast University in Nanjing[43–45] as well as Luming Li and coworkers at Tsinghua University in Beijing.[46,47] In conjugate electrospinning, two spinnerets or two groups of spinnerets are placed in an opposing configuration and connected to high voltage of positive and negative polarity respectively. The process is presented diagrammatically in Fig. 3.18. Oppositely charged fiber jets are ejected from the spinnerets and Coulombic attraction leads the oppositely charged fibers to collide with each other. The collision of the fibers leads to rapid neutralization of the charges on the fibers and rapid decrease in their flying speeds. In the processes described by both groups, the neutralized fibers are then collected onto take-up rollers to form yarns like the one depicted in Fig. 3.19. Each continuous yarn contains a large quantity of nanofibers, which are well aligned along the longitudinal axis of the yarn. Conjugate electrospinning works for a variety of polymers, composites and ceramics.

3.17 Nomex® yarn made with the gap-separated rotating rod process. Figure kindly supplied by Sphurti V. Doiphode and Darrell H. Reneker.

3.18 Conjugate electrospinning set-up. Image kindly supplied by Xinsong Li.
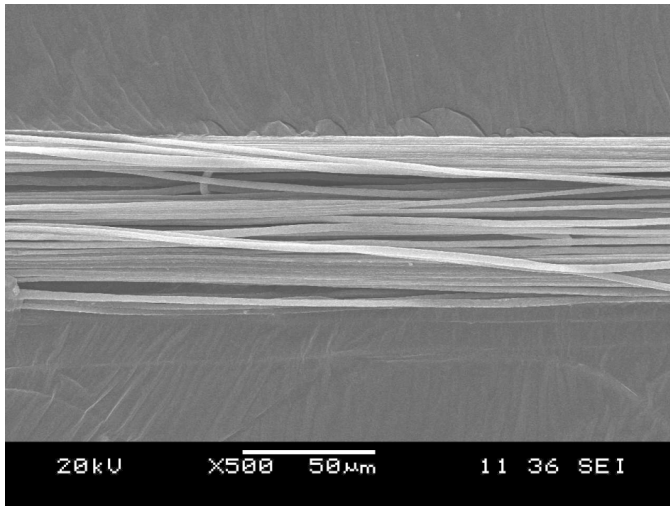
3.19 Yarn obtained through conjugate electrospinning. Image kindly supplied by Xinsong Li.

3.6   Summary and future trends

With only a few exceptions, most of the open literature on yarns from electrospun fibers focuses on the process of yarn formation, rather than on the yarns obtained. Although the process is certainly an important aspect, researchers should bear in mind that ultimately the intended end-user of their results will be the fibers and textiles manufacturing industry. With this in mind, future research should pay more attention to the properties of the yarns obtained, and report more on these with specific focus on tenacity, elasticity and linear density values.

To the best of our knowledge, there is currently no commercially available continuous nanofiber yarn produced through electrospinning. This is likely to change in the very near future and will lead to rapid worldwide evaluation of the product for numerous potential applications. This will also lead to evaluation of nanofiber yarn properties under 'real world' circumstances and results should indicate where further work is required.

Although electrospinning is more than a hundred years old and processes for producing electrospun nanofiber yarns have existed for more than 60 years, little is known about the mechanical and other properties of nanofibers, and especially their twisted yarns. Some recent work has focused on some of the properties of twisted yarns of specific polymers, as discussed in Sections 3.4 and 3.5, but many of the unknowns still need to be investigated.

There are certain drawbacks of the electrospinning process, such as low production rates, the requirement for proportionately large quantities of

industrial solvents, and the necessity for electrospinning through small, needle-like capillaries that tend to get blocked over time – through precipitation of small amounts of the spinning polymer at the capillary mouth. There are also certain challenges related to repeatably electrospinning core–shell and hollow-core fibers and obtaining sub-100 nm fiber diameters of all spinnable polymers without the formation of bead defects. Future work will undoubtedly be aimed at eliminating these drawbacks. Possible solutions to these problems could include multiple-jet, needleless spinning to overcome low production rates and needle blockage. The amounts of industrial solvents used in electrospinning could possibly be reduced or eliminated through application of supercritical fluid techniques or water-based emulsion chemistry.

In the field of tissue engineering, more information on and a better understanding of the wettability and permeability of nanofiber yarns, as well as their structural properties as a function of biodegradation, should lead to the development of highly functional tissue scaffolds and wound dressings. Successful electrospinning of other materials, such as metals and non-oxide ceramics, and better control over the crystallinity of electrospun polymer fibers will lead to significant advances in nanofiber reinforced composite materials.

Quality control methods for nanofiber yarn production processes will need to be developed for commercialization purposes, and other new problems, which will also arise once nanofiber yarns are spun on an industrial scale, will have to be dealt with. On a purely aesthetic level, once nanofibers are incorporated into wearable textiles, the question of coloration will arise. This might pose some problems, since fibers with diameters smaller than the optically visible wavelength range are seen through diffraction of light, not reflection, and therefore they usually appear white under normal circumstances.

3.7   Sources of further information and advice

As stated in the introduction, more general information on the topic of electrospinning can be obtained from some excellent review articles.[1,2] The reader is also referred to a recently published book '*An Introduction to Electrospinning and Nanofibers*' by Ramakrishna *et al*.[48] The book gives an introduction to electrospinning and also a basic background to a wide range of subdisciplines, such as polymer science, rheology and electrostatics, that someone new to the field might want to learn more about.

For more information on yarn terminology and definitions of textiles terms, the reader is referred to the Textiles Intelligence glossary of textiles terms (http://www.textilesintelligence.com/glo/). For more information on specific yarn formation processes discussed in the previous sections, the reader is referred to the specific publications or patents as cited.

3.8   References

1. Huang, Z.-M., Zhang, Y.-Z., Kotaki, M., Ramakrishna, S. 'A review on polymer nanofibers by electrospinning and their applications in nanocomposites', *Composites Science and Technology,* 2003, **63**, 2223–2253.

2. Frenot, A., Chronakis, I. S. 'Polymer nanofibers assembled by electrospinning', *Current Opinion in Colloid and Interface Science*, 2003, **8**, 64–75.

3. Yoshimoto, H., Shin, Y. M., Terai, H., Vacanti, J. P. 'A biodegradable nanofiber scaffold by electrospinning and its potential for bone tissue engineering', *Biomaterials*, 2003, **24**, 2077–2082.

4. Zong, X., Ran, S., Kim, K. S., Fang, D., Hsiao, B. S., Chu, B. 'Structure and morphology changes during *in vitro* degradation of electrospun poly(glycolide-co-lactide) nanofiber membrane', *Biomacromolecules*, 2003, **4**, 416–423.

5. Zong, X., Kim, K., Fang, D., Ran, S., Hsiao, B. S., Chu, B. 'Structure and process relationship of electrospun bio-absorbable nanofiber membranes', *Polymer*, 2002, **43**(16), 4403–4412.

6. Huang, L., McMillan, R. A., Apkarian, R. P., Pourdeyhimi, B., Conticello, V. P., Chaikof, E. L. 'Generation of synthetic elastinmimetic small diameter fibers and fiber networks', *Macromolecules*, 2000, **33**, 2989–2997.

7. Jin, H.-J., Fridrikh, S. V., Rutledge, G. C., Kaplan, D. L. 'Electrospinning *Bombyx mori* silk with poly(ethylene oxide)', *Biomacromolecules*, 2002, **3**, 1233–1239.

8. Kidoaki, S., Kwon, Il. K., Matsuda, T. 'Mesoscopic spatial designs of nano- and microfiber meshes for tissue-engineering matrix and scaffold based on newly devised multilayering and mixing electrospinning techniques', *Biomaterials*, 2005, **26**, 37–46.

9. Jiang, H., Fang, D., Hsiao, B. S., Chu, B. and Chen, W. 'Optimisation and characterization of dextran membranes prepared by electrospinning', *Biomacromolecules*, 2004, **5**, 326–333.

10. Bhattarai, S. R., Bhattarai, N., Yi, H. K., Hwang, P. H., Cha, D. Il., Kim, H. Y. 'Novel biodegradable electrospun membrane: scaffold for tissue engineering', *Biomaterials*, 2004, **25**, 2595–2602.

11. Fong, H., Reneker, D. H. 'Elastomeric nanofibers of styrene–butadiene–styrene triblock copolymer', *Journal of Polymer Science: Part B: Polymer Physics*, 1999, **37**, 3488–3493.

12. Laffin, C., McNally, G. M., Sanderson, R. D., Greyling, C. J. 'The manufacture of aligned poly(acrylonitrile) fibres by electrospinning', *Proceedings of ANTEC 2005*, Boston, pp. 1825–1829, 2005.

13. Zussman, E., Theron, A., Yarin, A. L. 'Formation of nanofiber crossbars in electrospinning', *Applied Physics Letters*, 2003, **82**, 973–975.

14. Dersch, R., Liu, T., Schaper, A. K., Greiner, A., Wendorff, J. H. 'Electrospun nanofibers: internal structure and intrinsic orientation', *Journal of Polymer Science Part B – Polymer Physics*, 2003, **41**, 545–553.

15. Katta, P., Alessandro, M., Ramsier, R. D., Chase, G. G. 'Continuous electrospinning of aligned polymer nanofibers onto a wire drum collector', *Nano Letters*, 2004, **4**, 2215–2218.

16. Li, D., Wang, Y., Xia, Y. 'Electrospinning of polymeric and ceramic nanofibers as uniaxially aligned arrays', *Nano Letters*, 2003, **3**, 1167–1171.

17. Li, D., Wang, Y., Xia, Y. 'Electrospinning nanofibers as uniaxially aligned arrays and layer-by-layer stacked films', *Advanced Materials,* 2004, **16**, 361–366.

18. Li, D., Ouyang, G., McCann, J. T., Xia, Y. 'Collecting electrospun nanofibers with patterned electrodes', *Nano Letters*, 2005, **5**, 913–916.
19. El-Aufy, A. K. 'Nanofibers and nanocomposites poly(3,4-ethylene dioxythiophene)/poly(styrene sulfonate) by electrospinning', PhD Thesis, March 2004, *Drexel University Online Library*, URL: http://dspace.library.drexel.edu/handle/1860/282, Access date: 10 May 2005.
20. Fennessey, S. F., Farris, R. J. 'Fabrication of aligned and molecularly oriented electrospun polyacrylonitrile nanofibers and the mechanical behaviour of their twisted yarns', *Polymer*, 2004, **45**, 4217–4225.
21. Deitzel, J. M., Kleinmeyer, J. D., Hirvonen, J. K., Beck Tan, N. C. 'Controlled deposition and collection of electro-spun poly(ethylene oxide) fibers', *US Army Research Laboratory Report - ARL-TR-2415*, 2001.
22. Deitzel, J. M., Kleinmeyer, J. D., Hirvonen, J. K., Beck Tan, N. C. 'Controlled deposition of electrospun poly(ethylene oxide) fibers', *Polymer*, 2001, **42**, 8163–8170.
23. Fong, H., Liu, W., Wang, C.-S., Vaia, R. A. 'Generation of electrospun fibers of nylon 6 and nylon 6-montmorillonite nanocomposite', *Polymer*, 2002, **43**, 775–780.
24. Dalton, P. D., Klee, D., Möller, M. 'Electrospinning with dual collection rings', *Polymer*, 2005, **46**, 611–614.
25. Formhals, A. 'Process and apparatus for preparing artificial threads', US Patent 1,975,504; 1934.
26. Cooley, J. F. 'Apparatus for electrically dispersing fluids', US Patent 692,631; 1902.
27. Morton, W. J. 'Method for dispersing fluids', US Patent 705,691; 1902.
28. Formhals, A. 'Method and apparatus for the production of fibers', US Patent 2,123,992; 1938.
29. Formhals, A. 'Artificial fiber construction', US Patent 2,109,333; 1938.
30. Formhals, A. 'Method and apparatus for spinning', US Patent 2,160,962; 1939.
31. Formhals, A. 'Artificial thread and method for producing same', US Patent 2,187,306; 1940.
32. Formhals, A. 'Production of artificial fibers from fiber forming liquids', US Patent 2,323,025; 1943.
33. Formhals, A. 'Method and apparatus for spinning', US Patent 2,349,950; 1944.
34. Lee, J.-R., Jee, S.-Y., Kim, H.-J., Hong, Y.-T., Kim, S., Park, S.-J. 'Filament bundle type nano fiber and manufacturing method thereof', PCT Application, WO 2005/123995 A1.
35. Ko, F., Gogotsi, Y., Ali, A., Naguib, N., Ye, H., Yang, G., Li, C., Willis, P. 'Electrospinning of continuous carbon nanotube-filled nanofiber yarns', *Advanced Materials*, 2003, **15**, 1161–1165.
36. Abd El-Fattah Ali, A. 'Carbon nanotube reinforced carbon nano composite fibrils by electro-spinning', PhD Thesis, October 2002, *Drexel University Online Library*, URL: http://dspace.library.drexel.edu/handle/1860/17, Access date: 19 May 2005.
37. Kim, H. Y., Kim, K. W., Lee, K. H., Yoo, E.-S., Farris, R. J. Fennessey, S. F. 'Electrospun hollow fibers of poly(e-caprolactone)', *Abstracts of Papers, 228th ACS National Meeting, Philadelphia, PA, United States, August 22–26, 2004*. American Chemical Society, Washington, DC, 2004.
38. Smit, E., Bűttner, U., Sanderson, R. D. 'Continuous yarns from electrospun fibers', *Polymer*, **46**, 2005, 2419–2423.
39. Kim, H.-Y. 'A process of preparing continuous filament composed of nanofibers', PCT Application, WO 2005/073442 A1.

40. Kim, H.-Y., Park, J.-C., 'A process of preparing continuous filament composed of nanofibers', PCT Application, WO 2006/052039 A1.
41. Teo, W. E., Ramakrishna, S. National University of Singapore, personal communication.
42. Doiphode, S. V., Reneker, D. H. University of Akron, personal communication.
43. Li, X., Sun, F., Yao, C., Song, T. 'Conjugate electrospinning: continuous yarns from oppositely charged nanofibers', *Preprint of Polymeric Materials Science and Engineering (PMSE): Electrostatic Polymer Processing, 231st American Chemical Society National Meeting, Atlanta, GA, March 26–30, 2006.*
44. Xinsong, L., Chen, Y., Tangyin, S. 'Method for the preparation of continuous nanofiber yarns', Chinese Patent No. CN1687493, 2005.
45. Xinsong, L., Chen, Y., Fuqian, S. 'Apparatus and methods for the preparation of continuous nanofiber yarns', Chinese Patent No. CN 1776033, 2005.
46. Pan, H., Li, L., Hu, L., Cui, X. 'Continuous aligned polymer fibers produced by a modified electrospinning method', *Polymer* 2006, **47**, 4901–4904.
47. Li, L., Pan, H., Hu, L, 'Device and method for electrospinning and fiber collecting', Chinese Patent No. CN 1766181, 2006.
48. Ramakrishna, S., Fujihara, K., Teo, W., Lim, L., Ma, Z. *An Introduction to Electrospinning and Nanofibers*. Singapore, World Scientific Publishing, 2005.

4

Producing polyamide nanofibers by electrospinning

M. A F S H A R I, R. K O T E K and A. E. T O N E L L I,
North Carolina State University, USA and D.-W.
J U N G, Hyosung Corporation, South Korea

4.1   Introduction

Conventional fiber spinning techniques such as wet spinning, dry spinning, melt spinning and gel spinning usually produce polymer fibers with diameters down to the micrometer range. If the fiber diameter is reduced from micrometers to nanometers, very large surface area to volume ratios are obtained and flexibility in surface functionalities and better mechanical performance may be achieved. These unique characteristics make polymer nanofibers optimal candidates for many important applications.[1] Polymer fibers can be generated from an electrostatically driven jet of polymer solution or polymer melt. This process, known as electrospinning, has received a great deal of attention in the past decade because of its ability to consistently generate polymer fibers that range from 5 to 500 nm in diameter.[2–5] The idea of electrospinning dates back more than 60 years. Formhals[6–10] introduced electrospinning methods and described fiber formation during the spinning process.

Because of the small pore size and high surface area inherent in electrospun textiles, these fabrics show promise for use in protective clothing for soldiers (to protect against extreme weather conditions, ballistics and nuclear, biological and chemical warfare), filtration applications, membranes, reinforcing fibers in composite materials, optical and electronic applications (piezoelectric, optical sensors), biomedical devices (cosmetics, skin healing and skin cleansing, wound dressing, drug delivery and pharmaceuticals, supports for enzymes or catalysts, scaffolds for tissue engineering, and templates for the formation of hollow fibers with inner diameters in the nanometer range.[1, 11–19]

4.2   The electrospinning process

Figure 4.1 shows a typical electrospinning apparatus. A high electrical potential, typically 5–30 kV, is applied to a polymer solution contained in a syringe. In electrospinning the tensile force is generated by the interaction of an applied electric field with the electrical charge carried by the jet rather than by the

71
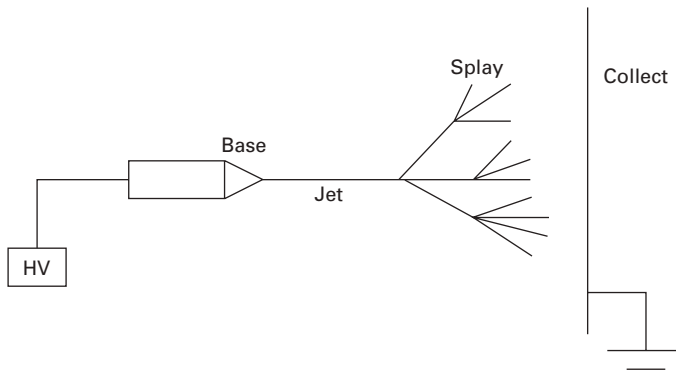
4.1 Schematic of electrospinning apparatus.

spindles and reels used in conventional spinning.[12] A stable electrospinning jet has four distinct regions (see Fig. 4.1). The jet emerges from the charged surface at the base region, travels through the jet region, divides into many fibers in the splaying region, and stops in the collection region. The base is the region where the jet emerges from the liquid polymer. The geometry of the jet near the base is a tapered Taylor cone in which the axial velocity of the liquid increases as the polymer is accelerated along the axis of the jet. The base may have a circular cross-section, or it may have some other shape if the surface tension of the liquid anchors the jet to the lip of a hole or some other stationary object. An electric field at the surface of a liquid produces a force that, if the electric field is strong enough, causes a jet of liquid to be ejected from a surface that was essentially flat before the field was applied. The jet is the region beyond the base where the electrical forces continue to accelerate the polymer liquid and then stretch the jet. In this region, the diameter of the jet decreases and the length increases in a way that keeps constant the amount of mass per unit time passing any point on the jet axis. Larrondo and Manley,[20, 21] through analysis of the flow field in an electrically driven jet, showed that the flow is a combination of parabolic and purely extensional flow. It was found, however, that the region about the symmetry axis of the jet is free of rotational components and is thus an area of pure extensional flow.[21] Splaying occurs in a region in which the radial forces from the electrical charges carried by the jet become larger than the cohesive forces within the jet, and the single jet divides into many charged jets with approximately equal diameters and charge per unit length. The collection region is where the jet is stopped. The polymer fibers that remain after the solvent has evaporated may be collected on a metal screen. The initiation and formation of the jet constitute a complex process with many variations.[12] In the electrospinning process the morphology of the fibers depends on various parameters, such as solution concentration, applied electric field

strength and tip-to-collector distance.[22–24] Although research has provided much fundamental understanding of the process, several difficulties remain.

Many parameters can influence the transformation of polymer solutions into nanofibers through electrospinning. These parameters include: (a) solution properties, such as viscosity, elasticity, conductivity and surface tension; (b) governing/operating variables, such as hydrostatic pressure in the capillary tube, electric potential at the capillary tip and the gap (distance between the tip and the collecting screen); and (c) ambient parameters such as solution temperature, humidity and air velocity in the electrospinning chamber.[14]

Sometimes electrospun fibers exhibit bead-on-string structures, which have been generally considered to be undesirable by-products or defects. Theoretical analyses in the literature predicted three types of instabilities for an electrically driven jet: the axisymmetric Rayleigh instability, the electric field-induced axisymmetric instability and whipping. The process of bead formation revealed that the formation of a beaded structure resulted from axisymmetric instabilities and flow of the electrospun jet. Applied voltage, solution surface tension and conductivity influenced the formation of beaded electrospun fibers.[25] Zuo and coworkers showed for poly(hydroxybutyrate-co-valerate) (PHBV) electrospun fibers that higher applied voltage favors formation of smooth fibers, and beads are likely to be formed at high solution feed rates. High surface tension promotes the formation of PHBV electrospun fibers with beads, whereas increased conductivity achieved with mixed solvents favors uniform smooth fibers.[25]

4.3   Properties of electrospun nanofibers

It is difficult to measure mechanical properties of each electrospun single nanofiber with existing test techniques, because of their very small diameters. Therefore, mechanical tests were performed instead on nano-scale nonwoven webs with conventional testing methods. Lee *et al.*[26] investigated the mechanical behavior of electrospun fiber webs of poly(vinyl chloride)/polyurethane (PVC/PU) polyblends with different blending ratios. Ding and coworkers[27] also tested mechanical properties of biodegradable nanofibrous mats comprising poly(vinyl alcohol)/cellulose acetate (PVA/CA), which were prepared by using multi-jet electrospinning methods. Mechanical properties of electrospun PU nanowebs were investigated by Pedicini and Farris.[28]

Among the many electrospun polymers reported in the literature are poly(*p*-phenylene terephthalamide), tri-block copolymers, polyethylene oxide and DNA from solution; and polyethylene and polypropylene from the melt.[2, 29] Nylon was the first commercialized synthetic fiber and is used throughout the world in many applications. It has been widely used as an important engineering plastic and synthetic fiber because of its good mechanical properties. It has been produced by traditional methods such as melt, wet and

dry spinning and is available in staple, tow, monofilament and multifilament forms.[30] Fiber diameters produced by these methods range from 10 to 500 μm.[31] Ryu et al.[32] examined morphology, pore size, surface area and gas transport properties of nylon-6 (N6) nonwoven electrospun mats. The crystallinity of nanocomposites of nylon-6 and nylon-6–montmorillonite was studied by Fong et al.[33] The ultra-large draw ratio and rapid solvent removal of electrospinning favors the formation of γ-phase nylon crystallites in pure N6 and montmorillonite–N6 fibers.[33] Bergshoef and Vancso[13] prepared nanocomposites with ultrathin, electrospun nylon-4,6 fibers and compared mechanical properties of nylon-4,6/epoxy composite films and epoxy films.

In an effort to understand the mechanism of jet formation from polymer melts Larrond and Manley[34] studied molten polymers of nylon-12 and polyethylene with the aid of an electric field. The drop formation was measured as a function of field intensity and frequency. There is qualitative agreement between the theory of Torza and experimental observation.

Schreuder-Gibson et al.[35] used nylon-6,6 (N6,6), polybenzimidazole (PBI) and poly(tetrafluoroethylene) membranes produced from electrospun fibers as protective layers. They measured properties of these electrospun membranes, including structural effects upon moisture transport, air convection, aerosol filtration, porosity and tensile strength.

Stephen et al.[36] using Raman spectroscopy showed that in the case of N6, the polymer crystalline structure was altered from α to γ form when electrospun. This, however, is not a permanent morphological conformational change and can be converted back to α form by solvent casting a film from the electrospun membrane. The ability of the electrospinning process to produce the γ form implies that the fibers are under high stress when they are being formed. Nylon-12 has only one preferred conformation, and the chain conformation is conserved after processing.

Supaphol and coworkers[37–39] studied the effects of electrode polarity and processing parameters (concentration, molecular weight, electrostatic field strength, solution temperature, addition of an inorganic salt and solvent system) on morphological appearance and size of the as-spun N6 fibers. An increase in the temperature of the spinning solutions decreased the size of the as-spun fibers. Addition of NaCl and increasing its concentration caused the conductivity of the spinning solutions to increase, which, in turn, caused the sizes of the as-spun fibers to increase. Fibers obtained from N6 of higher molecular weights appeared to be larger in diameter. An increase in the temperature of the solution during electrospinning resulted in a decrease in the fiber diameters. Increasing solution viscosity resulted in a reduced number of beads and increased fiber diameters. Diameters of fibers obtained under the negative electrode polarity were larger than those obtained under the positive electrode polarity.

Dersch et al.[40] showed that the intrinsic structure of N6 and poly(lactic acid) fibers do not differ to an appreciable extent from those found for much

thicker fibers obtained by melt extrusion. The annealing of polyamide fibers at elevated temperatures resulted in a transformation from the disordered γ from to the more highly ordered α form. The orientation of the crystals along the fiber axis was strongly inhomogeneous, and on average, was very weak.

In the literature there is little information on the effects of concentration, molecular weight, type of solvent, voltage and other parameters in the electrospinning process on jet stability and diameter of nylon nanofibers. In Section 4.2 we investigated the effects of voltage, distance between collector and tip of syringe, and solution concentration of N6 in formic acid on the diameters of electrospun fibers of N6 formed with stable solution jets. In Section 4.4, N6,6 nanofiber webs with different molecular weight were formed *via* the electrospinning method. The N6,6 solutions were produced by using the binary solvent formic acid/chloroform. Mechanical properties of two widely different molecular weight electrospun N6,6 nanowebs are compared by using conventional test methods. The main objective of this part of the study was to determine whether the use of high molecular weight N6,6 is a viable approach to improve the mechanical properties of electrospun nylon filaments.

4.4 Measuring the effects of different spinning conditions and the use of high molecular weight polymers on the properties of electrospun nanofibers

N6 chips of fiber grade from Parsilon Co., Iran, with relative viscosity 2.5–2.6 in H_2SO_4 (molecular weight around 17 000 g/mol) were used. Various polymer solution concentrations ranging from 5, 6, 8 and 9 wt% were prepared by dissolving N6 in formic acid (Merck).

High molecular weight N6,6 (MW = 170 000 g/mol) was prepared by using solid state polymerization of commercial N66 chips (Zytel®101, MW = 30 000 g/mol) that were supplied by Du Pont Co. Solid state polymerization of N6,6 was conducted under 0.4–5 torr at 255 °C for 8 hours, with the detailed procedure described in our previous paper.[41] Ninety per cent formic acid and chloroform were obtained from Aldrich Co.

4.4.1 Viscosity of nylon 6,6 polymer solutions

The different concentration polymer solutions for electrospinning were prepared by using a solvent mixture of 90% formic acid and chloroform with the ratio of 75/25 (v/v). Solution viscosity was determined at 25 °C using a DV-II viscometer from Brookfield Co., USA.

4.4.2   Electrospinning conditions

For electrospinning of N6, a variable high-voltage power supply was used to apply voltages of 5 and 30 kV to the vertically oriented syringe tip. The polymer solution was placed in a 5 ml syringe to which a capillary tip of 0.8 mm inner diameter was attached. The positive electrode of the high-voltage power supply is connected to a copper wire immersed in the polymer solution. The negative electrode was connected to a metallic collector wrapped with aluminum foil.

The process used in the electrospinning of N6,6 fibers is illustrated in Fig. 4.2. There are three components needed to fulfill the process: a high-voltage supply, a capillary tube with a needle of small diameter, and a metal collecting screen. A high-voltage power supply was used for creating an electrically charged polymer solution in electrospinning with voltages ranging from 0 to 30 kV. One electrode is attached to the metal capillary tip with 0.89 mm diameter and the other attached to the collector, a rotating cylindrical drum. The drum is 20 cm in diameter and 35 cm long and is covered with aluminum foil. The solution jet evaporates or solidifies and is collected as an interconnected web of small fibers. Electrospun nanowebs were produced by spinning N6,6 solutions from a 10 ml syringe with a back-pressure applied volume flow rate ranging from 90 μl/min to 0.040 ml/min.

4.4.3   Web morphology

The morphologies of electrospun low and high molecular weight N6,6 and N6 webs were observed by scanning electron microscopy (SEM, Hitachi Co., Japan) and their fiber diameters were measured with an Image J analyzer.
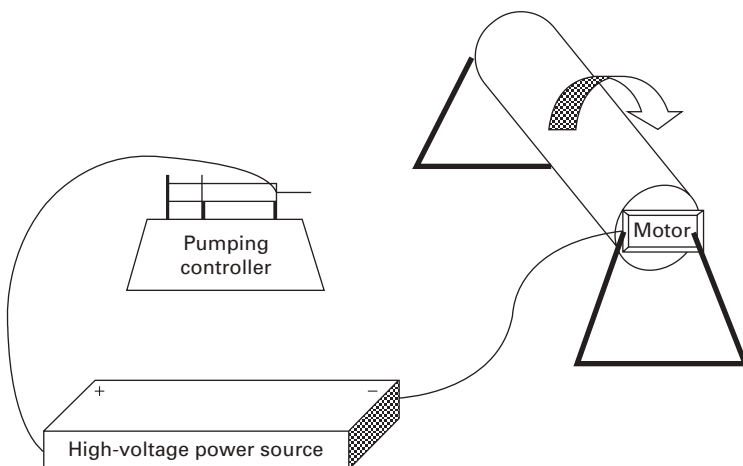
4.2 Schematic of electrospinning process used in this study.

4.4.4   Mechanical behavior

The tensile behavior of the electrospun low and high molecular weight N6,6 webs was tested on an Instron 5500R with a cross-head speed of 7 mm/min at room temperature. Rectangular-shaped tensile specimens (1 cm × 3 cm) were prepared for tensile tests. At least ten samples were tested for each fiber web.

4.5   Improving the properties of electrospun nanofibers: experimental results

It is well known that the morphologies of electrospun fibers depend on various processing parameters and environmental conditions, such as temperature and humidity.[11, 12, 22, 23] Optimal electrospinning conditions, such as polymer concentration, applied electric field strength and tip-to-collector distance, were examined. It was not easy to create fibers under some electrospinning conditions. First, the solution viscosity (controlled by the solution concentration) was too low to make fibers from solutions containing less than 3–4 wt% N6. Generally, the beads-on-string morphology produced at low concentrations was regarded as an undesirable by-product of electrospinning. The viscosity, net charge density and surface tension of solution are key parameters in the formation of the beads-on-string.[24] Second, the solvent was not completely evaporated owing to short tip-to-collector distances. With increased tip-to-collector distances, electrospinning did not facilitate the collection of fibers at the metallic collector, because of a relatively low electric field formed between the capillary tip and collector. The optimum tip-to-collector distance also depends on concentration of polymer solution, because as the solution concentration increased, so did the viscosity and surface tension of solution. Thus we needed to increase the voltage to overcome the solution surface tension to achieve splaying of the initial single jet into many charged jets. The type of solvent used for dissolving the polymer also has an effect on viscosity and surface tension.

Figure 4.3 shows the image of a nonwoven mat of electrospun N6 fibers on a foil of aluminum. The SEM micrographs in Figs 4.4 and 4.5 show some beads in electrospun N6 fibers. The results showed that with increasing applied voltage formation of beads decreased. The beads can be removed by controlling solution viscosities and electrical conductivities of the polymer solution.[22, 24]

Figure 4.6 shows the distribution of electrospun (5 kV) N6 fiber diameters. The average fiber diameter increased with increasing concentration of solution. Figure 4.7 shows that increasing voltage (30 kV) decreased average diameter of electrospun fibers. By increasing the voltage, the applied electric field for splaying the single jet increased producing many jets and the diameters of the electrospun fibers decreased.
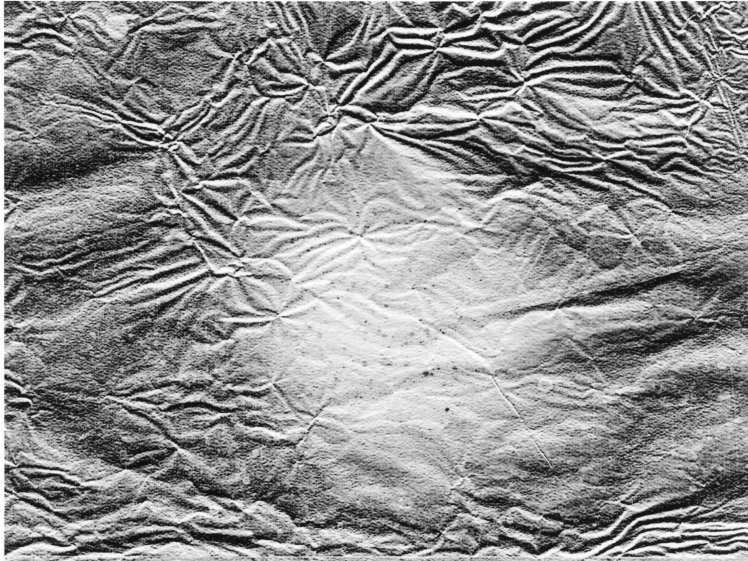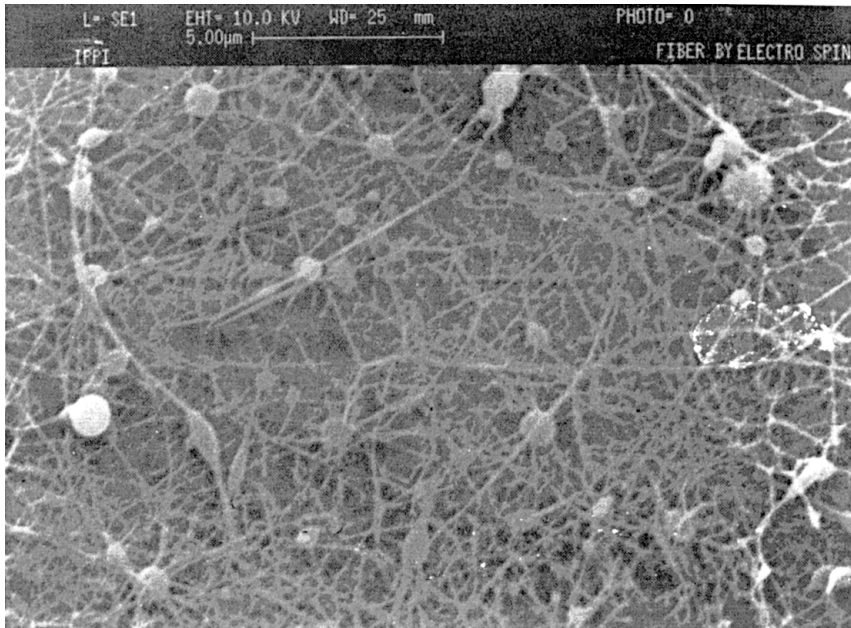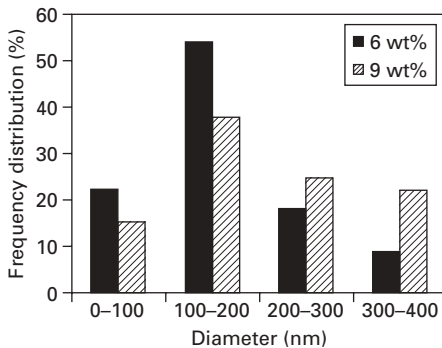
4.3 Nonwoven mat of N6 electrospun fibers on aluminum foil (8 wt% in formic acid at 10 kV).
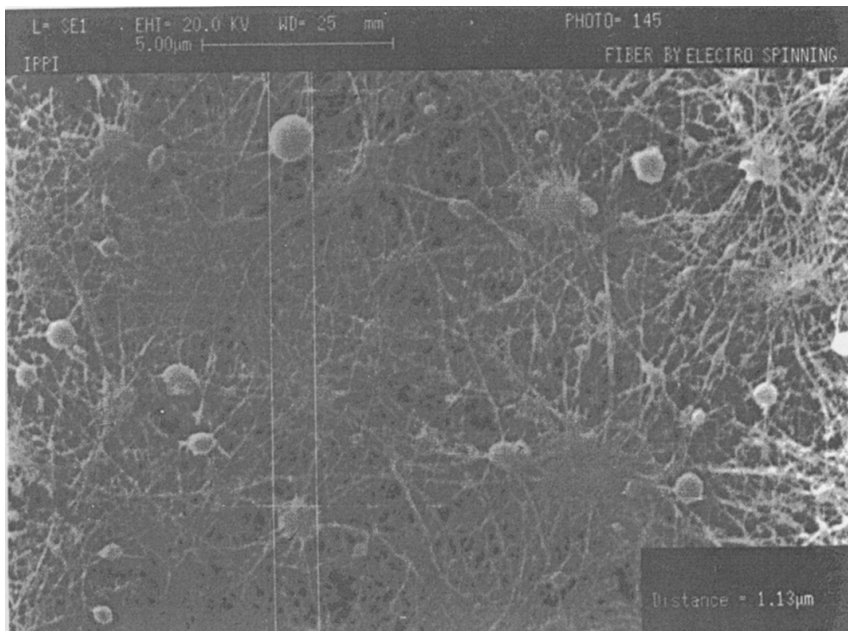
4.4 Scanning electron micrograph of N6 fibers spun from 6 wt% in formic acid solution at 5 kV.

4.5 Scanning electron micrograph of N6 fibers spun from 8 wt% at 10 kV.

4.6 Effect of solution concentration on diameter distribution of electrospun N6 fibers (voltage 5 kV).

The other important factor to the continuous production of electrospun N6 fibers is the distance between the tip of the syringe needle and the collector. To achieve splaying we needed to have an optimum distance between tip and collector. With increasing solution concentration of N6, the tip-to-collector distance has to increase. Tip-to-collector distances for 6 and 8 wt% solutions were about 3 and 5 cm, respectively. The fiber diameter generally decreased as the tip-to-collector distance increased. This is probably due to
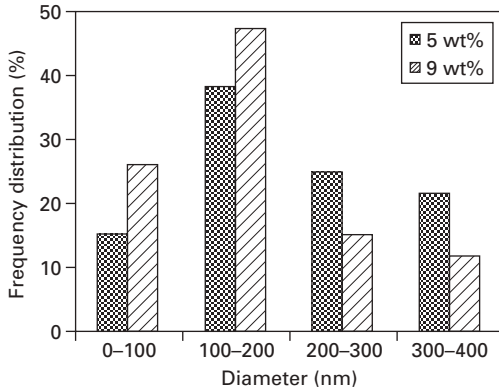
4.7 Distribution of diameter of N6 electrospun fibers.

Table 4.1 Viscosity of nylon-6,6 solutions

Molecular weight of nylon-6,6 (g/mol)	Concentration (%)	Viscosity (cP)
30000	10	350
30000	15	950
170000	3	340
170000	5	1000

splaying of the single jet into more charged jets or electrospun fibers. With a short tip-to-collector distance, the solvent cannot evaporate completely and the stretching of the jet is reduced.

4.5.1   Viscosity of nylon 6,6 solutions

It is well known that many parameters, such as viscosity, elasticity, conductivity, surface tension and distance between tip and collection screen, can influence the transformation of polymer solutions into nanofibers through electrospinning. Solution viscosity is one of the most important factors. Since both polymers have significantly different molecular weights, four different solutions of N6,6 with various concentrations were prepared. We used a mixed solvent consisting of formic acid and chloroform with the ratio of 75/25 (v/v). Table 4.1 shows the solution viscosities for each concentration of low and high molecular weight N6,6.

N6,6 with average molecular weight of 30 000 g/mol (called low molecular weight N6,6) was used to prepare two polymer solutions at concentrations of 10% and 15%. The corresponding Brookfield viscosities were 350 and 950 cPs, respectively. In order to prepare fiber-forming solutions, the concentrations

of N6,6 with average molecular weight 170 000 g/mol (called high molecular weight N6,6) were significantly lower. Correspondingly, the Brookfield viscosities were 340 and 1000 cPs for these solutions at 3% and 5%. Interestingly, as can be seen in Table 4.1, a 3% solution of high molecular weight N6,6 has comparable viscosity with that of a 10% solution of low molecular weight polymer. Similarly, a 5% solution of high molecular weight N6,6, has comparable viscosity with that of a 15% concentration solution of low molecular weight polymer.

Traditionally, formic acid is used as a solvent for the dissolution of N6 or N6,6. However, its boiling point of 100 °C is relatively high and therefore it is not very suitable for electrospinning. Nevertheless, the boiling point of formic acid can be lowered by addition of a cosolvent with a relatively low boiling point (bp), namely chloroform (bp of 61 °C). One may also expect that tensile strength of as-spun nylon fibers can be improved by changing ratios of formic acid and chloroform. Indeed, Gogolewski and Pennings[42] found that the morphology and tensile strength differences of dry-spun high molecular weight N6 fibers vary with different mixture ratios of formic acid and chloroform. They also documented that the ratio of formic acid to chloroform of 75/25 (v/v) gave a fiber with the highest tensile strength when a super high molecular weight N6 was used for making dry-spun fibers. Low-volatility solvents are required for both dry spinning and electrospinning processes. If solvent does not evaporate completely during electrospinning processing, it is very difficult to form a web or to remove the electrospun web from the collecting drum. Our experiments showed that the mixed solvent consisting of formic acid and chloroform is a good medium for electrospinning nylon-6,6.

4.5.2   Diameter distribution of nylon 6,6 electrospun webs

Bead formation is a very common phenomenon for electrospun fibers; therefore, we used scanning electron microscopy (SEM) to examine the appearance of our fibers. Figure 4.8 shows SEM micrographs of electrospun webs spun from low MW N6,6 at two concentrations of 10 and 15%. The webs formed with the high molecular weight N6,6 at $c = 3\%$ and $c = 5\%$ are shown in Fig. 4.9. Interestingly, no beads can be observed on all the fibers. If conditions of electrospinning, such as concentration of polymer solution, voltage power or flow rate, are not properly adjusted, beads occur on the surface of nanofilaments. Lee *et al.*[43] found the bead morphology on electrospun polystyrene fibers. Polymer concentration, applied voltage and tip-to-collector distance strongly affect the morphology of the formed beads on polystyrene fibers. At concentrations lower than 15%, beads occurred on the electrospun fibers. No beads were observed for polystyrene fibers when the polymer concentrations

(a)

(b)
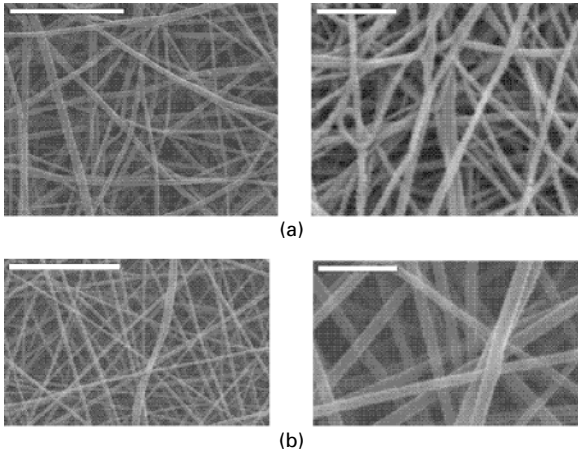
4.8 Scanning electron microscopy (SEM) micrograph of electrospun webs spun at: (a) c = 10%, low MW N6,6; (b) c = 15%, low MW N6,6. Left-hand scale bars are ~5 μm; right-hand scale bars are 1 μm.

(a)

(b)
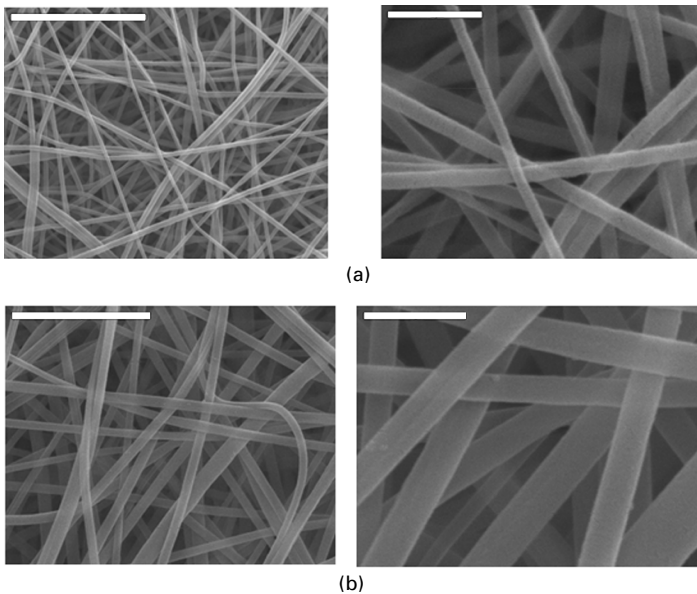
4.9 Scanning electron microscopy (SEM) micrograph of electrospun webs spun at: (a) c = 3%, high MW N6,6; (b) c = 5%, high MW N6,6. Left-hand scale bars are ~5 μm; right-hand scale bars are 1 μm.

were higher than 15%. Fong and coworkers[22, 44] also documented similar results from the electrospinning of polyethyleneoxide (PEO) polymer. As the concentration of PEO polymer increased, the beads disappeared. Furthermore, the bead shapes changed from spherical to spindle-like. The

bead formation is most likely related to the surface tension. At a low polymer concentration, the surface tension has the dominant influence and, therefore, the fibers with beads are formed, or dripping of polymer solution may even occur during spinning. At high concentrations, fibers without beads can be formed because of the cohesive nature of the high-viscosity solution. Usually, in the case of the low molecular weight N6,6, a polymer solution concentration greater than 10% is satisfactory for electrospinning, On the other hand, a polymer concentration of 3% is high enough to successfully conduct the electrospinning of the high MW N6,6.

Figures 4.10 and 4.11 show the diameter distribution of electrospun filaments. As can be seen, the fiber diameters depend on the concentration of the N6,6 polymers that were used in this study. Interestingly, the distribution was narrower and the fiber diameter varied from 100 to 200 nm for the web obtained from the low molecular weight N6,6, at a concentration of 10%. However, when the concentration was increased to 15%, the fiber diameter variability increased from 100 to 300 nm. More dramatic changes with polymer
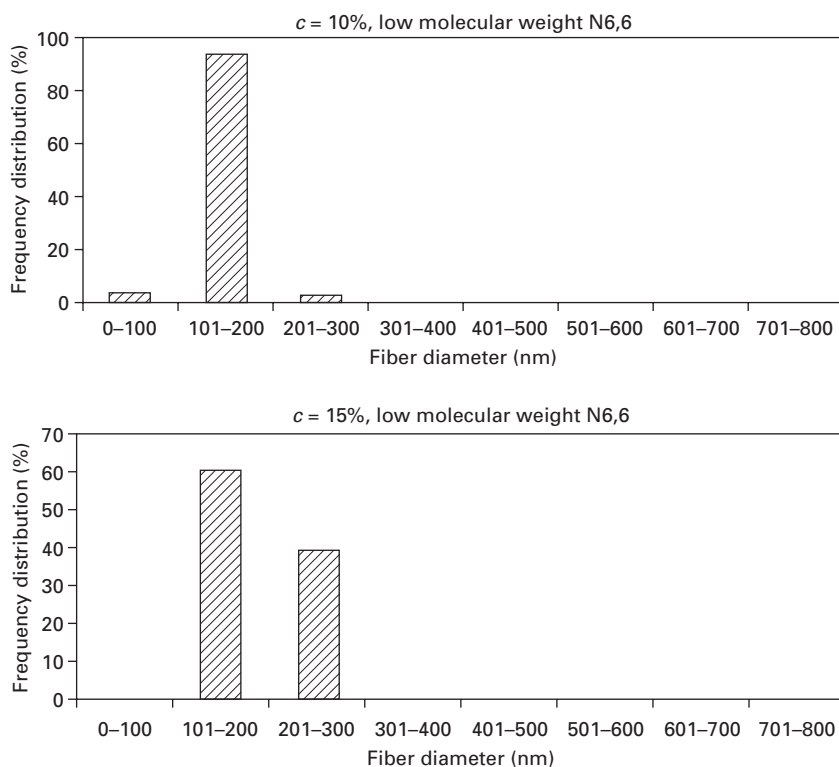
4.10 Fiber diameter distribution of the low molecular weight N6,6 electrospun webs.
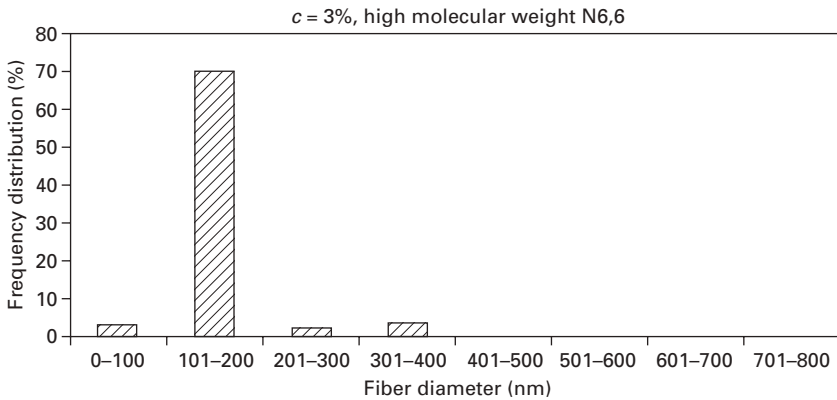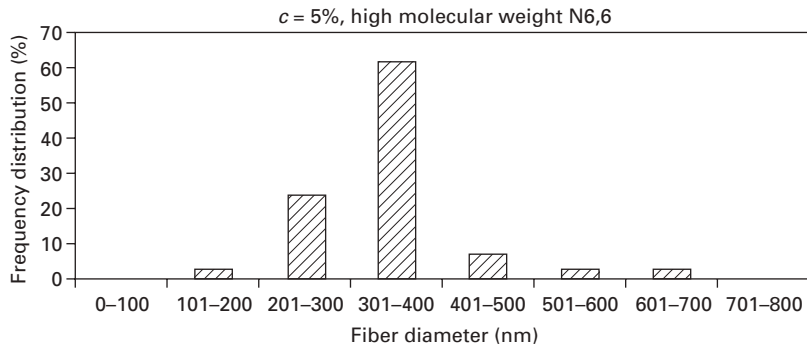
4.11 Fiber diameter distribution for high molecular weight N6,6 electrospun webs.

concentration were observed for the high molecular weight N6,6. At a concentration of 3% the fiber diameters were in the range 100–200 nm (Fig. 4.11). However, fibers spun from the higher molecular weight N6,6 solution at $c = 5\%$, had a higher average diameter and a greater diameter variability. As shown in Fig. 4.11, most fibers had diameters in the range 300–400 nm, but a small fraction of fibers exhibited diameters in the range 600–700 nm.

It is evident from our study that as the N6,6 concentration increases; the fiber diameter distribution of electrospun filaments becomes broader. Furthermore, the average diameter of electrospun filaments increases with increasing polymer concentration, and the increase in fiber diameters obtained between low and high concentrations of high molecular weight N6,6 solutions was larger than between those of the low molecular weight N6,6 solutions. Ryu et al.[32] reported similar results for their electrospun N6 nonwoven mats. The authors also reported a broader diameter distribution in the electrospun filaments at higher polymer concentrations. An increase in the filament diameter

(as the result of a higher viscosity or a higher polymer concentration) is a well-known phenomenon[11, 14, 22, 45] in electrospinning.

As shown in Figs 4.10 and 4.11, the electrospun fibers exhibit two different distributions at high concentrations for both low and high molecular weight N6,6. Although more detailed studies should be done to prove the generality of these observations, it appears that the bimodal distribution of fiber diameters might be common. Such behavior can be seen particularly for the filaments spun from 15 and 5% solutions of low and high molecular weight N6,6, respectively. Similar phenomena were reported by Ding *et al.*[27] and Deitzel *et al.*[11]

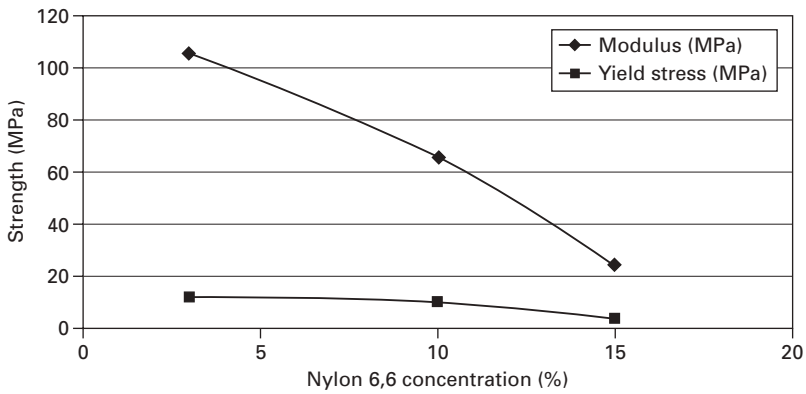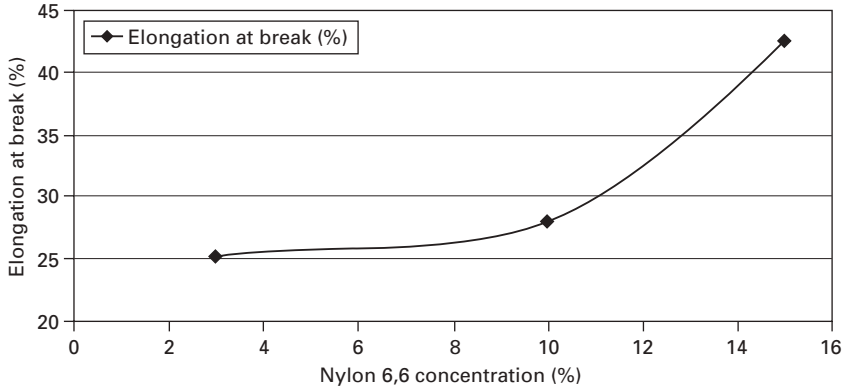### 4.5.3   Mechanical properties of nylon 6,6 electrospun webs

Table 4.2 shows the mechanical properties of electrospun N6,6 nonwoven webs that were made under various experimental conditions. It is evident that the polymer concentration and the molecular weight of N6,6 influence the fiber morphology and, therefore, the elongation at break and initial modulus, as well as the strength of these materials. Figure 4.12 gives the dependence of these properties as a function of N6,6 concentration. The lowest elongation at break of 25.4% can be seen for the fibers electrospun with the high MW N6,6 from a 3% solution. Interestingly, more concentrated polymer solutions (prepared from the low MW N6,6) seem to lead to an increase in the elongation at break of up to 42.4%.

It is well known that most electrospun filaments are not oriented and, therefore, exhibit poor mechanical properties, namely the initial modulus and strength. Interestingly, our study clearly shows that the modulus and the strength are much higher for the webs made from the high MW N6,6 (see Table 4.2 and Fig. 4.13). Thus, it is plausible to state that the use of N6,6 with a high molecular weight provides a simple approach for improving the mechanical properties of electrospun nylon filaments.

4.6   Conclusions

The following parameters have been suggested to affect the electrospinning process: solution properties, including viscosity, polymer concentration, polymer molecular weight, conductivity and surface tension; controlled process variables including hydrostatic pressure in the capillary, electric potential at the tip of needle, emitting electrode polarity, and the distance between the tip of the needle and the collection screen; and ambient parameters including temperature, humidity and air velocity in the electrospinning chamber. There are relationships between polymer solution concentration and electric field strength and the distance between tip and collection screen for achieving a

4.12 Mechanical properties of N6,6 electrospun webs as a function of polymer concentration. *c* = 3% high MW N6,6; *c* = 10%, low MW N6,6; *c* = 15%, low MW N6,6.

Table 4.2 Mechanical properties of electrospun low and high molecular weight nylon-6,6 nonwovens

Concentration (%)	Molecular weight (g/mol)	Modulus (MPa)	Yield stress (MPa)	Elongation at break (%)
3	170 000	106.7	12.1	25.3
10	30 000	65.8	10.2	27.9
15	30 000	23.2	3.5	42.4

steady jet of the polymer solution. Our results showed the voltage for producing electrospun N6 fibers increased with increasing concentration of polymer solution. The diameters of electrospun N6 fibers were affected by the concentration of polymer solution. The optimum tip-to-collector distance for producing a steady jet of the polymer solution depends on the concentration
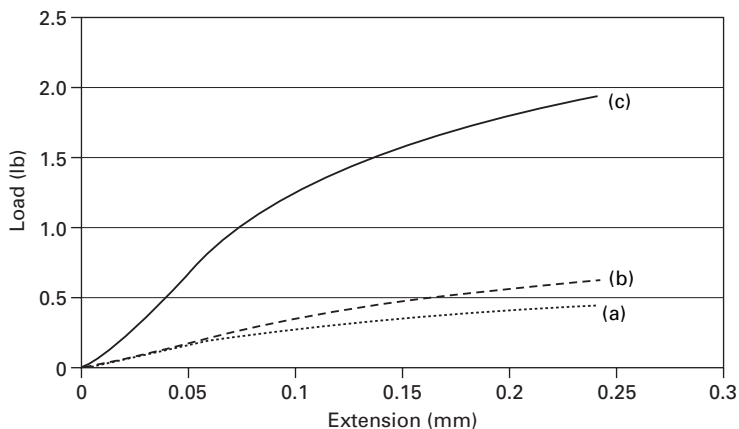
4.13 Load–extension curves for webs made at: (a) *c* = 15%, low MW N6,6; (b) *c* = 10%, low MW N6,6; (c) *c* = 3%, high MW N6,6.

of polymer solution and the voltage. Increasing voltage, up to a given limit, at a specific solution concentration decreased the diameters of electrospun N6 fibers.

Two N6,6 polymers having molecular weights of 30 000 (low MW polymer) and 170 000 g/mol (high MW polymer) were spun from mixed formic acid/ chloroform solutions. Electrospun nonwoven nano-webs were successfully made from 10 and 15% solutions of the low MW N6, while lower polymer concentrations of 3 and 5% were sufficient for electrospinning high MW N6,6. The morphologies and mechanical properties of these nano-scale nonwoven webs were examined. Fiber diameters increased and fiber diameter distributions were broader with increasing polymer concentration for both low and high molecular weight N6,6. Initial moduli of electrospun webs improved for high molecular weight N6,6, particularly when a low polymer concentration (3%) was used. This study demonstrates that the use of high MW N6,6 affords a simple approach for improving the mechanical properties of electrospun nylon filaments.

4.7   References

1. Huang Z., Zhang Y. Z., Kotaki M., Ramakrishna S. (2003), 'A review of polymer nano fibers by electrospinning and their applications in nanocomposites', *Comp Sci Technol*, **63**, 2223–2253.
2. Pedicini A., Farris R. J. (2004), 'Thermally induced color change in electrospun fiber mats', *J Polym Sci Part B: Polym Phys*, **42**, 752–757.
3. Deitze J. M., Kosik W., McKnight S. H., Beak Tan N. C., Desimone J. M., Crette S. (2002), 'Electrospinning of polymer nano-fibers with specific surface chemistry', *Polymer*, **43**, 1025–1029.

4. Ding B., Kim H. Y., Lee S. C., Shao C. L., Lee D. R., Park S. J., *et al.* (2002), 'Preparation and characterization of a nanoscale poly(vinyl alcohol) fiber aggregate produced by using electrospinning method', *J Polym Sci, Part B: Polym Phys*, **40**, 1261–1268.

5. Dai H., Gong J., Kim H. Y., Lee D. R. (2002), 'A novel method for preparing ultra-fine alumina-borate oxide fibers via an electrospinning technique', *Nanotechnology*, **13**, 674–677.

6. Formhals A. (1934), US patent 1,975,504.

7. Formhals A. (1939), US patent 2,160,962.

8. Formhals A. (1940), US patent 2,187,306.

9. Formhals A. (1943), US patent 2,323,025.

10. Formhals A. (1944), US patent 2,349,950.

11. Deitzel J. M., Kleinmeyer J., Harris D., Beck Tan N. C. (2001), 'The effect of processing variables on the morphology of electrospun nanofibers and textiles', *Polymer*, **1**(42), 261–272.

12. Reneker D. H., Chun I. (1997), 'Nanometer diameter fibers of polymer, produced by electrospinning', *Nanotechnology*, **7**, 216–223.

13. Bergshoef M. M., Vancso G. J. (1999), 'Transparent nanocomposites with ultrathin, electrospun nylon-4,6 fiber reinforcement', *Adv Mater*, **11**, 362–365.

14. Doshi J., Reneker D. H. (1995), 'Electrospinning process and applications of electrospun fibers', *J Electrostat*, **35**, 151–160.

15. Gibson P. W., Schreuder-Gibson H. L., Riven D. (1999), 'Transport properties of porous membranes based on electrospun nanofibers', *AIChE J*, **45**, 190–195.

16. Fong H., Renker D. H. (2001), 'Structure formation in polymeric fibers', in Salem D. R., Sussman M. V., Editors. *Electrospinning and Formation of Nanofibers*, Munich: Hanser, 2001, Chapter 6.

17. Hou H., Jun Z., Reuning A., Schaper A., Wendorff J. H., Greiner A. (2002), 'Poly(*p*-xylylene) nanotubes by coating and removal of ultrathin polymer template fibers', *Macromolecules*, **35**, 2429–2431.

18. Kenawy E. R., Bowlin G. L., Mansfield K., Layman J., Simpson D. G., Sanders E. H. (2002), 'Release of tetracycline hydrochloride from electrospun poly(ethylene-co-vinylacetate), polylactic acid and a blend', *J Controlled Release*, **81**, 57–64.

19. Scopelianos A. G. (1996), Pizoelectric biomedical device, US Patent, 5522879.

20. Larrondo L., Manley R. (1981), 'Electrostatic fiber spinning from polymer melts. I. Experimental observation on fiber formation and properties', *J Polym Sci Polym Phys Ed*, **19**, 909–920.

21. Larrondo L., Manley R. (1981), 'Electrostatic fiber spinning from polymer melts. II. Examination of the flow field in an electrically driven jet', *J Polym Sci Polym Phys Ed*, **19**, 921–932.

22. Fong H., Chun I., Reneker D. H. (1999), 'Beaded nanofibers formed during electrospinning', *Polymer*, **40**, 4585–4592.

23. Bognitzki M., Czado W., Frese T., Schaper A., Hellwig M., Steinhart M., *et al.* (2001), 'Nanostructured fibers via electrospinning', *Adv Mater*, **13**, 70–72.

24. Lee K. H., Kim Y. H., La Y. M., Lee D. R., Sung N. H. (2002), 'Influence of a mixing solvent with tetrahydrofuran and *N,N*-dimethylformamide on electrospun polyvinyl chloride nonwoven mats', *J Polym Sci Polym Phys*, **40**, 2259–2268.

25. Zuo W., Zhu M., Yang W., Yu H., Chen Y., Zhang Y. (2005), 'Experimental study on relationship between jet instability and formation of beaded fibers during electrospinning', *Polym Eng Sci*, **45**, 704–709.

26. Lee K. H., Kim H. Y., Ryu Y. J., Kim K. W., Choi S. W. (2003), 'Mechanical behavior of electrospun fiber mats of poly(vinyl chloride)/polyurethane polyblends', *J Polym Sci Part B Polym Phys*, **41**, 1256–1262.

27. Ding B., Kimura E., Sato T., Fujita S., Shiratori S. (2004), 'Fabrication of blend biodegradable nanofibrous nonwoven mats via multi-jet electrospinning', *Polymer*, **45**, 1895–1902.

28. Pedicini A., Farris R. J. (2003), 'Mechanical behavior of electrospun polyurethane', *Polymer*, **44**, 6857–6862.

29. Deitzel J. M., Kleinmeyer J. D., Hirvonen J. K., Beck Tan N. C. (2001), 'Controlled deposition of electrospun poly(ethylene oxide) fibers', *Polymer*, **42**, 8163–8170.

30. Zimmerman J., Mark H. F., Bikales N. M. (1988), in *Encyclopedia of Polymer Science and Engineering*, Vol. 6, New York: Wiley, 802–839.

31. Ziabicki A. (1976), *Fundamentals of Fiber Formation: The Science of Fiber Spinning and Drawing*, New York: Wiley.

32. Ryu Y. J., Kim H. Y., Lee K. H., Park H. C., Lee D. R. (2003), 'Transport properties of electrospun nylon 6 nonwoven mats', *Eur Polym J*, **39**, 1883–1889.

33. Fong H., Liu W., Wang C., Vaia R. A. (2002), 'Generation of electrospun fibers of nylon 6 and nylon 6-montmorillonite nanocomposite', *Polymer*, **43**, 775–780.

34. Larrond O., Manley R. (1981), 'Electrostatic fiber spinning from polymer melts. III. Electrostatic deformation of a pendant drop of polymer melts', *J Polym Sci Polym Phys*, **19**, 933–940.

35. Schreuder-Gibson H. L., Gibson P., Senecal K., Sennett M., Walker J., Yeomans W. (2002), 'Protective textile materials base on electrospun nanofibers', *J Adv Mater*, **34**, 44–55.

36. Stephen J. S., Chase D. B., Rabolt J. F. (2004), 'Effect of the electrospinning process on polymer crystallization chain conformation in Nylon 6 and Nylon 12', *Macromolecules*, **37**, 877–887.

37. Supaphol P., Uppatham C. M., Nithitanakul M. (2005), 'Ultrafine electrospun polyamide 6 fibers: effect of emitting electrode polarity on morphology and average fiber diameter', *J Polym Sci Polym Phys*, **43**, 3699–3712.

38. Uppatham C. M., Nithitanakul M., Supaphol P. (2004), 'Ultrafine electrospun polyamide 6 fibers: effect of solution conditions on morphology and average fiber diameter', *Macromol Chem Phys*, **205**, 2327–2338.

39. Supaphol P., Uppatham C. M., Nithitanakul M. (2005), 'Ultrafine electrospun polyamide 6 fibers: effects of solvent system and emitting electrode polarity on morphology and average fiber diameter', *Macromol Mater Eng*, **290**, 933–942.

40. Dersch R., Liu T., Schaper A. K., Greiner A., Wendorff J. H. (2003), 'Electrospun nanofibers: Internal structure and intrinsic orientation', *J Polym Sci Polym Chem*, **41**, 545–553.

41. Vasanthan N., Kotek R., Jung D. W., Shin D., Tonelli A. E. (2004), 'Lewis acid-base complexation of polyamide 66 to control hydrogen bonding, extensibility and crystallinity', *Polymer*, **45**, 4077–4085.

42. Gogolewski S., Pennings A. J. (1985), 'High-modulus fibres of nylon-6 prepared by a dry-spinning method', *Polymer*, **26**, 1394–1400.

43. Lee K. H., Kim H. Y., Bang H. J., Jung Y. H., Lee S. G. (2003), 'The change of bead morphology formed on electrospun polystyrene fibers', *Polymer*, **44**, 4029–4034.

44. Fong H., Reneker R. H. (1999), 'Elastomeric nanofibers of styrene-butadiene-styrene triblock copolymer', *J Polym Sci Part B Polym Phys*, **37**, 3488–3493.

45. Demir M. M., Yilgor, I., Yilgor, E., Erman, B. (2002), 'Electrospinning of polyurethane fibers', *Polymer*, **43**, 3303–3309.

5

Controlling the morphologies of electrospun nanofibres

T. L I N and X. G. W A N G, Deakin University, Australia

5.1   Introduction

Electrospinning is a unique method of producing continuous polymer fibres. It has received a great deal of attention in recent times due to its versatility in the spinning of a wide variety of polymeric fibres, and its consistency in producing polymer fibres with the fibre diameter on submicrometre or nanometre scales. The as-spun fibres, often in the form of a non-woven mat, have an extremely high surface area to mass ratio and a highly porous structure which has potential applications in areas such as tissue scaffolds (Li *et al*., 2002, Matthews *et al*., 2002, Yoshimoto *et al*., 2003, Subramanian *et al*., 2004), wound dressings (Khil *et al*., 2003, Kim *et al*., 2004), nano-catalysis (Jia *et al*., 2002, Dong and Jones, 2004), protective clothing (Gibson and Schreuder-Gibson, 2000, Gibson *et al*., 2001), filtration (Suthar and Chase, 2001, 2002, Tsai and Schreuder-Gibson, 2003) and optical electronics (Dong *et al*., 2003, El-Aufy *et al*., 2003).

Although the basic electrospinning technique was invented in the 1930s (Formhals, 1934), it is only in recent decades that fundamental research has led to great progress in this area. Studies on understanding the electrospinning process, its operating parameters and material properties have been extensive. Improved electrospinning methods, new fibre structures and potential applications are continually emerging. Professional reviews on the electrospinning process, and the advancement and applications of electrospun nanofibres in specific areas can be found in the literature (Reneker and Chun, 1996, Gibson *et al*., 1998, Bognitzki *et al*., 2001, Buer *et al*., 2001, Huang *et al*., 2003, Frenot and Chronakis, 2003, Jayaraman *et al*., 2004, Kameoka *et al*., 2004, Krishnan *et al*., 2004, Li and Xia, 2004b).

The electrospun nanofibres usually have a regular threadlike structure and some fibres can form a ribbon-like fibrous morphology. The fibre diameter varies in range from 5 nm to 10 μm. Defectives, such as colloid beads or beads-on-string fibres, occur among the resultant fibres, or even as the major product, depending on the operating conditions and the material properties.

90

Also, the electrospun fibres can be deposited either randomly to form a nonwoven web or in an oriented manner to give an aligned nanofibre array. Twisting nanofibre bundles can form nanofibre yarns. Within the fibre web, the nanofibres can be connected physically or bonded at 'cross-points' to form an interconnected 'spider web'. In addition, two polymer components have been combined to form side-by-side, or sheath–core, bicomponent electrospun fibres.

The production of nanofibres in a controlled manner, so that the process gives a high-quality fibre with precise fibre morphology, is a vital task, as the fibre morphology has a significant influence on the fibre performance. The control of fibre morphology has been based on a thorough understanding of the electrospinning process and the factors that affect the electrospinning process and the fibre morphologies. The fibre alignment is controlled through the fibre deposition process and the bicomponent nanofibres are electrospun using special spinnerets.

In this chapter, techniques on controlling the fibre morphology, the fibre orientation, the fibre component and the web morphology during the electrospinning process are discussed. This chapter is divided into seven sections. In Section 5.2, the electrospinning process is introduced briefly, and factors that affect the electrospinning process and the resultant nanofibres will be discussed. Possible approaches for controlling the fibre morphology in the electrospinning process will be introduced. Section 5.3 will discusses the effect of polymer concentration on the solution properties (e.g. viscosity, conductivity and surface tension) that adversely affect the fibre diameter and evenness. Tuning the fibre diameter via adjustments of the polymer concentration is described. Problems and limitations in changing polymer concentrations are discussed. In Section 5.4, fibre beads and approaches to eliminate the beads are presented. Section 5.5 discusses the orientation and assembly of nanofibres. The aligned nanofibre nonwovens and nanofibre yarns are described. The formation of interconnected nanofibre webs is also discussed. In Section 5.6, the preparation and potential applications of bicomponent nanofibres, e.g. core–sheath and side-by-side nanofibres, are given in detail. Section 5.7 discusses possibilities for further research on controlling the morphology of electrospun nanofibres.

5.2   The electrospinning process and fibre morphology

Electrospinning is an effective technique to produce continuous polymer fibres with diameters on submicrometre or nanometre scales (Reneker and Chun, 1996, Jayaraman *et al.*, 2004, Li and Xia, 2004b). It involves a process in which a polymer solution or melt is stretched into fine filaments under the action of a high electrical voltage. The basic electrospinning system, illustrated

in Fig. 5.1, consists of a charged polymer solution that is fed through a small opening or nozzle (usually a needle or pipette tip). When the polymer solution is delivered to the tip of a capillary and a high-voltage difference is established between the tip and the collector electrode, charge accumulates in the polymer solution and at the tip of the capillary a droplet is electrically attracted to the collector electrode, typically 5–30 cm away, deforming into a cone shape which is referred to as a 'Taylor cone'. With an increase in the applied voltage, the cone becomes sharper. When the voltage is larger than a critical value, the droplet overcomes the restriction of the surface tension: a jet is thus produced, forming fine filaments. Evaporation of the solvent from the filaments results in solid fibres.

Although both polymer solutions and polymer melts have been electrospun into fibres, most studies have been focused on the polymer solution. Literature is scarce on the polymer melt-based electrospinning process. Therefore, in this chapter, the discussion is limited to the solution-based electrospinning system.

It has been well established that both operating parameters and material properties affect the electrospinning process and the resulting fibre morphology. The operating parameters include the applied electrical field, the flow rate of the polymer solution, the distance between the nozzle and the collector (spinning distance), and the diameter of the spinneret, etc. A minute change in the operating parameters can lead to a considerable change in the fibre morphology. For example, finer nanofibres are electrospun from a nozzle of smaller diameter (Katti *et al*., 2004); increasing the flow rate leads to larger fibre diameter; and a higher applied voltage results in the emergence of fibre
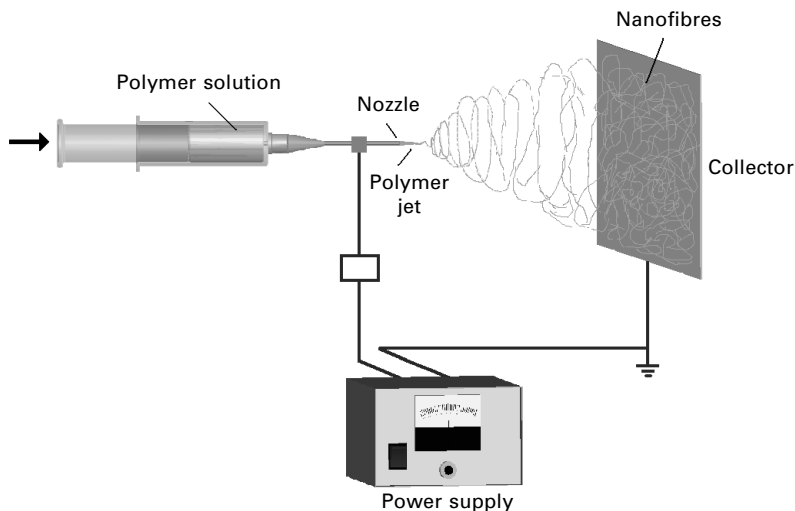
5.1 A basic electrospinning system.

beads, though reducing the fibre diameter (Deitzel *et al.*, 2001, Lee *et al.*, 2004).

The material properties that affect the electrospinning process and the fibre morphology include the polymer concentration, the solution viscosity, the solution conductivity, the surface tension and other properties concerning the solvent as well as the polymer itself. Among the material properties, the solution concentration plays a major role in stabilizing the fibrous structure because it also affects other solution properties, such as the solution viscosity, the surface tension and the conductivity. The solvent used is another important factor because it mainly determines the surface tension and the evaporation process. The volatility of the solvent affects the fibre surface morphology and the web structure.

The solution bulk properties come from intermolecular interactions among the solvent molecules and the polymer macromolecules. Any factors that interfere with these interactions change the solution properties that affect the electrospinning process, and the fibre morphology is thus altered accordingly. For example, the solution viscosity is closely related to the entanglement of polymer macromolecules. In a good solvent, polymer chains with a higher molecular weight tangle with each other more easily, which leads to a higher solution viscosity. Electrospinning such a polymer solution produces continuous and uniform fibres. However, when polymer of a lower molecular weight is electrospun, even at the same polymer concentration, the resultant fibre could have a colloid bead or beaded fibre morphology (Koski *et al.*, 2003).

In theory, any factor that affects the electrospinning process also provides a means to control the fibre morphology. In practice, however, only factors with a noticeable and reliable influence on fibre morphology can be employed for this purpose. Methods of controlling the fibre morphology have been reported based on either the operating parameters or the material properties.

5.3   Polymer concentration and fibre diameter

As the polymer concentration plays a major role in the electrospinning process, it is not surprising that the polymer concentration has been extensively exploited to change and control fibre morphology in electrospinning. This effort has also led to improved understanding on the effect of the polymer concentration on other solution properties, such as viscosity, surface tension and conductivity. Under the same electrospinning conditions, increasing the polymer concentration will increase the diameter of the electrospun fibres. However, a non-linear relationship between the solution concentration and the fibre diameter usually forms (Deitzel *et al.*, 2001). The reasons for this non-linear relationship can be attributed to the non-linear relationship between the polymer concentration and the solution viscosity. As illustrated in Fig. 5.2, when the polymer concentration is low, the solution viscosity increases slightly
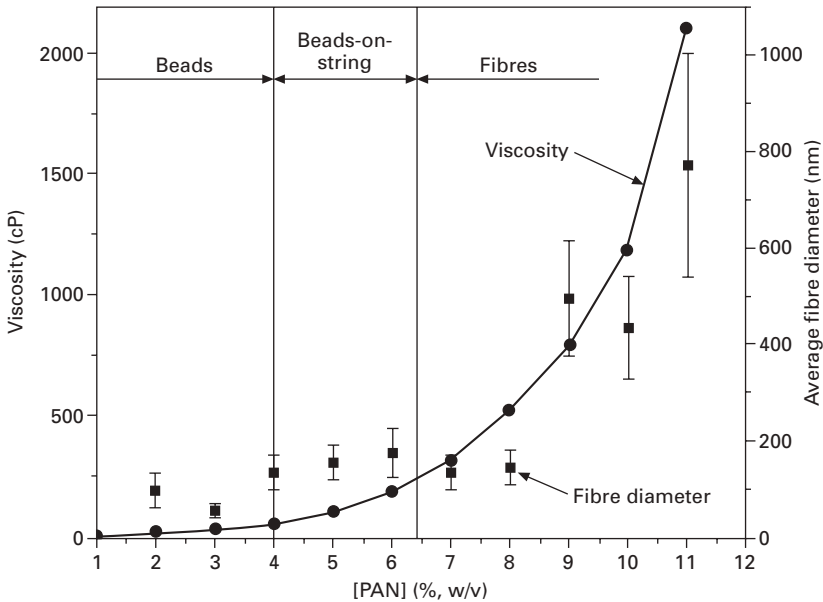
5.2 Relationship between polymer concentration, solution viscosity and diameter of electrospun polyacrylonitrile (PAN) fibres.

with the increase in the polymer concentration. As the polymer concentration increases, the viscosity increases gradually until the concentration reaches a specific value, after which the viscosity increases considerably (Lin *et al.*, 2005a).

In the electrospinning process, the solvent evaporates from the jet/filament continuously until the jet becomes dry. Stretching the jet increases the surface area, which accelerates the solvent evaporation. From the initial jet to dry fibres, the fibre stretching process is very quick, taking only tens of milliseconds (Shin *et al.*, 2001a). If the strength to stretch the filaments remains the same, electrospinning a polymer solution of higher viscosity could be much harder than that with a lower viscosity, because the concentration has a larger influence on the viscosity when the concentration is high. On the other hand, the polymer concentration affects the solution conductivity, which further influences the solution charge density (Shin *et al.*, 2001b). The stretching is enhanced as a result of increased charge density. This could compensate to some extent for the difficulty in stretching a solution of higher polymer concentration. In certain cases, the strength is improved to such an extent that it neutralizes the effect of the viscosity, which results in a similarly linear relationship between the concentration and the fibre diameter.

The relationship between the solution viscosity and the polymer concentration is highly dependent on the nature of the polymer (e.g. structure and molecular weight) and the intermolecular interactions within the polymer

solution (polymer–polymer, polymer–solvent, solvent–solvent, etc.). Because of these variants, it is almost impossible to establish a universal formula to include all polymer–solvent systems in a given electrospinning process. A conventional approach for controlling the fibre diameter is based on the understanding of the dependent relationship between the polymer concentration and the average diameter of the electrospun nanofibres, given the solvent system and specific operating conditions (e.g. the applied voltage, the flow rate and the spinning distance).

Although reducing the polymer concentration is a straightforward way to produce finer nanofibres, electrospinning a dilute polymer solution usually leads to the emergence of colloid beads or beads-on-string fibres (also called 'necklace fibres'). These defectives even become the main products when the polymer concentration is very low. Because of this, the electrospinning of bead-free and uniform nanofibres particularly for fibre diameters less than 100 nm still remains a great challenge.

The electrospinning of an extremely dilute polymer solution to produce colloid beads is usually called 'electrospraying' (Kebarle and Peschke, 2000). The suggested explanation is that the viscoelastic force in the jet is too small to hold the fibrous structure. The jet gets dissociated into individual charged sections, and these sections usually turn into droplets owing to the action of the surface tension. With the evaporation of the solvent, the droplet reduces its size. This leads to an increase in the surface charge density. The droplet can further split into smaller droplets due to the higher electrostatic repulsion (Fig. 5.3a).

As the polymer concentration increases, the solution viscosity also increases. The jet under the higher viscoelastic force is more difficult to break into
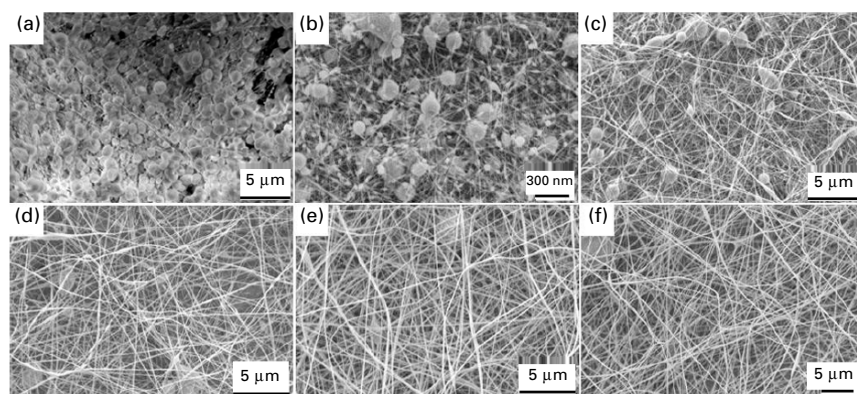
5.3 Product morphologies when electrospinning polyacrylonitrile/DMF(*N, N*-dimethylformamide) solution at different concentrations of (a) 2%, (b) 3%, (c) 4%, (d) 5%, (e) 6%, (f) 7% (w/v).

individual sections. Instead, the electrostatic repulsion among the like-charged sections elongates the thin 'links' between the sections, forming thinner filaments. As a result of the orientation of the macromolecular polymer, these filaments become hyper-stabilized (Yarin, 1993). Meanwhile, the relatively thicker sections get stretched thinner as well, although to a lesser extent than the 'links'. Under the action of surface tension, they tend to take the shape of a droplet or bead. With the evaporation of the solvent, an apparent beads-on-string structure is thus formed (Fig. 5.3b–d). Further increasing the solution viscosity provides a larger viscoelastic force to resist rapid changes in shape. This allows for more uniform stretching, resulting in a continuous and homogeneous fibre structure (Fig. 5.3e and f).

It has been well established that the solution viscosity is highly dependent on the intermolecular interaction of the polymer (Bercea *et al.*, 1999). Generally, in a dilute polymer solution, the intermolecular distance is so large that the intermolecular interactions are very weak. The intermolecular interactions become predominant gradually with the increase in polymer concentration. At a certain concentration, c^*, the domains of the polymer molecules begin to overlap and eventually an entanglement may develop. Thus, c^* is a critical concentration to distinguish whether an obvious intermolecular interaction will happen in the polymer solution. The higher concentration regime, named as semi-dilute, is characterized by the intermolecular interaction and eventual entanglements. In addition, it is worth noting that a high applied voltage also leads to the formation of a beaded fibre (Deitzel *et al.*, 2001).

5.4   Fibre bead formation and fibre surface morphology

The formation of beaded fibres has been attributed to a low solution viscosity (Fong *et al.*, 1999, Lee *et al.*, 2003). Increasing the polymer concentration, which results in an increase in the solution viscosity, has been the conventional approach to prevent the formation of the beads. However, increasing the solution viscosity is not always effective. With some polymers, polystyrene for instance, even a high concentration of polymer solution does not guarantee bead-free electrospun fibres.

Our research indicates that for a given solution viscosity, the solution conductivity has a significant effect on the formation of beaded fibres. The addition of a small amount of ionic surfactant into the polymer solution is able to suppress the formation of beads effectively (Lin *et al.*, 2004). As shown in Fig. 5.4a, beads proliferate as a result of electrospinning a normal polystyrene solution. Increasing the flow rate increased the number of beads. Efforts to eliminate the beaded fibres by adjusting the operating conditions and changing the polymer concentrations were unsuccessful. However, when a small amount of cationic surfactant was added to the same polymer solution,
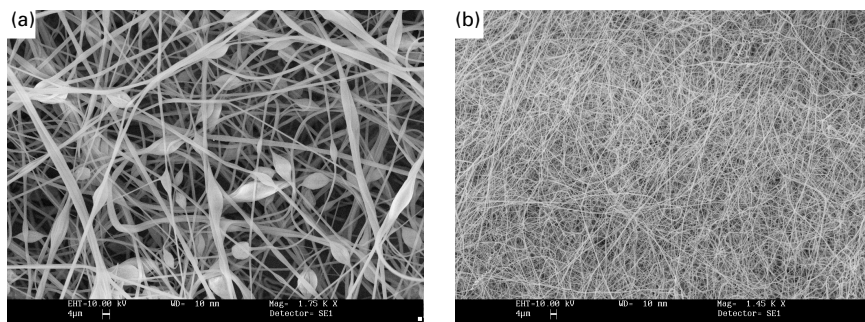
5.4 Electrospun polystyrene fibres: (a) non-uniform beaded fibres electrospun from an ordinary electrospinning process; (b) bead-free fibres electrospun from the same polymer solution with the addition of a cationic surfactant.

the same electrospinning process produced non-beaded fibres. The SEM image (Fig. 5.4b) reveals bead-free and uniform fibres as a result of surfactants added to the polymer solution. No isolated beads and beads-on-string structures were found. The surfactant was so effective that a concentration as low as 10^{-6} mol/l was enough to prevent the formation of the beaded fibres.

Reasons as to why the addition of ionic surfactant prevents the formation of beaded fibres can be found in the effect of ionic surfactant on polymer properties. When the polymer concentration is the same, with the increase in surfactant concentration, the solution viscosity has a slight increase and the surface tension has a minor reduction; however, the solution conductivity increases considerably. Increasing the solution conductivity leads to an increase in the solution charge density. With increased charges within the filaments, their interaction with the external electric field and their repulsion to each other are enhanced, which improves the stretch of the filaments. Under the stronger stretching forces, the liquid filaments are extended in a more rapid and uniform way, which prevents the filaments from forming beaded sections. When the electrospun fibres become uniform, further addition of the ionic surfactant into the polymer solution reduces the fibre diameter. As shown in Fig. 5.5, as the surfactant concentration increases, the average fibre diameter decreases gradually, and the fibre distribution becomes narrow as well (Lin *et al.*, 2004).

Both the anionic and the cationic surfactants have been found to improve the solution charge density that enhances the fibre stretching process. It appears that there is no difference between adding an anionic and a cationic surfactant into the polystyrene solution, because they both lead to bead-free and uniform fibres. However, when a surfactant molecule is able to associate with the polymer linkage in the solution, it gives rise to an improvement in fibre evenness, because this polymer–surfactant interaction tends to make
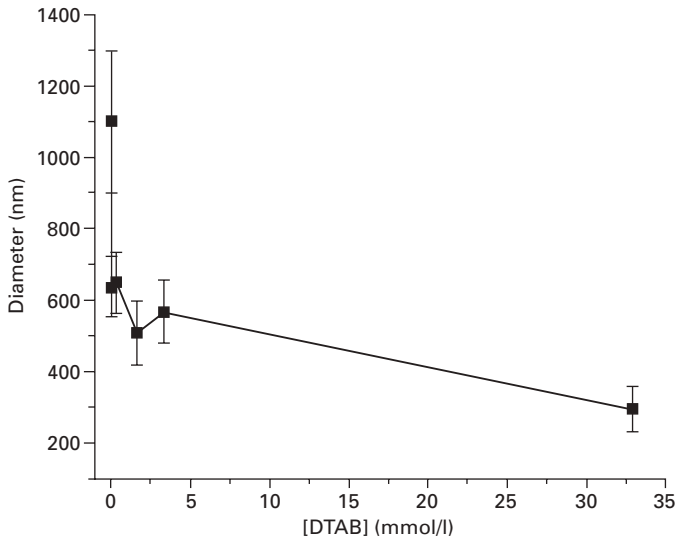
5.5 Average fibre diameter vs surfactant concentration. The surfactant used is dodecyltrimethylammonium bromide (DTAB).

the polymer–surfactant become polyions. Other additives, such as NaCl, pyridinium formate and polyelectrolyte, have also been reported to improve fibre evenness (Fong *et al*., 1999, Jun *et al*., 2003, Won *et al*., 2004).

By comparison with the ionic surfactants, a non-ionic surfactant, Triton X-405, was added to the polystyrene solution, and the solution was electrospun in the same operating conditions. It was observed that the beaded fibres were still produced, but the fibre and bead morphologies are different from those that were electrospun from a polystyrene solution not containing surfactants. The addition of surfactant into the solution would affect the formation of 'Taylor corn', as observed by other researchers (Yao *et al*., 2003), who also found that a non-ionic surfactant made the electrospinning process stable.

The feasibility of stopping the formation of fibre beads by adding ionic surfactants to a dilute polymer solution has also been studied (Lin et al., 2005a). As shown in Fig. 5.6, when a small amount of ionic surfactant was added to the dilute polymer solution, beads changed to a beads-on-string structure. Also, when the ionic surfactant was added to a semi-dilute polymer solution the fibres became quite uniform.

5.4.1   Surface morphology

The surface morphology of electrospun fibres is affected by the polymer used, the voltage applied and the solvent, as well as the environmental conditions (e.g. humidity). The fibres may have either a smooth or a porous/
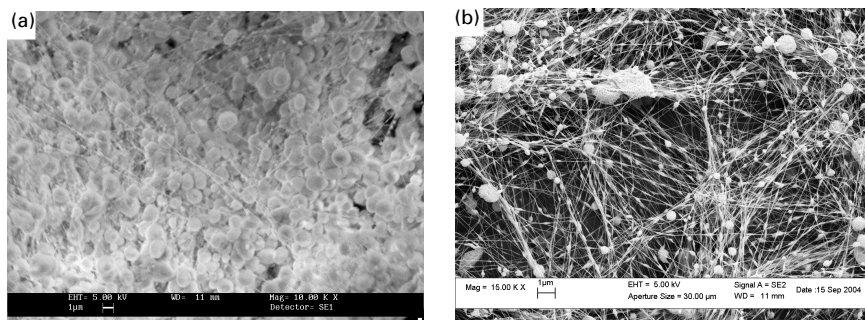
5.6 SEM images of fibres electrospun from 2% PAN/DMF solution: (a) the solution does not contain any additives; (b) the solution contains 0.1% (w/v) dodecyltrimethylammonium bromide (DTAB).
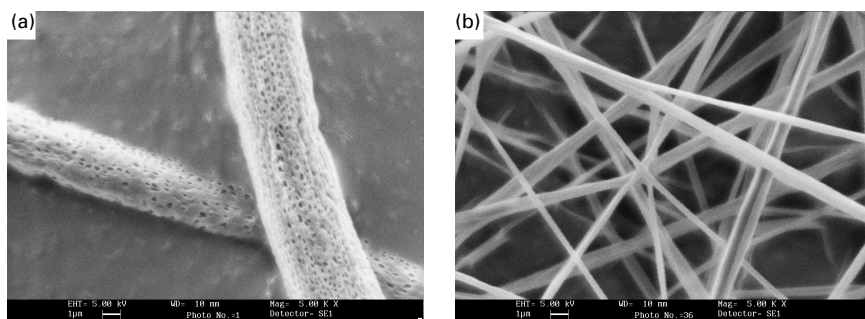
5.7 SEM images of electrospun PLA fibres: (a) chloroform as the solvent; (b) chloroform–DMF mixture (50:50 v/v) as the solution.

rough surface. A higher applied voltage leads to a rougher fibre surface (Deitzel et al., 2001).

Porous fibres containing lots of ellipse-like holes on the fibre surface layer have been electrospun from a polylactic acid (PLA)–chloroform solution (Fig. 5.7a). However, when the solution used chloroform–DMF mixture as the solvent, the same operating condition gave a finer nanofibre with a smooth fibre surface (Fig. 5.7b). Porous fibres have also been electrospun from polycarbonate, poly (methyl methacrylate) and polystyrene (Megelski et al., 2002).

Reasons for the formation of the porous surface have been explained as a phase separation occurring during the cooling of fibres. The rapid solvent evaporation and subsequent condensation of moisture into water particles result in the formation of nano- or micropores on the fibre surface (Casper et al., 2004). When the environment humidity increases, the pore size becomes larger. However, this result was observed only when the solution used a highly volatile organic solvent, such as chloroform, tetrahydrofuran and acetone.

5.5   Controlling fibre alignment and web morphologies

The driving forces for the deposition of electrospun fibres come from an electric field between the charged spinneret and the grounded collector. Owing to the existence of electric charges, the as-spun fibres increase the local electric potential of the collector. The deposition of the as-spun fibres on the collector is affected by the local electric potential. The fibres or fibre sections later deposited on the collector are electrically repulsed by the previously deposited fibres. Thus they adjust their direction automatically towards an area that has a lower electric potential. A dynamic change in the electric potential profile leads to random deposition of fibres, which results in a nonwoven fibrous web, as usually observed in an ordinary electrospinning process. However, orientated or aligned nanofibres can be formed if the fibres are deposited in a controlled way.

5.5.1   Fibre orientation

Earlier works on controlling the fibre orientation used a moving roller (Pedicini and Farris, 2003) (Fig. 5.8a) or a vibrating metal plate (Sundaray *et al*., 2004, Teo *et al*., 2005) (Fig. 5.8b) as the collector. When the roller rotated at a high speed (surface velocity 9–10 m/s), the fibre sections deposited first on the roller would move with the collector at the same speed. This additional movement drew other fibre sections which had not deposited on the collector to move with the movement of the collector. As a result, the fibres were deposited with their direction parallel to the direction of the movement, thus giving a partially orientated fibre mat. When the moving speed was high enough, the collector was able to further elongate the as-spun fibres, thus leading to a higher molecular orientation within the fibres (Fennessey and Farris, 2004).

A sharp-edged metal disc has also been used to control the fibre alignment (Fig. 5.8c). Although the roller rotates at a relatively lower speed, fibres with very good alignment can be produced (Theron *et al*., 2001, Xu *et al*., 2004). Using a motionless metal frame (2 cm × 6 cm) as the electrode (Fig. 5.8d), the aligned nanofibres can be easily collected (Dersch *et al*., 2003). During the fibre deposition, a fibre first attaching to one side of the frame makes the local electric potential increase instantly. The electrical repulsion leads fibre sections arriving later to be deposited at the opposite side of the frame. This results in the fibres being deposited vertically to the frame side in order to avoid the repulsing force. Fibres deposited later on the frame are repulsed electrically by the fibres deposited previously, which therefore results in a parallel arrangement. The electrospinning process finally gives an aligned nanofibre array. When the collector uses an inter-parallel grounded electrode
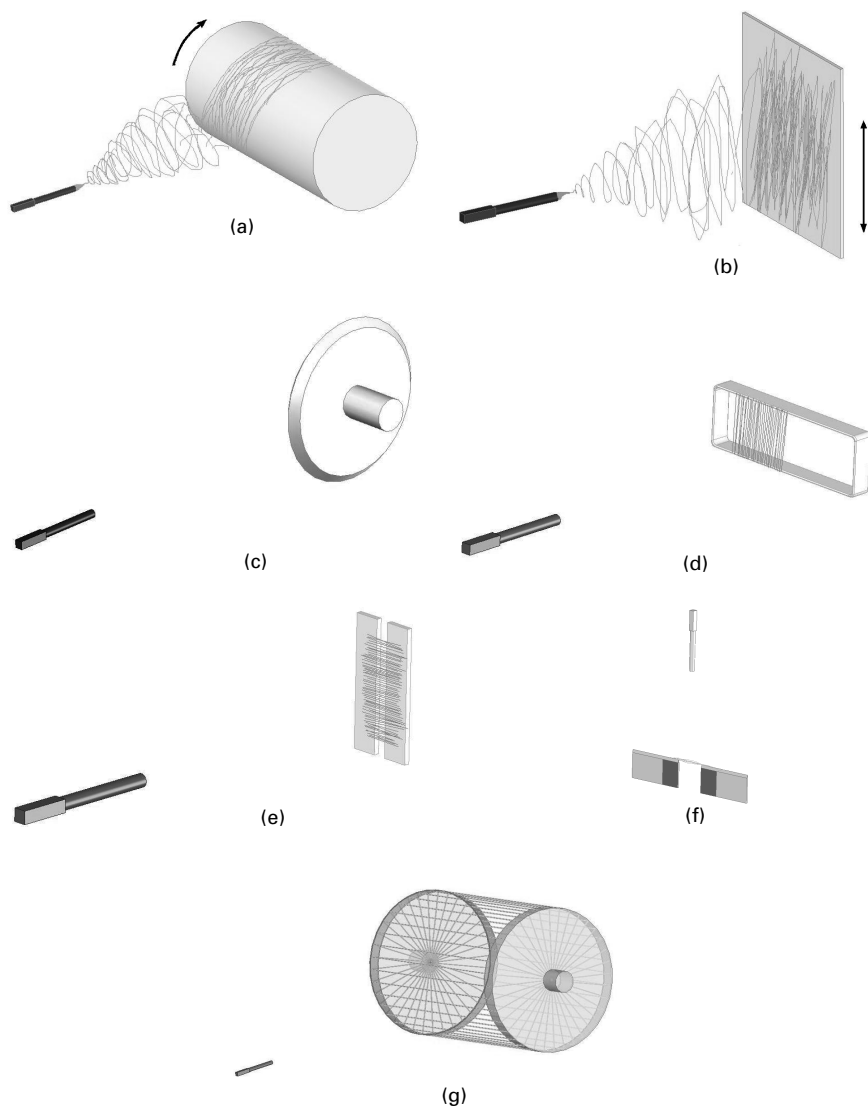
5.8 Collectors used for regulating the fibre collection process: (a) rotating roller; (b) vibrating plate; (c) sharp edged rotating disc; (d) frame; (e) fork; (f) point collector; (g) drum.

couple (the distance between micrometres to millimetres) (Fig. 5.8e), the nanofibres are aligned in the same way (Li *et al*., 2003).

Based on the above concept, a silicon wafer, containing four couples of inter-paralleled Au stripes, has been used as the collector. The selective connection of one electrode couple to the ground electrode each time in

sequence in the electrospinning process enables the deposition of fibres layer-by-layer, with fibres parallel to each other within each layer, yet having a different orientation among the layers (Li *et al*., 2004b). A wire drum collector (Fig. 5.8g), consisting of a group of metal frames in the form of a cylindrical collector, has been used to produce the aligned nanofibres continuously (Katta *et al*., 2004). With rotating the drum slowly, a wire with the closest distance to the spinneret will be deposited by a fibre section firstly, followed by the deposition of other fibre sections on the next wire, due to the electric field attraction. With the movement of the collector, the fibres are deposited from one wire to the next. Because of the electrostatic forces, the fibres stretch across the shortest distance between the wires and thus cause the fibres to align. In addition, a well-aligned nanofibre bundle has been prepared using two fixed points as the collector (Teo and Ramakrishna, 2005) (Fig. 5.8f).
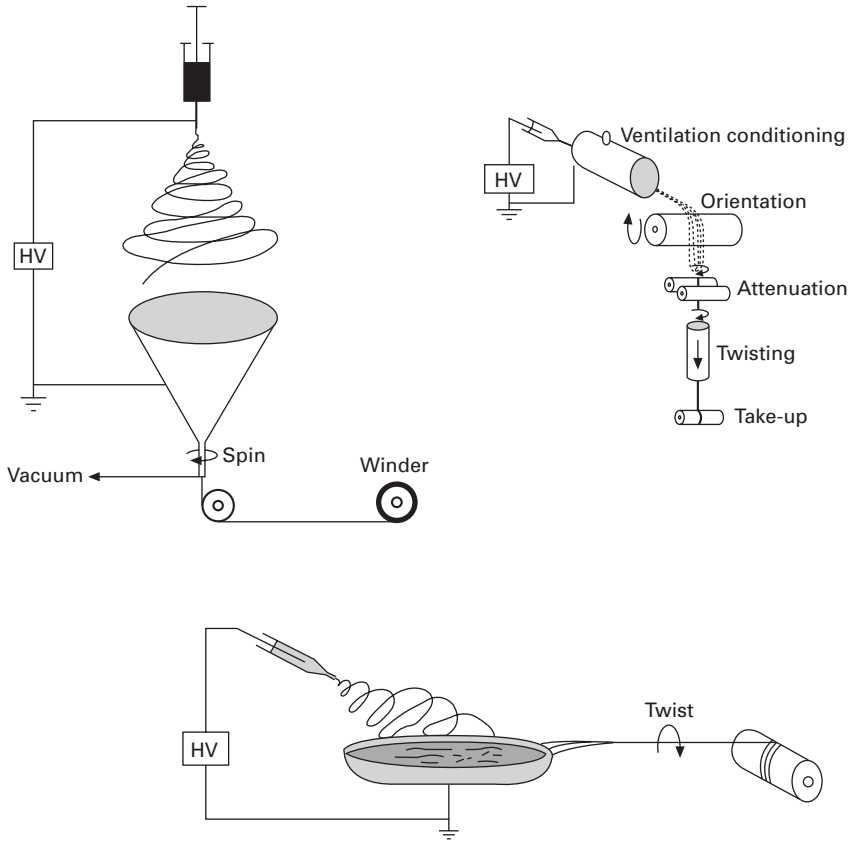
5.5.2   Nanofibre yarns

Yarns are continuous fibre bundles with the fibres partially oriented. The preparation of yarn has been based on either an *in situ* or a postspinning twisting process. The preparation of a continuous nanofibre yarn consists of a special deposition system which collect the fibres continuously and twists in sequence so as to form a continuous yarn. A metal cylinder (Ko *et al*., 2003) and a funnel-like collector (Kim *et al*., 2003) have been employed for this purpose, and when the nanofibres are electrospun to the inner side of the collector, they are drawn mechanically, or with the aid of vacuum, into a continuous thread, and twisted by rotating the collector or by using an additional twisting system, to form a continuous yarn (Fig. 5.9).

Water has also been used as the collecting medium. When the fibres are directly electrospun in to water, they are usually floated on the water surface to form a thin fibre membrane. Drawing and twisting this nanofibre membrane results in a nanofibre yarn (Smit *et al*., 2005) (Fig. 5.9). In addition, simply twisting a thin nanofibre stripe cut from a regular electrospinning nanofibre mat also gives a nanofibre yarn (Fennessey and Farris, 2004). The twisting treatment leads to a partially orientated nanofibre bundle and the twisting angle affects the yarn's mechanical strength.

5.5.3   Web structure

Although a random deposition of electrospun fibres gives a nonwoven fibre structure, the web morphology varies depending on the polymer properties and the operating conditions. Usually, the nanofibres are accumulated by a simple physical interaction and the fibres do not bond with each other. However, when the electrospinning distance is very short, the solvent has insufficient

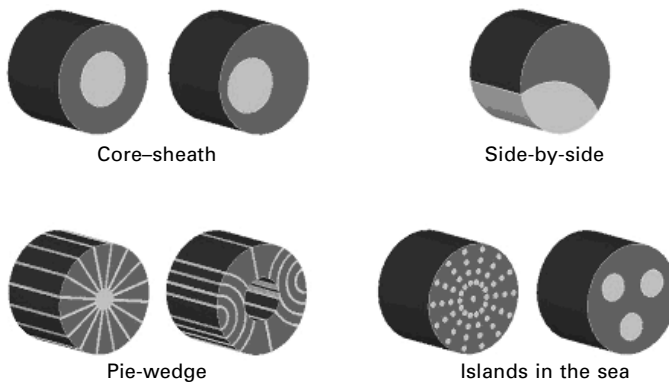*5.9* Process for the preparation of nanofibre yarns.

time to evaporate from the filaments because of the short flying time. Wet or semidry nanofibres are stuck and bonded together, forming an interconnected fibre web (Buchko *et al.*, 1999). Even with dry electrospun fibres, if they come from an elastomeric polymer, an interconnected web structure could also be formed, because the polymer has a low glass transition temperature. As shown in Fig. 5.10, the elastomeric nanofibres merge at their 'crossover points' to form an interconnected web, or combine into larger fibres.

5.6   Bicomponent cross-sectional nanofibres

As with conventional bicomponent fibres, a bicomponent nanofibre consists of two or more polymer components within the same filament, with each component existing separately (Khatwani and Yardi, 2003). According to the cross-sectional morphology, the bicomponent fibres can be classified into

EHT= 5.00 kV   WD= 14 mm   Mag= 8.00 K X
1µm   Photo No.=478   Detector= SE1
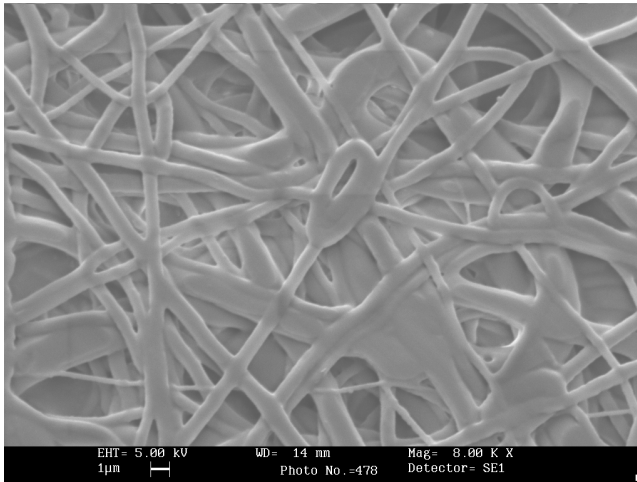
5.10 An interconnected nanofibre web electrospun from elastomeric polyurethane.

Core–sheath

Side-by-side

Pie-wedge

Islands in the sea

5.11 Cross-sectional morphologies of the bicomponent fibres.

four main types: 'core–sheath', 'side-by-side', 'pie-wedge' and 'islands in the sea'. Their cross-sectional morphologies are illustrated in Fig. 5.11.

Although the existing fibre-making technique is able to produce a bicomponent fibre of many cross-sectional structures, the production of bicomponent nanofibres has been limited to two basic types of cross-sectional structures, the 'core–sheath' and the 'side-by-side'. These bicomponent nanofibres are electrospun via special spinnerets. Two polymer solutions flow within the spinneret as the sheath and core, or side-by-side, to the tip of the nozzle and then are subjected to a co-electrospinning process. The formation of bicomponent nanofibres is determined by the laminar bicomponent jet.

5.6.1   'Core–sheath' nanofibres and hollow nanofibres

The core–sheath nanofibres are prepared by using a co-axial spinneret as the nozzle (Sun *et al*., 2003, Yu *et al*., 2004). In the electrospinning process, the two polymer solutions are delivered to the tip of the nozzle via the small tube and the interlayer between this small tube and the larger co-axial tube, separately, and then co-electrospun into 'core–sheath' nanofibres (Fig. 5.12). The dimensions of the core and the sheath can be adjusted via the solution concentration and their relative flow rates. The two polymer solutions can use either the same or different types of solvents. Such a co-electrospinning process is also suitable for a polymer couple which generates a precipitate while mixing (Li *et al*., 2004a). Even a pure liquid or a solution of a small molecule which is not able to be electrospun alone can also be used as the core solution, and the co-axial bicomponent electrospinning process still works very well (Li and Xia, 2004a).

'Hollow nanofibres' (also called 'nanotubes') can be prepared easily from this core–sheath nanofibre by selectively removing the 'core' from the bicomponent nanofibres. To facilitate removal, a heavy mineral oil is used as the core material, which can therefore be removed by a simple dissolving/ extracting process (Li and Xia, 2004a). SEM and TEM images can clearly confirm the tubulous morphology.

Another approach to prepare the hollow nanofibres used electrospun nanofibres as the template ('tubes-by-fibre-template' technique, TUFT). The nanofibres are firstly coated with a layer of shell material and then the fibre material is removed by dissolving or calcination, giving tubulous fibres.
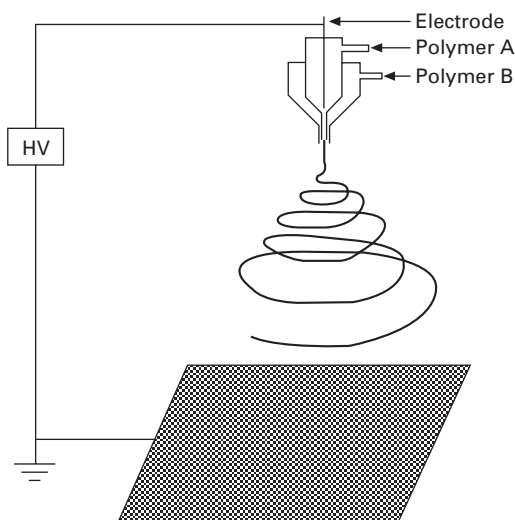
*5.12* Apparatus for electrospinning 'core–sheath' nanofibres.

This technique has been used to prepare metal (Pinto *et al*., 2004), polymer (Bognitzki *et al*., 2000, Hou *et al*., 2002) and inorganic oxide (Caruso *et al*., 2001, Zhang *et al*., 2005) nanotubes.

### 5.6.2   'Side-by-side' nanofibres and sharp-edged cross-sectional nanofibres

Early attempts to prepare the 'side-by-side' bicomponent nanofibres were also based on a co-electrospinning process (Gupta and Wilkes, 2003). In the experiment, two charged polymer solutions were delivered via different syringes to the tip of a single nozzle and then electrospun into nanofibres. Although energy dispersive X-ray spectrometry (EDS) analysis confirmed that the as-spun nanofibre mat had both polymer components, there is no clear proof to indicate whether the fibre has a 'side-by-side' bicomponent cross-sectional morphology.

Using a microfluidic device as the nozzle and putting two polymer solutions into the same microfluidic channel side-by-side, Lin *et al.* (2005b) have electrospun the side-by-side bicomponent nanofibres successfully (Fig. 5.13). The 'side-by-side' fibre morphology can be clearly proved by selective removal of one of the polymer components from the nanofibres. As shown in Fig. 5.14b, when the polyurethane moiety is removed from a polyacrylonitrile–polyurethane (PAN-PU) bicomponent nanofibre, the residual PAN moiety retains its fibrous structure, except that one side is removed from the fibre.

Further proof can be found in the cross-sectional view of the nanofibres. As shown in Fig. 5.14c and d, the TEM image indicates that all the PU-PAN
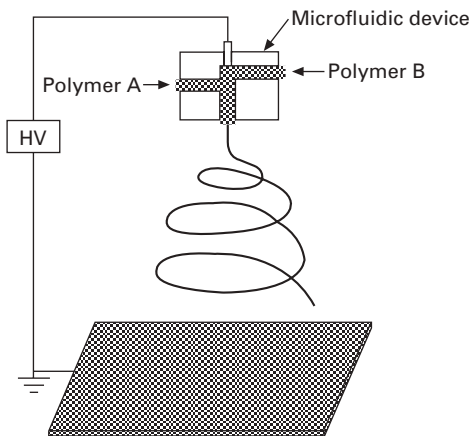
5.13 Schematic for electrospinning the 'side-by-side' bicomponent nanofibres.
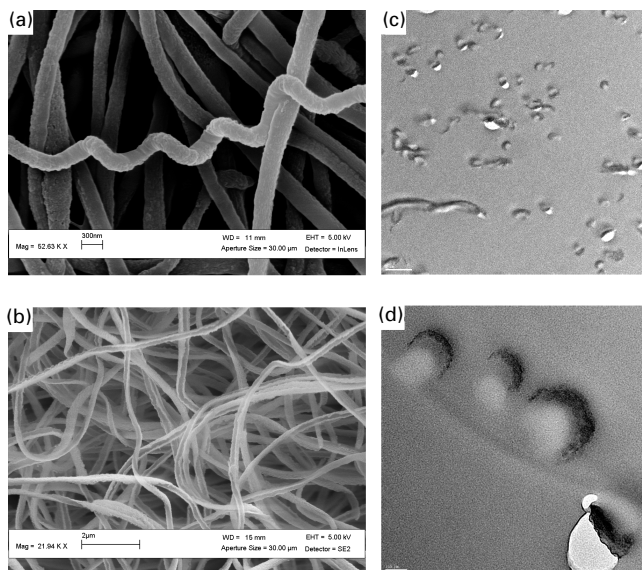
5.14 SEM image of PU-PAN side-by-side nanofibres (a) and the same side-by-side nanofibre after dissolving the PU moiety (b). TEM image of the cross-sectional morphology of PU-PAN side-by-side nanofibres (c, d). Scale bars are 1 µm (c) and 100 nm (d).

fibres have both a light and a dark area in the fibre cross-sections, which suggests that the fibre has two side-by-side components. The light area has been confirmed to be the polyurethane, while the dark area is the PAN moiety. The PAN side has a 'U'-shaped cross-section. Selective removal of the PU 'side' from the nanofibres leaves a sharp-edged cross-sectional nanofibre (Fig. 5.14b).

It is very interesting to observe that when the 'side-by-side' bicomponent nanofibres are electrospun from an elastomeric polymer and a thermal plastic, the as-spun nanofibres have curly or helically crimped fibre morphologies (Fig. 5.14a). The diameter of the helix can be as small as 500 nm. Therefore, the side-by-side co-electrospinning process could be an effective route for the production of helical or crimped polymer nanofibres.

5.7   Future trends

Although significant progress has been made in electrospinning in recent times, theoretical research on electrospinning nanofibres in a controlled way is still at an early stage. There is considerable potential for the improvement of the electrospinning process and for the modification of fibre morphology.

One of the challenges to the electrospinning technique is for the production of uniform and fine nanofibres (with fibre diameter less than 100 nm) from

different types of polymers. Other challenges include controlling the fibre morphology in a precise way, such as preparing the nanofibres with specific dimension, morphology and web structure, or with specific component arrangement. The 'core–sheath' and 'side-by-side' bicomponent fibres are the basic structures of bicomponent fibres. Methods for the preparation of more complex bicomponent nanofibres such as 'island-in-the-sea' and 'pie-wedges' have yet to be developed.

In addition, electrospinning of polymer melt is also interesting as no solvent is involved in the process. Further research is warranted to examine the effects of both operating conditions and material properties on the properties and morphologies of nanofibres electrospun from polymer melts.

5.8   Acknowledgements

5.9   References

Bercea, M., Morariu, S., Ioan, C., Ioan, S. and Simionescu, B. C. (1999) *European Polymer Journal*, **35**, 2019–2024.

Bognitzki, M., Hou, H., Ishaque, M., Frese, T., Hellwig, M., Schwarte, C., Schaper, A., Wendorff, J. H. and Greiner, A. (2000) *Advanced Materials (Weinheim, Germany)*, **12**, 637–640.

Bognitzki, M., Czado, W., Frese, T., Schaper, A., Hellwig, M., Steinhart, M., Greiner, A. and Wendroff, J. H. (2001) *Advanced Materials (Weinheim, Germany)*, **13**, 70–72.

Buchko, C. J., Chen, L. C., Shen, Y. and Martin, D. C. (1999) *Polymer*, **40**, 7397–7407.

Buer, A., Ugbolue, S. C. and Warner, S. B. (2001) *Textile Research Journal*, **71**, 323–328.

Caruso, R. A., Schattka, J. H. and Greiner, A. (2001) *Advanced Materials (Weinheim, Germany)*, **13**, 1577–1579.

Casper, C. L., Stephens, J. S., Tassi, N. G., Chase, D. B. and Rabolt, J. F. (2004) *Macromolecules*, **37**, 573–578.

Deitzel, J. M., Kleinmeyer, J., Harris, D. and Beck Tan, N. C. (2001) *Polymer*, **42**, 261–272.

Dersch, R., Liu, T., Schaper, A. K., Greiner, A. and Wendorff, J. H. (2003) *Journal of Polymer Science*, *Part A: Polymer Chemistry*, **41**, 545–553.

Dong, H. and Jones, W. E. (2004) In *Abstracts of Papers*, *228th ACS National Meeting*, *Philadelphia*, *PA*, *United States*, *August 22–26*, *2004*, pp. INOR-317.

Dong, H., Megalamane, U. and Jones, W., Jr (2003) *Polymer Preprints (American Chemical Society*, *Division of Polymer Chemistry)*, **44**, 124–125.

El-Aufy, A. K., Naber, B. and Ko, F. K. (2003) *Polymer Preprints (American Chemical Society*, *Division of Polymer Chemistry)*, **44**, 134–135.

Fennessey, S. F. and Farris, R. J. (2004) *Polymer*, **45**, 4217–4225.

Fong, H., Chun, I. and Reneker, D. H. (1999) *Polymer*, **40**, 4585–4592.

Formhals, A. (1934) US Patent 1975504 (Schreiber-Gastell, Richard).

Frenot, A. and Chronakis, I. S. (2003) *Current Opinion in Colloid & Interface Science*, **8**, 64–75.

Gibson, P. and Schreuder-Gibson, H. (2000) *Materials Division (American Society of Mechanical Engineers)*, **91**, 45–61.

Gibson, P., Schreuder-Gibson, H. and Pentheny, C. (1998) *Journal of Coated Fabrics*, **28**, 63–72.

Gibson, P., Schreuder-Gibson, H. and Rivin, D. (2001) *Colloids and Surfaces*, *A: Physicochemical and Engineering Aspects*, **187–188**, 469–481.

Gupta, P. and Wilkes, G. (2003) *Polymer Preprints (American Chemical Society*, *Division of Polymer Chemistry)*, **44**, 82–83.

Hou, H., Jun, Z., Reuning, A., Schaper, A., Wendorff, J. H. and Greiner, A. (2002) *Macromolecules*, **35**, 2429–2431.

Huang, Z.-M., Zhang, Y.-Z., Kotaki, M. and Ramakrishna, S. (2003) *Composites Science and Technology*, **63**, 2223–2253.

Jayaraman, K., Kotaki, M., Zhang, Y., Mo, X. and Ramakrishna, S. (2004) *Journal of Nanoscience and Nanotechnology*, **4**, 52–65.

Jia, H., Zhu, G., Vugrinovich, B., Kataphinan, W., Reneker, D. H. and Wang, P. (2002) *Biotechnology Progress*, **18**, 1027–1032.

Jun, Z., Hou, H., Schaper, A., Wendorff, J. H. and Greiner, A. (2003) *e-Polymers*, Paper No. 9.

Kameoka, J., Czaplewski, D., Liu, H. and Craighead, H. G. (2004) *Journal of Materials Chemistry*, **14**, 1503–1505.

Katta, P., Alessandro, M., Ramsier, R. D. and Chase, G. G. (2004) *Nano Letters*, **4(11)**, 2215–2218.

Katti, D. S., Robinson, K. W., Ko, F. K. and Laurencin, C. T. (2004) *Journal of Biomedical Materials Research*, *Part B: Applied Biomaterials*, **70B**, 286–296.

Kebarle, P. and Peschke, M. (2000) *Analytica Chimica Acta*, **406**, 11–35.

Khatwani, P. A. and Yardi, S. S. (2003) *Man-Made Textiles in India*, **46**, 19–23.

Khil, M. S., Cha, D. I., Kim, H. Y., Kim, I. S. and Bhattarai, N. (2003) *Journal of Biomedical Materials Research*, *Part B: Applied Biomaterials*, **67B**, 675–679.

Kim, H. Y., Khil, M. S., Kim, H. J., Jung, Y. H. and Lee, D. R. (2003) In *IEEE-Nano 2003*, San Francisco, CA, USA, pp. 801–803.

Kim, H. Y., Lee, B. M., Kim, I. S., Jin, T. H., Ko, K. H. and Ryu, Y. J. (2004) *Polymeric Materials: Science and Engineering*, **91**, 712–713.

Ko, F., Gogotsi, Y., Ali, A., Naguib, N., Ye, H., Yang, G., Li, C. and Willis, P. (2003) *Advanced Materials (Weinheim*, *Germany)*, **15**, 1161–1165.

Koski, A., Yim, K. and Shivkumar, S. (2003) *Materials Letters*, **58**, 493–497.

Krishnan, J., Kotaki, M., Yanzhong, Z., Xiumei, M. and Ramakrishna, S. (2004) *Journal of Nanoscience and Nanotechnology*, **4**, 52–65.

Lee, J. S., Choi, K. H., Ghim, H. D., Kim, S. S., Chun, D. H., Kim, H. Y. and Lyoo, W. S. (2004) *Journal of Applied Polymer Science*, **93**, 1638–1646.

Lee, K. H., Kim, H. Y., Bang, H. J., Jung, Y. H. and Lee, S. G. (2003) *Polymer*, **44**, 4029–4034.

Li, D. and Xia, Y. (2004a) *Nano Letters*, **4**, 933–938.

Li, D. and Xia, Y. (2004b) *Advanced Materials (Weinheim*, *Germany)*, **16**, 1151–1170.

Li, D., Wang, Y. and Xia, Y. (2003) *Nano Letters*, **3**, 1167–1171.

Li, D., Babel, A., Jenekhe, S. and Xia, Y. (2004a) *Advanced Materials (Weinheim*, *Germany)*, **16** (22) 2062–2066.

Li, D., Wang, Y. and Xia, Y. (2004b) *Advanced Materials (Weinheim, Germany)*, **16**, 361–366.

Li, W. J., Laurencin, C. T., Caterson, E. J., Tuan, R. J. and Ko, F. K. (2002) *Journal of Biomedical Materials Research*, **60**, 613–621.

Lin, T., Wang, H., Wang, H. and Wang, X. (2004) *Nanotechnology*, **15**, 1375–1381.

Lin, T., Wang, H., Wang, H. and Wang, X. (2005a) *Journal of Material Science and Technology*, **21**, 9–12.

Lin, T., Wang, H. and Wang, X. (2005b) *Advanced Materials (Weinheim, Germany)*, **17**, 2699–2703.

Matthews, J. A., Wnek, G. E., Simpson, D. G. and Bowlin, G. L. (2002) *Biomacromolecules*, **3**, 232–238.

Megelski, S., Stephens, J. S., Chase, D. B. and Rabolt, J. F. (2002) *Macromolecules*, **35**, 8456–8466.

Pedicini, A. and Farris, R. J. (2003) *Polymer*, **44**, 6857–6862.

Pinto, N. J., Carrion, P. and Quinones, J. X. (2004) *Materials Science & Engineering*, *A: Structural Materials: Properties*, *Microstructure and Processing*, **366**, 1–5.

Reneker, D. H. and Chun, I. (1996) *Nanotechnology*, **7**, 216–223.

Shin, Y. M., Hohman, M. M., Brenner, M. P. and Rutledge, G. C. (2001a) *Applied Physics Letters*, **78**, 1149–1151.

Shin, Y. M., Hohman, M. M., Brenner, M. P. and Rutledge, G. C. (2001b) *Polymer*, **42**, 9955–9967.

Smit, E., Buttner, U. and Sanderson, R. D. (2005) *Polymer*, **46(8)**, 2419–2423.

Subramanian, A., Lin, H. Y., Vu, D. and Larsen, G. (2004) *Biomedical Sciences Instrumentation*, **40**, 117–122.

Sun, Z., Zussman, E., Yarin, A. L., Wendorff, J. H. and Greiner, A. (2003) *Advanced Materials (Weinheim, Germany)*, **15**, 1929–1932.

Sundaray, B., Subramanian, V., Natarajan, T. S., Xiang, R.-Z., Chang, C.-C. and Fann, W.-S. (2004) *Applied Physics Letters*, **84**, 1222–1224.

Suthar, A. and Chase, G. (2001) *The Chemical Engineer*, **726**, 26–28.

Suthar, A. and Chase, G. (2002) *Fluid/Particle Separation Journal*, **14**, 58–64.

Teo, W. E. and Ramakrishna, S. (2005) *Nanotechnology*, **16(9)**, 1878–1884.

Teo, W. E., Kotaki, M., Mo, X. M. and Ramakrishna, S. (2005) *Nanotechnology*, **16(6)**, 918–924.

Theron, A., Zussman, E. and Yarin, A. L. (2001) *Nanotechnology*, **12**, 384–390.

Tsai, P. and Schreuder-Gibson, H. L. (2003) *Advances in Filtration and Separation Technology*, **16**, 340–353.

Won, K. S., Ji, H. Y., Taek, S. L. and Won, H. P. (2004) *Polymer*, **45**, 2959–2966.

Xu, C. Y., Inai, R., Kotaki, M. and Ramakrishna, S. (2004) *Biomaterials*, **25**, 877–886.

Yao, L., Haas, T. W., Guiseppi-Elie, A., Bowlin, G. L., Simpson, D. G. and Wnek, G. E. (2003) *Chemistry of Materials*, **15**, 1860–1864.

Yarin, A. L. (1993) *Free Liquid Jets and Films: Hydrodynamics and Rheology*, John Wiley & Sons Inc., New York.

Yoshimoto, H., Shin, Y. M., Terai, H. and Vacanti, J. P. (2003) *Biomaterials*, **24**, 2077–2082.

Yu, J. H., Fridrikh, S. V. and Rutledge, G. C. (2004) *Advanced Materials (Weinheim, Germany)*, **16(17)**, 1562–1566.

Zhang, G., Kataphinan, W., Teye-Mensah, R., Katta, P., Khatri, L., Evans, E. A., Chase, G. G., Ramsier, R. D. and Reneker, D. H. (2005) *Materials Science & Engineering*, *B: Solid-State Materials for Advanced Technology*, **B116(3)**, 353–358.